AVERAGE FREQUENCY TRAJECTORY CONTROL: NORMAL MODE

by

Khaled Ibrahim Yared

B.E., American University of Beirut

1974

SUBMITTED IN PARTIAL FULFILLMENT OF THE
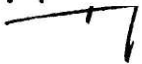
REQUIREMENTS FOR THE DEGREE OF

MASTER OF SCIENCE

at the

MASSACHUSETTS INSTITUTE OF TECHNOLOGY

February, 1976

Signature of Author ..Signature redacted......
Department of Electrical Engineering
and Computer Science, December 19, 1975.

Certified by . Signature redacted ....
Thesis Supervisor

Accepted by ... Signature redacted ....
Chairman, Departmental Committee on Graduate Students

AVERAGE FREQUENCY TRAJECTORY CONTROL: NORMAL MODE

by

Khaled Ibrahim Yared

Submitted to the Department of Electrical Engineering and Computer Science
on December 19, 1975 in partial fulfillment of the requirements for the
Degree of Master of Science.

ABSTRACT

In this thesis, a linear-plus-deadband controller is implemented on an
average system frequency model of a power system, under normal mode oper-
ation, and where only unknown-but-bounded disturbances of the loads are
considered. The deadband is added to both a conventional AGC as well as
a full state feedback control ; its design is based on set theoretic re-
lations which are then translated to relations between bounding ellipsoids.

Computational problems are solved by adding fictitious noise to the model
during the design process. This additional degree of freedom results in
sizeable savings in control signals. The deviations of frequency and tie-
line flow between areas are not significantly increased as compared to
the case where no deadband is used. Moreover, slightly better results are
obtained for the full state feedback deadband controller.

THESIS SUPERVISOR: Nils R. Sandell Jr.

TITLE: Assistant Professor of Electrical Engineering and
       Computer Science

ACKNOWLEDGEMENT

TABLE OF CONTENTS

C H A P T E R 1

INTRODUCTION

The oldest and most widely used power system central control is
Automatic Generation Control (AGC). It is essentially a feedback of tie-
line interchange power and system frequency which, integrated, provides
an appropriate supplementary control signal to power plant governors
when a mismatch between generation and demand occurs [1].

More sophisticated AGC laws, using modern control theory techniques,
have been investigated during the past few years. Most of them, inspired
by the success of the Optimal Linear Regulator, have called for a linear
feedback of all the state variables of the system while attempting to
minimize some quadratic cost function. Examples of these are given in
[2,3].

Also, a refinement of AGC, the "Error Adaptive Control Computer"
[4], has reduced inefficient control commands sent to power houses and
is presently often used.

The purpose of all those ideas was two fold. On one hand, the goal
was to improve the normal AGC function of keeping frequency and tie-line
power flow within scheduled limits by feeding back additional variables,
resulting therefore in a "smarter" control signal. On the other hand, it

was also useful to reduce wear and tear on control equipment (turbine valves) and the inefficiency of continuously pulsing machines by ignoring random disturbances which would anyway be eliminated by the natural damping of the power system. Moreover, it has been observed that in several instances conventional AGC needlessly pulses machines up and down [9].

From another point of view, the difference in magnitude of time constants associated with different elements of a power system suggests different dynamic models. And, in connection with AGC, predominant interest should be given to the slower speed dynamics by ignoring the much faster individual intermachine oscillations. The "Average System Frequency" concept is one such way to approach to problem and has been already presented in several instances [5,6].

This thesis proposes to investigate a control strategy based on the ideas presented above. The motivation for that is the ultimate aim of designing an average frequency trajectory controller which would have, in the normal mode of system behavior, the desired performance of:

· following the long term changes in demand while ignoring small rapid variations.

· keeping frequency (and time) within limits.

· keeping tie-line flows (and energy) within limits about schedule.

· causing a minimum number of changes in turbine valve positions.

A brief outline of the different chapters of the thesis is presented below:

In chapter 2, the average system frequency model is presented and derived for a specific test example of a two areas - three generators interconnected power system.

Chapter 3 presents the control strategy to be used. The derivation involves the use of different sets and it is found useful, for computational purposes, to derive ellipsoidal bounds to those sets. A simple two dimensional example is given to illustrate the problem before going to the more abstract geometry of the fifteen dimensional test system modeled in chapter 2.

In chapter 4, a hypothetical set of data is chosen for the two areas-three sources example of chapter 2 and the resulting continuous time model is discretized. Then a linear plus deadband control is designed, first using conventional AGC for the linear feedback, and second resorting to optimal control theory for a full state feedback. In both cases simulations are run and results discussed.

Chapter 5 draws a general conclusion to the thesis and provides a few suggestions for future research.

C H A P T E R 2

AVERAGE SYSTEM FREQUENCY MODEL

2.1 Introduction

In general, one can distinguish three parts in a power system: the power plants, the transmission network and the loads. Also, each one of these parts could lend itself to quite detailed mathematical models involving a large number of nonlinear differential equations. But, if a model is to be of any practical use, it has to be simplified in most of the cases to retain only the significant features relative to the problem at hand.

The purpose of this chapter is therefore to obtain a state variable model, i.e. first order differential equations, of an interconnected power system, making it possible to use modern control techniques. Moreover, this model should retain only the slow speed dynamics of the system since the rapid intermachine oscillations are not the concern of the control problem under study here. Finally, in view of the control strategy which will be used later, a linear and time-invariant model is also sought.

It is with those requirements in mind that one can proceed in developping the system model.

2.2 General Description

2.2.1 Power Plants

Different energy sources can be used to feed a power system. The only one to be considered here is the fossil-fuel steam boiler source. A common simplification is to neglect the boiler dynamics which are much slower than those of the remaining parts of the system but to include the boiler effects on the reheats. As a result, the turbine-governor model presented by Chan, Dunlop and Schweppe [7] is chosen to represent the incremental mechanical dynamics of the power plants. Mechanical deadbands are neglected and the bloc digram is shown in figure 2.1. The different parameters, for the kth power plant are:

R_k : droop of the speed governor

$T_{s,k}$: time constant of the speed control

$T_{v,k}$: time constant of the steam bowl

$T_{1,k}$: time constant of the first reheat

$T_{2,k}$: time constant of the second reheat

$M_{max,k}, M_{min,k}$: upper and lower margin of power due to valve limits

$\Delta f_k(t)$: frequency deviation from 1 p.u (60 c/s)

$\Delta P_{M,k}(t)$: total change (in p.u) in mechanical output power.

Also, the equivalent representation of the turbine-steam bowl model suggested by Grandez-Gomez [5] will be used. The model is shown in figure

GOVERNOR-STEAM BOWL MODEL
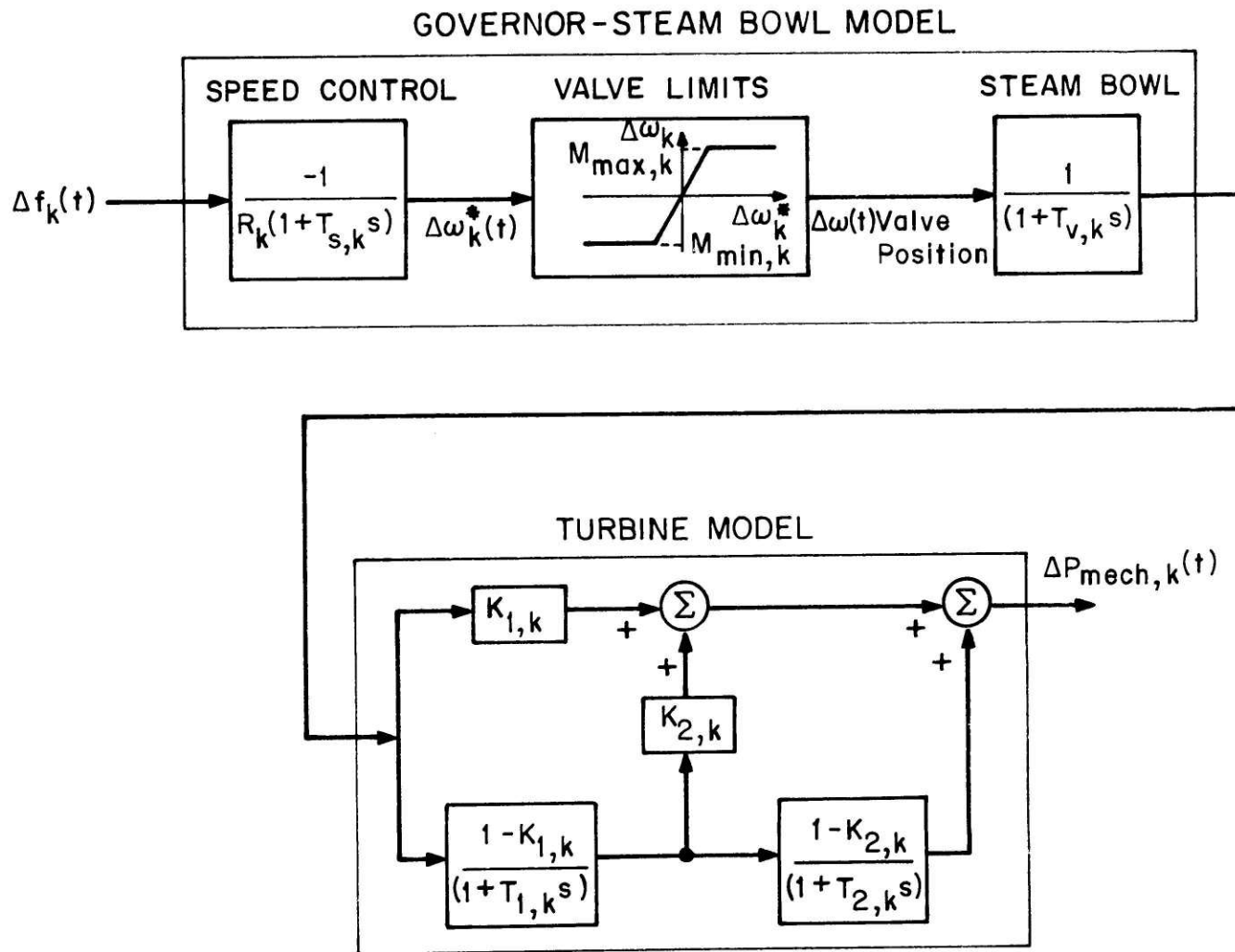
Figure 2-1

Governor-Turbine Model for K[th] Generator

2.2 along with the expressions for the new gains.

On the electrical side, the generator will be considered as a voltage source of constant magnitude. This is also common practice since the voltage regulator/excitor loop is much faster than the mechanical turbine loop.

Finally, the mechanical and electrical models are connected by the usual swing equations, which, for the Kth power plant, is:

$$M_k \frac{d\Delta f_k}{dt} = \Delta P_{M,k} - \Delta P_{E,k} - P_{D,k}$$

where M_k is the inertia coefficient of the kth generator

$\Delta P_{M,k}$ is the change in mechanical power delivered by the kth turbine (per unit)

$\Delta P_{E,k}(t)$ is the change in electrical output power of the kth generator (per unit)

$P_{D,k}(t) = K_{D,k} f_k(t)$ is the damping power with $K_{D,k}$, the damping coefficient.

Using the parameters of figures 2.1 and 2.2 the equations of the kth power plant can now be written:

$$\frac{d\Delta w_k^*}{dt} = - \frac{1}{T_{S,k}} \left(\frac{\Delta f_k}{R_k} + \Delta w_k^* \right) \tag{2.1}$$

$$\frac{c_{1,k}}{1 + d_{1,k}^{-1} s}$$

$$\frac{c_{2,k}}{1 + d_{2,k}^{-1} s}$$

$$\frac{c_{3,k}}{1 + d_{3,k}^{-1} s}$$

$\Delta w_k(t)$

$\Delta P_{M,k}(t)$
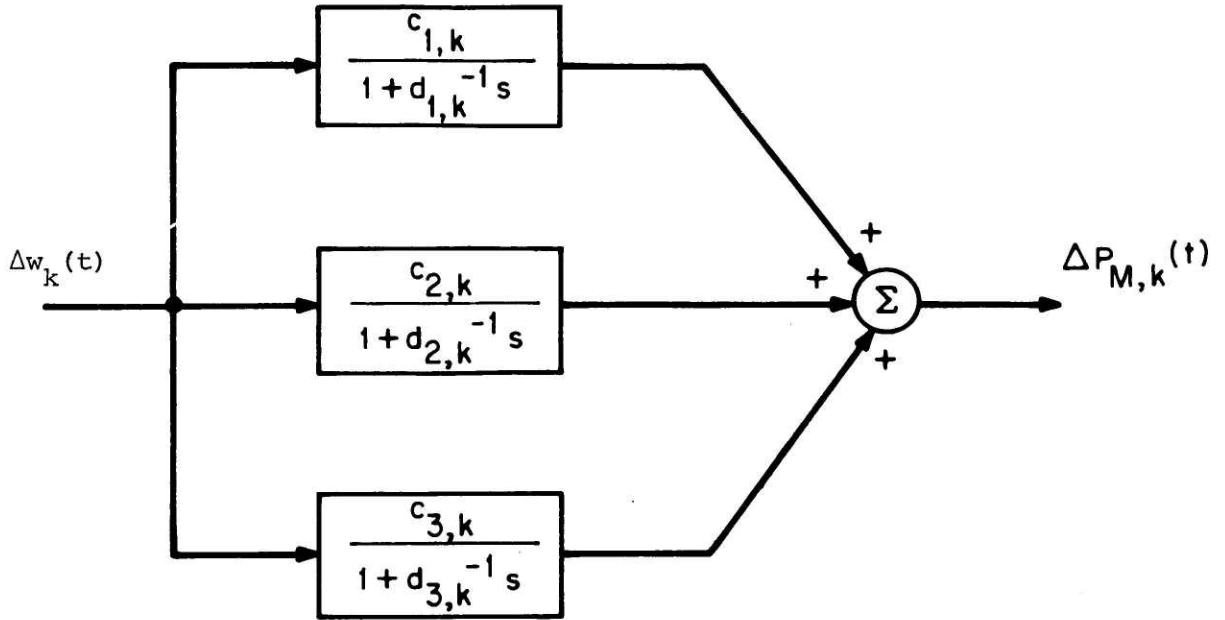
$$d_{1,k}^{-1} = T_{1,k}$$

$$d_{2,k}^{-1} = T_{2,k}$$

$$d_{3,k}^{-1} = T_{v,k}$$

$$C_{1,k} = \frac{\left(1 - K_{1,k}\right)\left(1 - K_{2,k}\frac{T_{2,k}}{T_{1,k}}\right)}{\left(1 - \frac{T_{2,k}}{T_{1,k}}\right)\left(1 - \frac{T_{v,k}}{T_{1,k}}\right)}$$

$$C_{2,k} = \frac{\left(1 - K_{1,k}\right)\left(1 - K_{2,k}\right)}{\left(1 - \frac{T_{1,k}}{T_{2,k}}\right)\left(1 - \frac{T_{v,k}}{T_{2,k}}\right)}$$

$$C_{3,k} = K_{1,k} + \frac{\left(1 - K_{1,k}\right) K_{2,k}}{\left(1 - \frac{T_{1,k}}{T_{v,k}}\right)} + \frac{\left(1 - K_{1,k}\right)\left(1 - K_{2,k}\right)}{\left(1 - \frac{T_{1,k}}{T_{v,k}}\right)\left(1 - \frac{T_{2,k}}{T_{v,k}}\right)}$$

Figure 2-2: Equivalent Turbine-Steam Bowl Model

$$\Delta w_k = \begin{cases} \Delta w_k^* & M_{min,k} < \Delta w_k^* < M_{max,k} \\[3mm] M_{max,k} & \Delta w_k^* \geq M_{max,k} \\[3mm] M_{min,k} & \Delta w_k^* \leq M_{min,k} \end{cases} \qquad (2.2)$$

$$\frac{d\Delta P_{M,j,k}}{dt} = d_{j,k}\left(c_{j,k}\Delta\omega_k - \Delta P_{M,j,k}\right) \qquad j = 1,2,3 \qquad (2.3)$$

$$\Delta P_{M,k} = \sum_{j=1}^{3} P_{M,j,k} \qquad (2.4)$$

$$M_k \frac{d\Delta f_k}{dt} = \Delta P_{M,k} - \Delta P_{E,k} - P_{D,k} \qquad (2.5)$$

And those will have to be combined with the equations of the transmission network to be developped next.

2.3.2. Transmission network:

In general, the real power flowing into a transmission line from bus i towards bus m can be expressed as:

$$P_{im} = Re\left\{\overline{v}_i^* \, \overline{I}_{im}\right\}$$

where, in phasor notation,

$\overline{Y}_{im} = Y_{im}e^{+j\theta_{im}}$ is the i-m line admittance

$\overline{v}_i^* = V_i e^{-j\delta_i}$ is the conjugate of voltage at bus i

$\overline{I}_{im}$ is the current in the i-m line

$$\text{then,} \quad P_{im} = \text{Re}\left\{\left(V_i e^{-j\delta_i}\right)\left[Y_{im}\left(V_i e^{j\delta_i} - V_m e^{j\delta_m}\right)e^{j\theta_{im}}\right]\right\}$$

$$= \text{Re}\left\{Y_{im}V_i^2 e^{j\theta_{im}} - Y_{im}V_i V_m e^{j(\theta_{im}-\delta_i+\delta_m)}\right\}$$

$$= Y_i V_i^2 \cos\theta_{im} - Y_i V_i V_m \cos\left(\theta_{im} - \delta_i + \delta_m\right)$$

It is therefore to linearize and simplify this equation that the following assumptions are now made. Those are also of standard practice when a linear model is needed to replace a more exact load flow study [8].

Assume, first, the transmission lines to be modeled by a pure reactance, thus, neglecting in effect the real power loss in the transmission network. As a result $\theta_{im} = -\frac{\pi}{2}$ rad. and we get:

$$P_{im} = Y_{im}V_i V_m \sin(\delta_i - \delta_m)$$

Second, assume the magnitudes of the voltages to be all aproximately equal to a same value V and we get:

$$P_{im} = Y_{im}V^2 \sin(\delta_i - \delta_m)$$

Finally, assume the differences in phase angles δ to be small enough so that

$$P_{im} = Y_{im}V^2(\delta_i - \delta_m) \tag{2.6}$$

And now, in a network containing N_t lines and N_b busses, a linear relationship between the line flows and the bus powers can be found [8].

Let $\underline{P}_t$ be the N_t-vector of line flows P_{im}

              $\underline{Y}_t$ be the $N_t \times N_t$ diagonal matrix of line admittances Y_{im}

              $\underline{\delta}$ be the (N_b-1)-vector of phase angles with respect to the reference bus

              $\underline{A}_r$ be the $N_t \times (N_b-1)$ reduced bus incidence matrix

              $\underline{P}_b$ be the (N_b-1)-vector of bus powers, omitting the reference bus

The elements a_{ij} of $\underline{A}_r$ are:

        $a_{ij}=+1$ if transmission line i is connected to bus j and directed away from the bus.

        $a_{ij}=-1$ if transmission line i is connected to bus j and directed towards the bus.

        $a_{ij}=0$ if transmission line i is not connected to bus j

From equation (2.6)

$$\underline{P}_t = V^2 \underline{Y}_t \, \underline{A}_r \, \underline{\delta} \tag{2.7}$$

On the other hand, conservation of power yields:

$$\underline{P}_b = \underline{A}_r^T \, \underline{P}_t$$

Substituting for $\underline{P}_t$:

$$\underline{P}_b = V^2 \, [\underline{A}_r^T \, \underline{Y}_t \, \underline{A}_r] \, \underline{\delta}$$

If the network has no isolated buses and since a reference bus has been used, it can be shown [8] that $\underline{B} = [\underline{A}_r^T \, \underline{Y}_t \, \underline{A}_r]$ has an inverse

Then

$$\underline{\delta} = \frac{1}{V^2} \, \underline{B}^{-1} \, \underline{P}_b$$

and

$$\underline{P}_t = \underline{Y}_t \, \underline{A}_r \, [\underline{A}_r^T \, \underline{Y}_t \, \underline{A}_r]^{-1} \, \underline{P}_b$$

Since the relations above are linear, they are aslo valid for deviations from nominal values. Thus:

$$\Delta\underline{P}_t = \underline{Y}_t \, \underline{A}_r \, [\underline{A}_r^T \, \underline{Y}_t \, \underline{A}_r]^{-1} \, \Delta\underline{P}_b \qquad (2.8)$$

and this will be connected to the power plant equations in section 2.3. A model for the loads is still needed to complete the picture.

2.2.3 Loads

In general, transient characteristics of the load at a bus k, are a function of f_k, V_k, $\dot{f}_k$, $\dot{V}_k$. But since a slow speed dynamics model of the system will be set up, "constant" power loads will be assumed so that,

if bus k is disturbed

$$P_{L,k}(t) = P_{L,k}(nominal) + \Delta P_{L,k}(t)$$

where no **explicit** dependance on frequency or voltage is retained.

Now the issue of modeling load disturbances $\Delta P_{L,k}(t)$ is a very delicate one, since those actually depend on a great number of factors (location, time, customers, accidents, etc...) This is why, in most of the simulations, simple test models are used, such as steps, ramps or completely random disturbances.

To be able to set up a simple regulator problem, load disturbances are chosen as "unbiased uncertainties". Possible models would be a white Gaussian random process or also a completely unknown-but-bounded in magnitude function[10]. Due to the structure of the control strategy which will be used later the latter model is chosen for $\Delta P_{L,k}(t)$.

2.3 Average System Frequency Model

The average system frequency concept has often been used to study the slow speed dynamics of an interconnected power system [5].

Using the same definitions for M_k, $\Delta P_{M,k}$, $\Delta P_{E,k}$, $P_{D,k}$ as above, and for a system containing N_g generators, let:

$$M_T = \sum_{k=1}^{N_g} M_k \quad \text{be the total inertia coefficient of the system}$$

$$\Delta P_{MT}(t) = \sum_{k=1}^{N_g} \Delta P_{M,k}(t) \quad \text{be the total change in mechanical input power}$$

$$\Delta P_{ET}(t) = \sum_{k=1}^{N_g} \Delta P_{E,k}(t) \quad \text{be the total change in electrical output power}$$

$$P_{DT}(t) = \sum_{k=1}^{N_g} P_{D,k}(t) \quad \text{be the total damping power}$$

The definition of the average system frequency deviation is

$$\Delta f_{av}(t) = \frac{\sum_{k=1}^{N_g} M_k \Delta f_k(t)}{M_T} \tag{2.9}$$

It is the weighted average of the individual frequency deviations of the system's generators, with the inertia coefficients as weighting factors.

Also, in view of equations (2.5) and (2.9) one gets the relation:

$$M_T \frac{d\Delta f_{av}(t)}{dt} = \Delta P_{MT}(t) - \Delta P_{ET}(t) - P_{DT}(t) \tag{2.10}$$

which does not contain, so far, any additional approximation.

Now, an average system frequency model can be obtained by neglect-

ing the effects of $(\Delta f_k - \Delta f_{av})$ throughout the power system.

2.3.1 Power Plants

The mechanical power output of the kth turbine $\Delta P_{M,k}$ is a function of governor action and therefore of Δf_k. If, in the governor-turbine model, Δf_k is replaced by Δf_{av}, the implicit assumption is that $\Delta P_{M,k}$ now depends only on Δf_{av}. One can argue, in support of this, that, if the disturbances are such that the system remains in synchronism, and the transmission system is not too weak [6], $(\Delta f_k - \Delta f_{av})$ is a high frequency oscillatory quantity relative to the large time constants of the turbine, and tends to be filtered out as a result.

A similar argument holds for $P_{D,k}$.

Showing explicitly the dependance on Δf_{av}, Equation (2.10) becomes, using the above assumptions,

$$M_T \frac{d\Delta f_{av}(t)}{dt} = \Delta P_{MT}[\Delta f_{av}(t)] - \Delta P_{ET}(t) - P_{DT}[\Delta f_{av}(t)] \qquad (2.11)$$

As for $P_{ET}(t)$, the total electrical power output of all the generators, since we are neglecting the losses in the transmission network, it depends on the total electric power delivered to the loads $P_{LT}(t)$; and here again, it is "physically reasonable" to assume dependance on the average frequency only.

As a result, the N_g swing equations are reduced to an approximate single one for Δf_{av} and equations (2.1) to (2.5) become, for the kth power plant:

$$\frac{d\Delta w_k^*}{dt} = -\frac{1}{T_{s,k}} \left(\frac{\Delta f_{av}}{R_t} + \Delta w_k^* \right) \qquad (2.12)$$

$$\Delta w_k = \begin{cases} \Delta w_k^* & M_{min,k} < \Delta w_k^* < M_{max,k} \\ M_{max,k} & \Delta w_k^* \geq M_{max,k} \\ M_{min,k} & \Delta w_k^* \leq M_{min,k} \end{cases} \qquad (2.13)$$

$$\frac{d\Delta P_{Mj,k}}{dt} = d_{j,k} \left(C_{j,k} \Delta w_k - \Delta P_{Mj,k} \right) \qquad j = 1,2,3 \qquad (2.14)$$

$$\Delta P_{M,k} = \sum_{j=1}^{3} \Delta P_{Mj,k} \qquad (2.15)$$

$$\frac{d\Delta f_{av}}{dt} = \frac{1}{M_T} \left\{ \Delta P_{MT}[\Delta f_{av}(t)] - \Delta P_{ET}(t) - P_{DT}[\Delta f_{av}(t)] \right\} \qquad (2.16)$$

This average system frequency model for the power plants, coupled to a nonlinear AC load flow solution for the transmission network, has been tested (see [5]) and shown to be an effective model for slow speed system dynamics. However, in view of the present task of putting together a linear model, the next section will develop a linear load flow study, considering real power flows only.

2.3.3 Transmission Network

Substracting (2.10) from (2.5) one gets the following relation:

$$M_k \frac{d}{dt} (\Delta f_k - \Delta f_{av}) = \Delta P_{M,k} - \Delta P_{E,k} - P_{D,k} - \frac{M_k}{M_T} [\Delta P_{MT} - \Delta P_{ET} - P_{DT}]$$

On the grounds of the same assumptions used already one can argue (see appendix D of [6]) that, integrated over a "period" of oscillation of $(\Delta f_k - \Delta f_{av})$, the left hand side vanishes. But the expression on the right hand side is much "slower" than $(\Delta f_k - \Delta f_{av})$ and can be therefore considered as constant over the period of integration. In other words, to a good approximation:

$$\Delta P_{E,k} \stackrel{\sim}{=} \Delta P_{M,k} - P_{D,k} - \frac{M_k}{M_T} [\Delta P_{MT} - \Delta P_{ET} - P_{DT}] \qquad (2.17)$$

Now, for every bus of the transmission network described in section 2.2.2 the change in bus power ΔP_{bi} is equal to the difference in changes

of electric power $\Delta P_{E,i}$ generated at that bus and load $\Delta P_{L,i}$ connected to the bus.

So

$$\Delta P_{b,i} = \Delta P_{E,i} - \Delta P_{L,i}$$

Substituting (2.17) for $\Delta P_{E,i}$

$$\Delta P_{b,i} = \Delta P_{M,i} - P_{D,i} - \frac{M_i}{M_T} [\Delta P_{MT} - \Delta P_{ET} - P_{DT}] - \Delta P_{L,i}$$

But since the power losses in the network are neglected:

$$\Delta P_{ET} = \sum_{i=1}^{N_b} \Delta P_{Li} = \Delta P_{LT}$$

and

$$\Delta P_{b,i} = \Delta P_{M,i} - P_{D,i} - \frac{M_i}{M_T} [\Delta P_{MT} - \Delta P_{LT} - P_{DT}] - \Delta P_{L,i}$$

So that, in view of (2.8), changes in tie-line power flows can be expressed as a function of changes in mechanical and load powers.

2.4 Model of an Interconnected System - A Two **Areas** - Three Sources

      Example

The different parts studied above can now be assembled to construct a linear, state variable, average system frequency model of an interconnected system. The working example will be that shown in fig. 2.3.
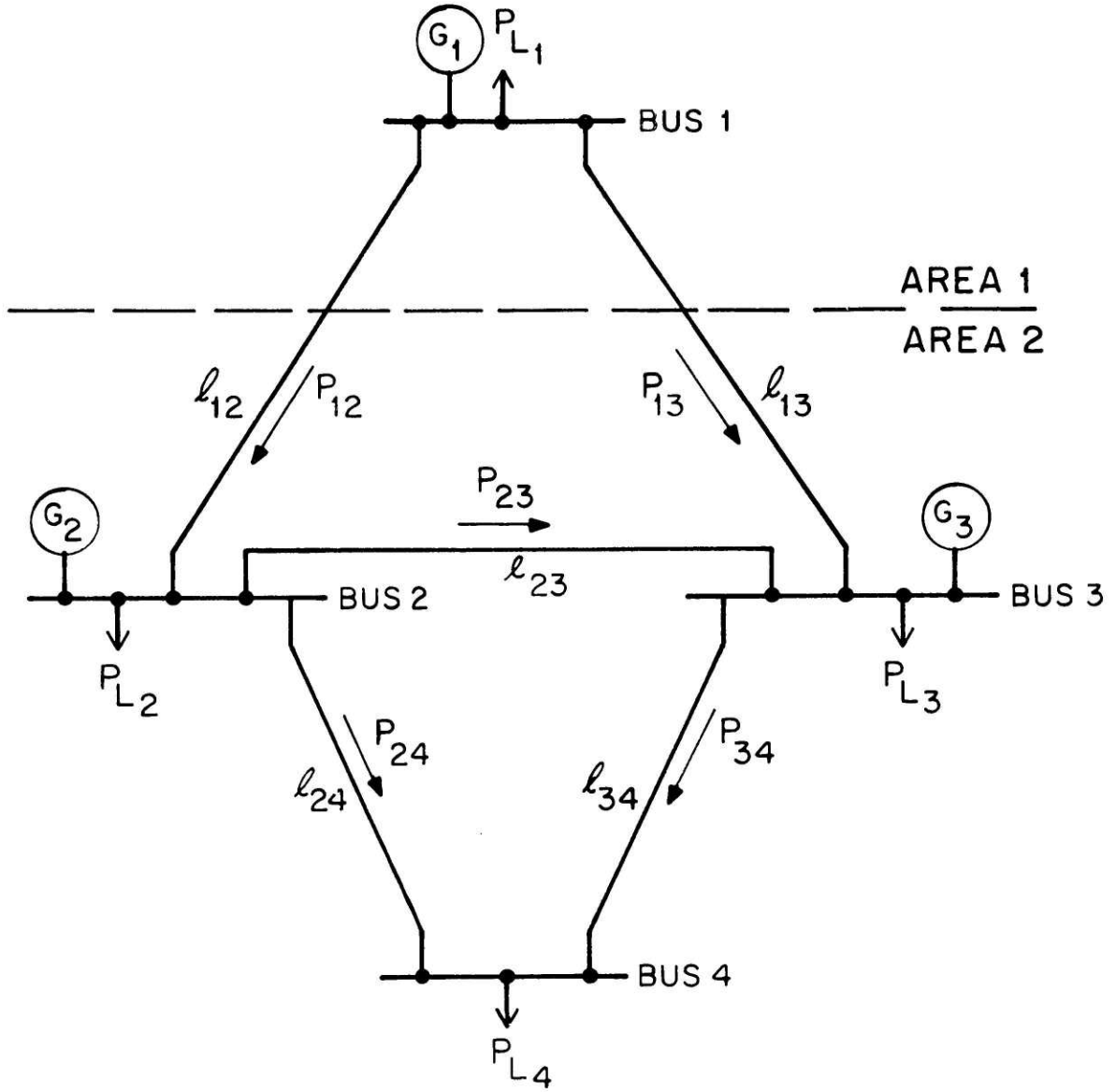
Figure 2-3

Two Areas-Three Sources Interconnection

To obtain a totally linear model, the valves of the power plant turbines are assumed never to hit their limits. Once the control design is carried out, one can go back and check the validity of this assumption. Note that only normal mode operation of the system with no emergency type disturbances occuring is under study here.

Damping power will also be neglected for simplicity.

With those changes in effect, equations (2.12) to (2.16) show that each power plant requires four states of its own. All power plants share a common fifth state: the average frequency deviation. Two states, the integral of average frequency deviation and the integral of tie-line power interchange between the two areas are added to the model, in view of the AGC action which will be used later.

Tie-line power interchange is

$$\Delta P_{tie} = \Delta P_{12} + \Delta P_{13}$$

Using the developments of sections 2.2.2 and 2.3.2, with

$$\underline{\Delta P}_t = \begin{bmatrix} \Delta P_{12} \\ \Delta P_{13} \\ \Delta P_{23} \\ \Delta P_{24} \\ \Delta P_{34} \end{bmatrix} \quad ; \quad \underline{Y}_t = \begin{bmatrix} Y_{12} & & & \\ & Y_{13} & & \underline{0} \\ & & Y_{23} & \\ \underline{0} & & & Y_{24} \\ & & & & Y_{34} \end{bmatrix}$$

and bus #4 as the reference bus, so that

$$\Delta \underline{P}_b = \begin{bmatrix} \Delta P_{b1} \\ \Delta P_{b2} \\ \Delta P_{b3} \end{bmatrix} \quad ; \qquad \underline{A}_r = \begin{bmatrix} +1 & -1 & 0 \\ +1 & 0 & -1 \\ 0 & +1 & -1 \\ 0 & +1 & 0 \\ 0 & 0 & +1 \end{bmatrix}$$

$$\Delta P_{tie} = [\ 1 \quad 1 \quad 0 \quad 0 \quad 0\ ] \ \Delta \underline{P}_t$$

$$= [\ 1 \quad 1 \quad 0 \quad 0 \quad 0\ ] \ \underline{Y}_t \ \underline{A}_r \ [\ \underline{A}_r^T \ \underline{Y}_T \ \underline{A}_k\ ]^{-1} \ \Delta \underline{P}_b$$

$$\Delta P_{tie} = [\ C_1 \ C_2 \ C_3\ ] \ \underline{P}_b$$

$$= \begin{cases} C_1 \left[\Delta P_{M1} - \dfrac{M_1}{M_T} \left(\Delta P_{MT} - \Delta P_{LT} \right) - \Delta P_{L1} \right] \\[2mm] + C_2 \left[\Delta P_{M2} - \dfrac{M_2}{M_T} \left(\Delta P_{MT} - \Delta P_{LT} \right) - \Delta P_{L2} \right] \\[2mm] + C_3 \left[\Delta_{M3} - \dfrac{M_3}{M_T} \left(\Delta P_{MT} - \Delta P_{LT} \right) - \Delta P_{L3} \right] \end{cases}$$

$$= [a_1 \ a_2 \ a_3] \begin{bmatrix} \Delta P_{M1} \\ \Delta P_{M2} \\ \Delta P_{M3} \end{bmatrix} - [\ a_1 \ a_2 \ a_3 \ a_4] \begin{bmatrix} \Delta P_{L1} \\ \Delta P_{L2} \\ \Delta P_{L3} \\ \Delta P_{L4} \end{bmatrix}$$

where

$$a_i = c_i - \frac{\displaystyle\sum_{i=1}^{3} C_i M_i}{M_T} \quad ; \qquad i = 1, 2, 3$$

$$a_4 = - \frac{\displaystyle\sum_{i=1}^{3} C_i M_i}{M_T}$$

Remark: the result should be independant of the choice of bus reference

since network losses are neglected and a linear model is used.

Finally, the control signals act directly on the governor servo, as shown in fig. 2-4 and equation 2.12 becomes, when a control is applied:

$$\frac{d\Delta w_k}{dt} = - \frac{1}{T_{s,k}} \left(\frac{\Delta f_{av}}{R_k} + \Delta w_k \right) + \frac{u_k}{T_{s,k}}$$

The model can now written in the form

$$\underline{\dot{x}}(t) = \underline{A}\, \underline{x}(t) + \underline{B}_c\, \underline{u}(t) + \underline{G}_c\, \Delta \underline{P}_L(t)$$

where $\underline{A}$, $\underline{B}_c$ and $\underline{G}_c$ are given in figure 2-5 and the physical interpretation of the state variables is given in figure 2-6.

Note: There has been increasing interest in the idea of aggregation in

connection with the study of large scale systems (e.g. [15]). In

relation to that, the model developed in this chapter can be

considered as an approximate aggregation, based, though, on physical

assumptions and approximations.
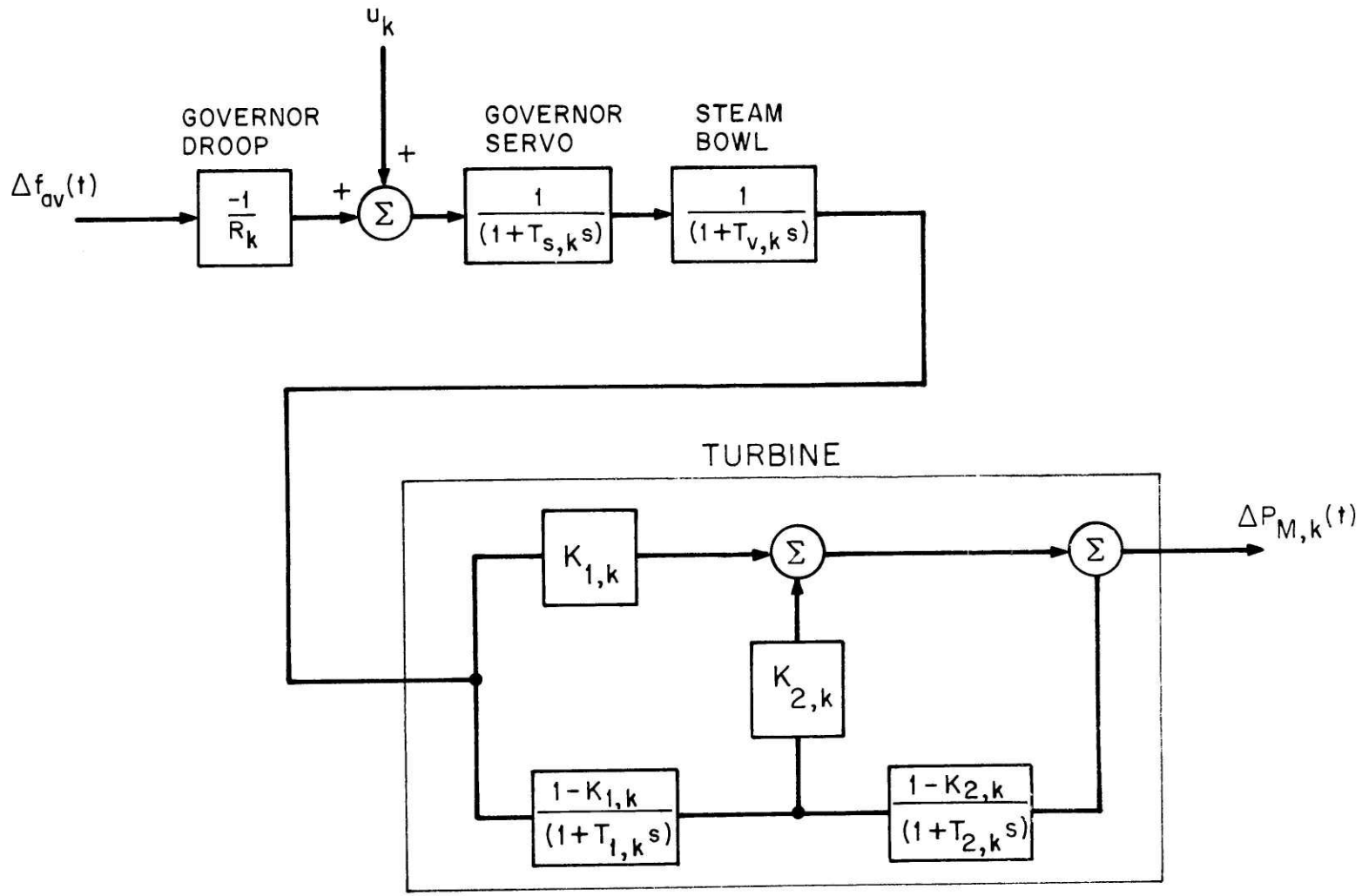
Figure 2-4 Linear Average System Frequency Model of the kth Power Plant with Control Signal Applied

$$\underline{\dot{x}} =$$

$$
\begin{bmatrix}
-d_{11} & & & d_{11}c_{11} & & & & & & & -\frac{1}{T_{S1}R_1} & \\
& -d_{21} & & d_{21}c_{21} & & & & & & & & \\
& & -d_{31} & d_{31}c_{31} & & & & & & & & \\
& & & -\frac{1}{T_{S1}} & & & & & & & \\
& & & & -d_{12} & & d_{12}c_{12} & & & & & \\
& & & & & -d_{22} & d_{22}c_{22} & & & & & \\
& & & & & -d_{32} & d_{32}c_{32} & & & & & \\
& & & & & & -\frac{1}{T_{S2}} & & & & -\frac{1}{T_{S2}R_2} & \\
& & & & & & & -d_{13} & & d_{13}c_{13} & & \\
& & & & & & & & -d_{23} & d_{23}c_{23} & & \\
& & & & & & & & -d_{33} & d_{33}c_{33} & & \\
& & & & & & & & & -\frac{1}{T_{S3}} & -\frac{1}{T_{S3}R_3} & \\
\frac{1}{M_T} & \frac{1}{M_T} & \frac{1}{M_T} & & \frac{1}{M_T} & \frac{1}{M_T} & \frac{1}{M_T} & \frac{1}{M_T} & \frac{1}{M_T} & \frac{1}{M_T} & & \\
& & & & & & & & & & 1 & \\
a_1 & a_1 & a_1 & & a_2 & a_2 & a_2 & a_3 & a_3 & a_3 & &
\end{bmatrix}
\underline{x}
$$

$$
+
\begin{bmatrix}
\\
\frac{1}{T_{S1}} \\
\\
\\
\frac{1}{T_{S2}} \\
\\
\\
\frac{1}{T_{S3}} \\
\\
\end{bmatrix}
\begin{bmatrix}
u_1 \\
u_2 \\
u_3
\end{bmatrix}
+
\begin{bmatrix}
\\
\\
\\
\\
\\
\frac{-1}{M_T} & \frac{-1}{M_T} & \frac{-1}{M_T} & \frac{-1}{M_T} \\
\\
-a_1 & -a_2 & -a_3 & -a_4
\end{bmatrix}
\begin{bmatrix}
\Delta P_{L1} \\
\Delta P_{L2} \\
\Delta P_{L3} \\
\Delta P_{L4}
\end{bmatrix}
$$
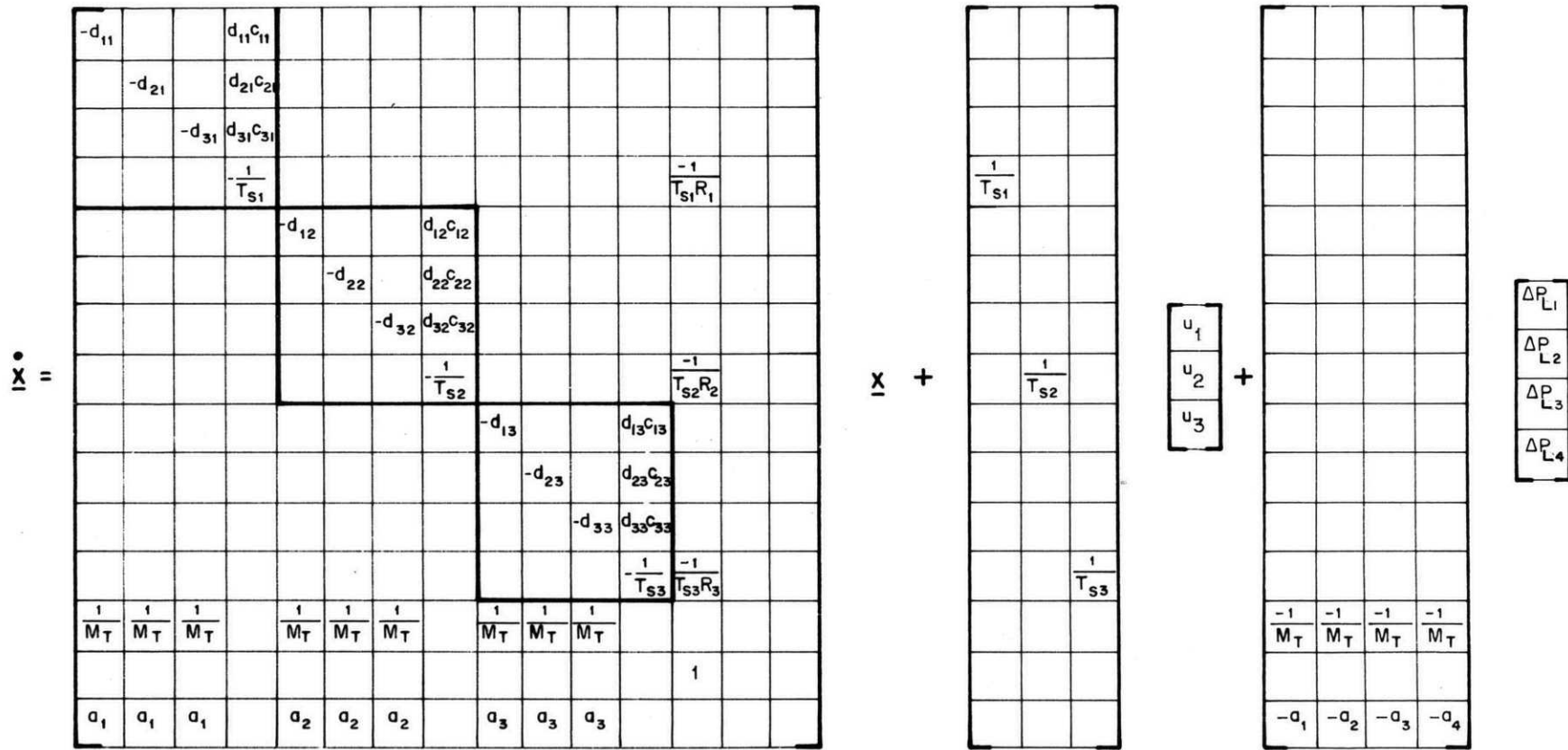
$$\underline{\dot{x}} = \underline{A}\,\underline{x} + \underline{B}_c\,\underline{U} + \underline{G}_c\,\Delta\underline{P}_L$$

Figure 2-5

Linear Model of the Interconnected System

$$x_1 = \Delta P_{M1,1}$$
$$x_2 = \Delta P_{M2,1} \qquad x_1 + x_2 + x_3 = \Delta P_{M1}$$
$$x_3 = \Delta P_{M3,1}$$
$$x_4 = \Delta w_1$$

$$x_5 = \Delta P_{M1,2}$$
$$x_6 = \Delta P_{M2,2} \qquad x_5 + x_6 + x_7 = \Delta P_{M2}$$
$$x_7 = \Delta P_{M3,2}$$
$$x_8 = \Delta w_2$$

$$x_9 = \Delta P_{M1,3}$$
$$x_{10} = \Delta P_{M2,3} \qquad x_9 + x_{10} + x_{11} = \Delta P_{M3}$$
$$x_{11} = \Delta P_{M3,3}$$
$$x_{12} = \Delta w_3$$

$$x_{13} = \Delta f_{av}$$
$$x_{14} = \Delta\delta av = \int \Delta f_{av}$$
$$x_{15} = \int \Delta P_{Tie} = \int (\Delta P_{12} + \Delta P_{13})$$

$$\Delta P_{MT} = x_1 + x_2 + x_3 + x_5 + x_6 + x_7 + x_9 + x_{10} + x_{11}$$

Figure 2.6:

Physical Interpretation of State Variables

C H A P T E R 3

CONTROL STRATEGY

3.1 Introduction

In the modeling process of the previous chapter, individual inter-
machine oscillations were ignored by using the average system frequency
concept. This chapter concerns itself with the problem of reducing the
number of signals sent to power plants and therefore causing a minimum
number of changes in turbine valve positions. The motivation for this is
of course the resulting reduction in wear and tear on control equipment
and, moreover, the increase in efficiency in the operation of the turbine.
The problem is dealt with by using the linear-plus-deadband control
concept [3,11].

Because of the sampled data nature of AGC, as presently used in the
power industry, it will be found convenient, in the next chapter to
convert the continuous time model of the system into a discrete time model
before going further into the design of a controller. Therefore, the
discussion in the present chapter will be based on a general discrete time
linear system.

Moreover, in view of the aim of finding a deadband set for control
action, space sets containing the state variables will be considered rather
than assuming a probabilistic structure.

This is why the load disturbances were chosen, is section 2.2, to be only set constrained.

In the sequel, the control problem will be stated and the logic behind the strategy will be first presented with set theoretic relations. Then, equations giving more manageable bounds to these sets will be developed to match the working model assembled in Section 2.4. Finally a simple numerical two dimensional example will illustrate the different steps of the design procedure.

3.2 Linear - Plus - Deadband Control

3.2.1 Problem Statement

Consider the linear, time invariant system given in discrete time by:

$$\underline{x}(n\Delta+\Delta) = \underline{\Phi}\ \underline{x}(n\Delta) + \underline{B}\ \underline{u}(n\Delta) + \underline{G}\ \underline{w}(n\Delta) \qquad (3.1)$$

$$\underline{y}(n\Delta) = \underline{H}\ \underline{x}(n\Delta) \qquad (3.2)$$

where $\underline{x}(n\Delta)$ is the N_s-dimensional state vector.

$\underline{u}(n\Delta)$ is the N_c-dimensional control vector

$\underline{w}(n\Delta)$ is the N_ℓ-dimensional disturbance vector

$\underline{y}(n\Delta)$ is the N_0-dimensional output vector

$\underline{\Phi}$, $\underline{B}$, $\underline{G}$, $\underline{H}$ are constant matrices of proper dimensions.

Let the disturbances $\underline{w}(n\Delta)$ be unknown-but-bounded:

$$\underline{w}(n\Delta) \in \Omega_w, \quad \Omega_w \text{ is in } R^{N_\ell} \tag{3.3}$$

Find a **control** of the form:

$$\underline{u}(n\Delta) = \begin{cases} \underline{0} & , \quad \text{if} \quad \underline{x}(n\Delta) \in \Omega_c \\ \underline{K} \, \underline{x}(n\Delta) & , \quad \text{if} \quad \underline{x}(n\Delta) \notin \Omega_c \end{cases} \tag{3.4}$$

where Ω_c is a deadband set in R^{N_s}, and such that

$$\underline{y}(n\Delta) \in \Omega_y \qquad \forall \, n, \quad n = 0,1,\ldots$$

where Ω_y is a specification set in R^{N_0}.

In other words, the control law is such that, if, at time $n\Delta$, the state lies within a certain deadband or switching region Ω_c no control action is taken and if, due to the disturbances of the loads, the state has drifted out of Ω_c a control signal proportional to the state is fed back.

The problem is to design the linear feedback gain $\underline{K}$ and the deadband set Ω_c such that, with a minimum number of **control** signals the vector of outputs $\underline{y}$ we are interested in keeping within specified limits about schedule (frequency, tie line flows), does indeed remain within those limits.

At this point, and in order to reconnect the control problem formulation with the task at hand of controlling an interconnected power system,

one can note the following.

Several approaches could be taken to design the linear part of the control law (3.4). These include conventional automatic generation control or, alternatively, a full state feedback linear regulator which minimizes some quadratic cost function using optimal control theory. However, in both cases, the closed loop should be of course stable. From Schweppe's discussion [10] of dynamic systems driven by an unknown-but-bounded disturbance, and for a time-invariant stable system given by:

$$\underline{x}(n\Delta+\Delta) = \underline{\Phi}\ \underline{x}(n\Delta) + \underline{G}\ \underline{w}(n\Delta),\ \underline{w}(n\Delta)\ \varepsilon\ \Omega_w$$

the steady-state value of $\underline{x}(n\Delta)$ will itself be constrained to some constant set $\Omega_x(ss)$ which depends on the dynamics of the system i.e. the transition matrix $\underline{\Phi}$, as well as on the "size" of Ω_w.

On the other hand, in the model derived in chapter 2, the regulated variables, i.e. the frequency, the integral of frequency (time), and the area interchange of energy, are included in the state vector so that the matrix $\underline{H}$ of equation (3.2) is of the form:

$$\underline{H} = [\ \underline{0}\ \underline{I}\ ]$$

where $\underline{I}$ is the $N_0 \times N_0$ identity matrix.

On the grounds of those remarks, the control problem can be restated roughly in the following manner:

For the system given by (3.1), (3.2) and (3.3), find a control of the form given by (3.4) such that:

    i) the size of Ω_c in R^{N_s} is maximum (minimum number of control

       signals)   (3.5)

    ii) $\Omega_{x|y}(ss; \underline{K}) \subset \Omega_y$ (3.6)

where Ω_y is the specification set in R^{N_0}.

$\Omega_{x|y}(ss; \underline{K})$ is the projection of $\Omega_x(ss)$ in R^{N_s} down on to

(see appendix G of [10]) the N_0-dimensional subspace of $\underline{y}$.

Explicit dependance of the steady-state set on the closed loop matrix (and therefore on the feedback gain $\underline{K}$) is shown.

3.2.2 Set theoretic relations

Two approaches to linear-plus-deadband control have been discussed by Glover and Schweppe, [11]; However, it is the first one that has been found more suitable to the problem as stated above.

Consider the system given by (3.1), (3.2) and (3.3); assume that a linear control law

$$\underline{u}(n\Delta) = \underline{K}\,\underline{x}(n\Delta) \qquad\qquad (3.7)$$

is chosen so that, for the closed loop:

$$\underline{x}(n\Delta+\Delta) = (\underline{\Phi} + \underline{B}\,\underline{K})\,\underline{x}(n\Delta) + \underline{G}\,\underline{w}(n\Delta) = \underline{\Phi}_{c\ell}\,\underline{x}(n\Delta) + \underline{G}\,\underline{w}(n\Delta)$$
$$(3.8)$$

there exists a steady state set $\Omega_x(ss; \underline{K})$ in R^{N_s} that contains $\underline{x}(n\Delta)$, $\forall n$, and $\forall \underline{w}(n\Delta) \in \Omega_w$, if the control (3.7) is applied for all n, and which satisfies relation (3.6).

Furthermore, let $\Omega_c^{\sim}$ be defined as the largest set in R^{N_s} that satisfies:

$$\underline{\Phi} \, \Omega_c^{\sim} \, \oplus \, \underline{G} \, \Omega_w \subset \Omega_x(ss; \underline{K}) \tag{3.9}$$

where $\oplus$ denotes a vector sum

$\underline{\Phi} \, \Omega_c^{\sim}$ denotes the set $\Omega_c^{\sim}$ translated by $\underline{\Phi}$

$$= \{\underline{\Phi} \, \underline{x} : \underline{x} \in \Omega_c^{\sim}\}$$

$\underline{G} \, \Omega_w$ denotes the set Ω_w translated by $\underline{G}$

$$= \{\underline{G} \, \underline{w} : \underline{w} \in \Omega_w\}$$

As a result, if $\underline{x}(n\Delta) \in \Omega_c^{\sim}$ and $\underline{u}(n\Delta) = 0$, $\underline{x}(n\Delta+\Delta) \in \Omega_x(ss; \underline{K})$ and:

$$\begin{cases} \underline{y}(n\Delta+\Delta) \in \Omega_{x|y}(ss; \underline{K}) \\ \Omega_{x|y}(ss; \underline{K}) \subset \Omega_y \end{cases}$$

Finally, since $\underline{y}(n\Delta) \in \Omega_{x|y}(ss;\underline{K})$ as well, define the deadband set Ω_c as:

$$\Omega_c = \Omega_c^{\sim} \cap \Omega_x(ss;\underline{K}) \tag{3.10}$$

In other words, the deadband set Ω_c is a subset of $\Omega_x(ss;K)$ such

that, if at time $n\Delta$ it contains the state $\underline{x}(n\Delta)$, one can afford not to apply a control $\underline{u}(n\Delta)$ and keep $\underline{x}(n\Delta+\Delta)$ in $\Omega_x(ss;\underline{K})$. It follows that using the control law

$$\underline{u}(n\Delta) = \begin{cases} \underline{0} & , \quad \text{if} \quad \underline{x}(n\Delta) \in \Omega_c \\ \underline{K} \, \underline{x}(n\Delta) & , \quad \text{if} \quad \underline{x}(n\Delta) \notin \Omega_c \end{cases}$$

will give, for all n:

$$\underline{y}(n\Delta) \in \Omega_y$$

And since Ω_c is chosen as large as possible, the number of control signals applied will be kept at a minimum level.

Figure 3.1 illustrates the approach taken in this section.

Note that the design of $\underline{K}$, using either conventional AGC or optimal linear regulator theory, is not carried to maximize the size of Ω_c directly. It follows that the control law will be, in terms of the deadband, only suboptimal in some sense.

Note also that it has been implicitly assumed all along in the development that the states of the system can be measured perfectly. This has the advantage of simplifying the problem to concentrate only on the performance of the linear-plus-deadband control. If found promising, this approach could be always extended to include a state estimator.

$\Omega_x(ss; \underline{k})$

in here use
$\underline{u} = \underline{k}\,\underline{x}$

Ω_c
in here use
$u = 0$

$\Omega_{\tilde{c}}$

Space R^{N_s}
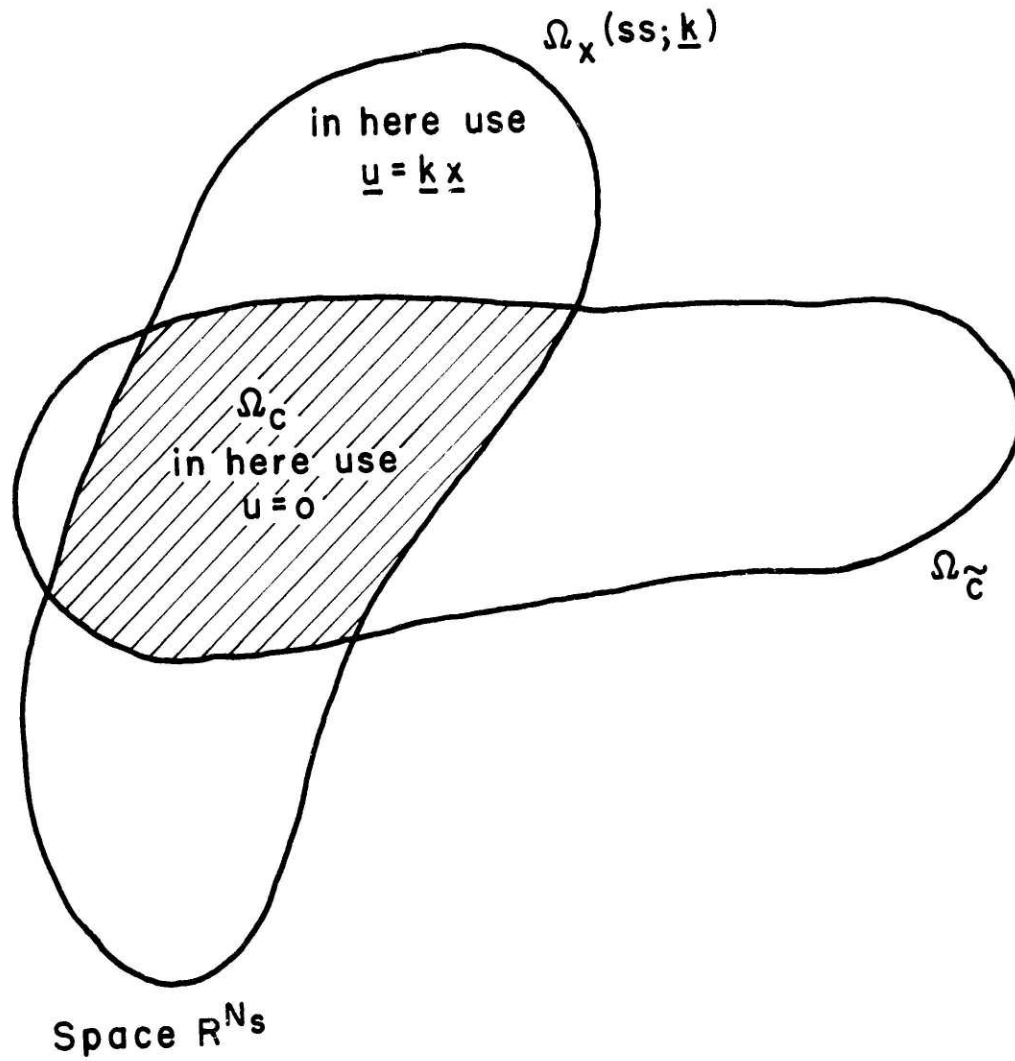
Figure 3-1

Linear-Plus-Deadband Control

Finally, the set theoretic relations developped above are not suitable for a computer design. On the other hand, ellipsoidal sets are defined by matrices which can be manipulated on a digital computer. They are therefore very practical from a computational point of view; and this is why bounding ellipsoids to the sets of the previous relations will now be derived.

3.2.3 Bounding Ellipsoids:

The relevant mathematical material to the subsequent development is gathered from [10, 11] in an Appendix for the sake of completeness.

Consider the system given by (3.1), (3.2) and (3.3); and assume Ω_w to be given by the following ellipsoid:

$$\Omega_w = \{\underline{w} \in R^{N_\ell} : \underline{w}' \underline{Q}^{-1} \underline{w} \leq 1\}$$

where $\underline{Q}$ is a specified positive definite matrix.

If a linear control (3.7) is chosen so that the closed loop system (3.8) is stable, then there exists (Appendix) a steady state bounding ellipsoid $\Omega_{x,b}(ss; \underline{K})$ given by:

$$\Omega_{x,b}(ss; \underline{K}) = \{\underline{x} \in R^{N_s}, \quad \underline{x}' \underline{\Gamma}^{-1}_{ss} \underline{x} \leq 1\}$$

$$\Omega_x(ss; \underline{K}) \subset \Omega_{x,b}(ss; \underline{K})$$

where $\underline{\Gamma}_{ss} = \left(\dfrac{1}{1-\beta} \right) \underline{\Phi}_{c\ell} \, \underline{\Gamma}_{ss} \, \underline{\Phi}'_{c\ell} + \dfrac{1}{\beta} \, \underline{G} \, \underline{Q} \, \underline{G}'$ (3.11)

where $0 < \beta < 1$ is chosen so that $\underline{\Gamma}_{ss}$ is positive definite

Note that β is a design parameter which enters the picture when an ellipsoidal bound to the set $\Omega_x(ss;\ \underline{K})$ is desired; and although, Ω_w is itself chosen as an ellipsoid, $\Omega_x(ss;\underline{K})$ will not be one in general. Moreover, equation (3.11) shows that a β close to "zero" tends to amplify the effect of the disturbance bound whereas a β close to "one" tends to amplify the dynamics of the system.

Note also that the ellipsoids considered here are all centered at the origin since no deterministic quantities drive the system.

As for the output,

$$\Omega_{x,b|y}(ss;\ \underline{K}) = \left\{ \underline{y} \in R^{N_0}:\ \underline{y}' \ [\underline{H} \ \underline{\Gamma}_{ss} \ \underline{H}']^{-1} \ \underline{y} \le 1 \right\}$$

(see Appendix H of [10]), and condition (3.6) becomes

$$\Omega_{x,b|y}(ss;\ \underline{K}) \subset \Omega_y$$

Then, let Ω_c be defined as the largest set in R^{N_s} that satisfies

$$\underline{\Phi} \ \Omega_c + \underline{G} \, \Omega_w \subset \Omega_{x,b}(ss:\ \underline{K})$$

Since Ω_w is an ellipsoid in R^{N_ℓ} with matrix $\underline{Q}$, its translation $\underline{G}\Omega_w$ is an ellipsoid in R^{N_s} with matrix $\underline{G}\,\underline{Q}\,\underline{G}'$ (Appendix)

Here again, although $\Omega_{x,b}(ss;\ \underline{K})$ and $\underline{G}\Omega_w$ are ellipsoidal, in general Ω_{c} is not. If $(\underline{\Gamma}_{ss} - \underline{G}\,\underline{Q}\,\underline{G}')$ is positive definite, i.e. $\Omega_{x,b}$ is bigger than $\underline{G}\Omega_w$, then an inner ellipsoidal bound $\Omega_{c,b}$ to Ω_c is given by (Appendix)

$$\Omega_{c,b} = \{\ \underline{x} \in R^{N_s} : \underline{x}'\ \Gamma_c^{-1}\underline{x} \leq 1\}$$

where $\underline{\Phi}\,\underline{\Gamma}_c\,\underline{\Phi}' = \dfrac{\alpha}{1+\alpha}\,\underline{\Gamma}_{ss} - \alpha\,\underline{G}\,\underline{Q}\,\underline{G}'$ \hfill (3.12)

where

$$0 < \alpha < [\lambda_{\min}(\underline{\Theta}'\ \underline{\Gamma}_{ss}\ \underline{\Theta}) - 1] > 0$$

$\lambda_{\min}(\underline{\Theta}'\ \underline{\Gamma}_{ss}\ \underline{\Theta}) = $ minimum eigenvalue of $\underline{\Theta}'\ \underline{\Gamma}_{ss}\ \underline{\Theta}$

$\underline{\Theta}$ is the matrix which transforms $\underline{G}\,\underline{Q}\,\underline{G}'$ into

a **sphere** $(\ \underline{\Theta}'\underline{G}\,\underline{Q}\,\underline{G}'\ \underline{\Theta} = \underline{I}\ )$

A derivation and geometrical interpretation of the limits on the design parameter α are presented in the Appendix, Note that if $(\underline{G}\,\underline{Q}\,\underline{G}')$ has not full rank, $(\underline{\Theta}'\ \underline{G}\,\underline{Q}\,\underline{G}'\ \underline{\Theta})$ could be only of the form

$$\begin{bmatrix} \underline{0} & \underline{0} \\ \underline{0} & \underline{I} \end{bmatrix}$$

Geometrically this means that the ellipsoid $\underline{G}\Omega_w$, considered in the basis defined by the eigenvectors of $\underline{G}\,\underline{Q}\,\underline{G}'$, is flat in the directions corresponding to the zero eigenvalues of $\underline{G}\,\underline{Q}\,\underline{G}'$. This will be the case in the physical problem treated in chapter 4 and the parameter α will be chosen using such geometrical arguments.

The deadband set is now

$$\Omega_c = \tilde{\Omega}_{c,b} \cap \Omega_{x,b}(ss;\underline{k})$$

Here again, an ellipsoidal inner bound to Ω_c could be found. But with every bounding process the design gets more and more conservative. This last step can therefore be avoided by replacing the test:

$$\underline{x}(n\Delta) \ \varepsilon \ \Omega_c$$

by the combined:

$$\left\{ \begin{array}{l} \underline{x}(n\Delta) \ \varepsilon \ \Omega_{x,b}(ss;\underline{K}) \\[2ex] \underline{x}(n\Delta) \ \varepsilon \ \tilde{\Omega}_{c,b} \end{array} \right\} \longleftrightarrow \left\{ \begin{array}{l} \underline{x}'\,\underline{\Gamma}_{ss}^{-1}\,\underline{x} \leq 1 \\[2ex] \underline{x}'\,\underline{\Gamma}_c^{-1}\,\underline{x} \leq 1 \end{array} \right\}$$

in the linear-plus-deadband control strategy (3.4).

The design procedure can be now summarized by the flow chart shown in fig. 3-2.

Given: $\underline{\phi}$, $\underline{B}$, $\underline{G}$; the model

$\underline{Q} > 0$; Disturbance bound

$\underline{\text{Design}}$ $\underline{K}$ (Conventional AGC
or optimal control)

$$\underline{\phi}_{c\ell} = \underline{\phi} + \underline{B}\ \underline{K}$$

Choose β and   Solve   for $\underline{\Gamma}_{ss}$
$$\Gamma_{ss} = \frac{1}{1-\beta}\ \underline{\phi}_{c\ell}\underline{\Gamma}_{ss}\ \underline{\phi}'_{c\ell} + \frac{1}{\beta}\ \underline{G}\ \underline{Q}\ \underline{G}'$$

Is $\underline{\Gamma}_{ss}$ acceptable ?

no

yes

Choose α and Solve for $\underline{\Gamma}_C$

$$\underline{\phi}\ \underline{\Gamma}_C\ \underline{\phi}' = \frac{\alpha}{1+\alpha}\ \underline{\Gamma}_{ss} - \alpha\ \underline{G}\ \underline{Q}\ \underline{G}'$$
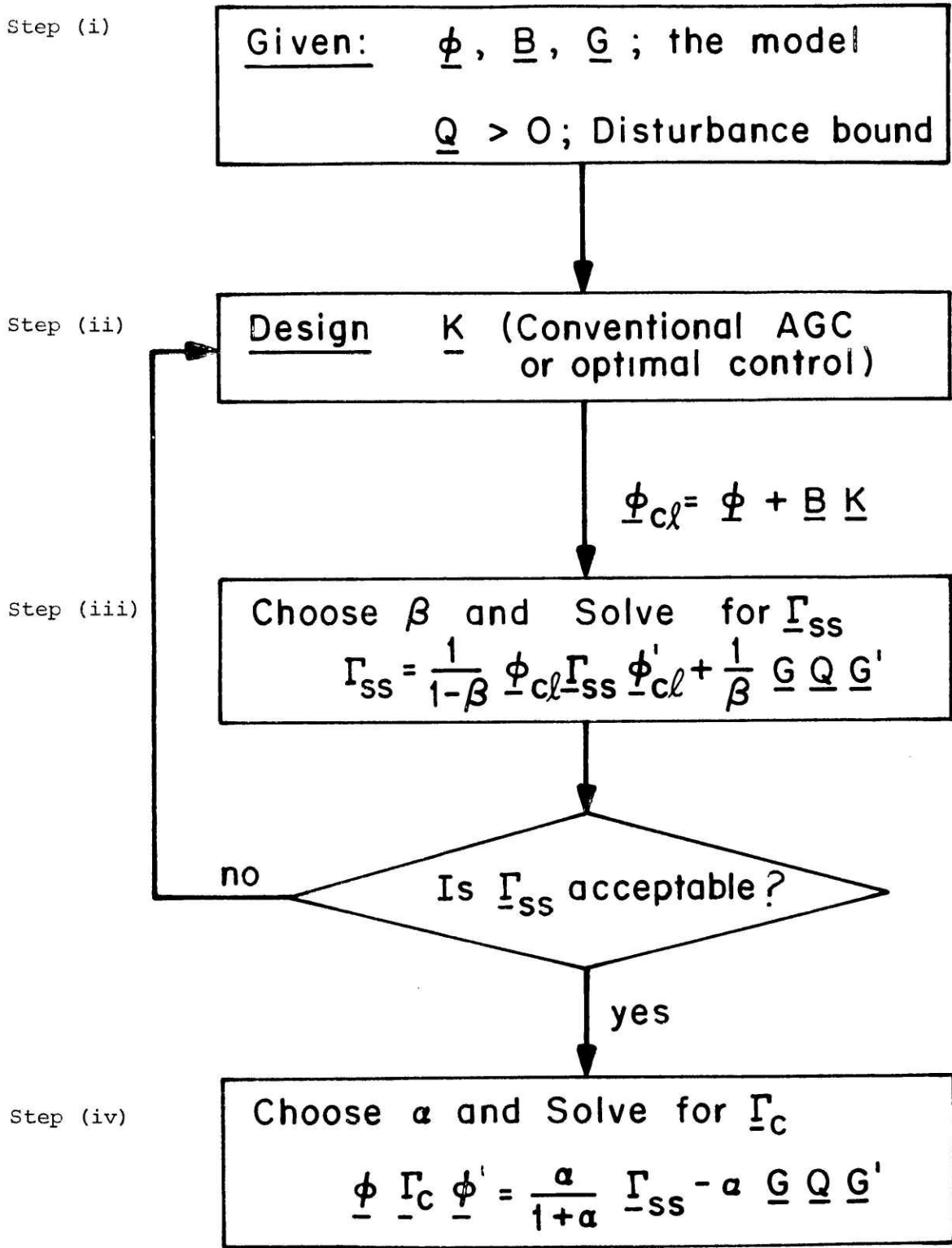
Figure 3-2   Summary of Design Procedure

Note the similarity between equation (3.11) and the discrete version of the algebraic Lyapunov equation where $\underline{\Gamma}_{ss}$ and $\underline{Q}$ would be covariance matrices rather than magnitude bounds. This similarity leads to the conclusion that equation (3.11) will have a unique positive definite solution $\underline{\Gamma}_{ss}$, if and only if [12]:

i) $\quad \left| \lambda_i\left(\frac{1}{\sqrt{1-\beta}} \underline{\Phi}_{c\ell} \right) \right| < 1 \qquad , \qquad i = 1, \ldots N_s$

ii) $\quad$ the pair $\left\{ \frac{1}{\sqrt{1-\beta}} \underline{\Phi}_{c\ell} , \underline{G} \right\} \quad$ is controllable

where β is of course chosen between 0 and 1.

As for equation (3.12), provided α is chosen properly (see previous discussion), it could always be solved for $\underline{\Gamma}_c$ since $\underline{\Phi}$ is a result of a discretization process and is, therefore, invertible; So:

$$\underline{\Gamma}_c = \underline{\Phi}^{-1} \left[\frac{\alpha}{1+\alpha} \underline{\Gamma}_{ss} - \alpha \underline{G} \underline{Q} \underline{G}' \right] \underline{\Phi}'^{-1}$$

The design procedure described in this section will now be tried on a simple two dimensional hypothetical system. The motivation for this, is that some of the ideas are based on geometrical arguments and a two dimensional example can be illustrated by exact figures. Those will give a better picture of what the equations derived above represent before they are applied to the fifteen dimensional model of chapter 2.

3.3 A Two Dimensional Example

Consider the hypothetical system given by the continuous time state variable model:

$$\underline{\dot{x}}(t) = \begin{bmatrix} \dot{x}_1(t) \\ \\ \dot{x}_2(t) \end{bmatrix} = \underline{A}\ \underline{x}(t) + \underline{B}_c u(t) + \underline{G}_c w(t)$$

where

$$\underline{A} = \begin{bmatrix} -2 & -1 \\ 1 & 0 \end{bmatrix} \quad , \quad \underline{B}_c = \begin{bmatrix} 1 \\ 0 \end{bmatrix} \quad , \quad \underline{G}_c = \begin{bmatrix} 0 \\ -1 \end{bmatrix}$$

Its structure was chosen to present as close features as possible to those of the model of figure 2.5. The first state takes the place of the first four states of a power plant and the second state that of the average system frequency deviation (or x_{13} in fig. 2-6). The control $u(t)$ and load disturbance $w(t)$, both scalars here, are applied accordingly.

A discrete time equivalent is now derived, lending itself to the control strategy described in this chapter. The discretization is done over a period Δ of two seconds and assuming $u(t)$ and $w(t)$ to be constant over this period of time. This is to duplicate the discretization which will be applied to the physical model in chapter 4 and where the assumptions will be discussed and physically justified.

i) $\underline{\Phi} = e^{\underline{A}\Delta} = \begin{bmatrix} -e^{-2} & -2e^{-2} \\ 2e^{-2} & 3e^{-2} \end{bmatrix} = \begin{bmatrix} -0.135 & -0.270 \\ 0.270 & 0.406 \end{bmatrix}$

$\underline{B} = \int_0^\Delta e^{\underline{A}(\Delta-\tau)} d\tau \begin{bmatrix} 1 \\ 0 \end{bmatrix} = \begin{bmatrix} 2e^{-2} \\ 1-3e^{-2} \end{bmatrix} = \begin{bmatrix} 0.270 \\ 0.594 \end{bmatrix}$

$\underline{G} = \int_0^\Delta e^{\underline{A}(\Delta-\tau)} d\tau \begin{bmatrix} 0 \\ -1 \end{bmatrix} = \begin{bmatrix} 1-3e^{-2} \\ 4e^{-2}-2 \end{bmatrix} = \begin{bmatrix} 0.594 \\ -1.46 \end{bmatrix}$

$\underline{Q}$ is here a scalar, arbitrarily chosen as $Q = 1$

$\underline{G}\,\underline{Q}\,\underline{G}' = \begin{bmatrix} 0.353 & -0.867 \\ -0.867 & 2.132 \end{bmatrix}$

ii) Since this example has no physical meaning, $\underline{K}$ is also chosen arbitrarily as $\underline{K} = [0 \ -1]$ for simplicity (the only requirement here is to keep $\underline{\Phi}_{c\ell}$ stable). Then

$\underline{\Phi}_{c\ell} = \underline{\Phi} + \underline{B}\,\underline{K} = \begin{bmatrix} -0.135 & -0.54 \\ 0.270 & -0.188 \end{bmatrix}$

iii) Again, choosing β arbitrarily to be 0.5

$$\underline{\Gamma}_{ss} \overset{\sim}{=} \begin{bmatrix} 3.73 & -0.78 \\ -0.78 & 5.34 \end{bmatrix}$$

Diagonalized, $\underline{\Gamma}_{ss}$ becomes

$$\begin{bmatrix} 3.41 & 0 \\ 0 & 5.65 \end{bmatrix}$$

where $\sqrt{\lambda_1} = \sqrt{3.41} = 1.85$ and $\sqrt{\lambda_2} = \sqrt{5.65} = 2.38$ are the lengths of the semimajor axes of $\Omega_{x,b}(ss)$

iv) $\underline{G} \underline{Q} \underline{G}'$ has rank 1

Diagonalized, it becomes

$$\begin{bmatrix} 0 & 0 \\ 0 & 2.49 \end{bmatrix} \qquad \text{where } \sqrt{\lambda_2} = \sqrt{2.49} = 1.58$$

In this problem both $\Omega_{x,b}$ and $\underline{G}\Omega_w$ have the same axis. So, from the geometrical discussion of the appendix,

$$\alpha < \frac{2.38}{1.58} - 1 \overset{\sim}{=} 0.51$$

Taking $\alpha = 0.5$

$$\underline{\Gamma}_c = \begin{bmatrix} 659 & -409 \\ -409 & 256 \end{bmatrix}$$

$\Omega_{x,b}(s)$, $\underline{G}\,\Omega_w$, $\underline{\Phi\Omega}_{c,b}$ and $\Omega_{c,b}$ are shown in figure 3.3.
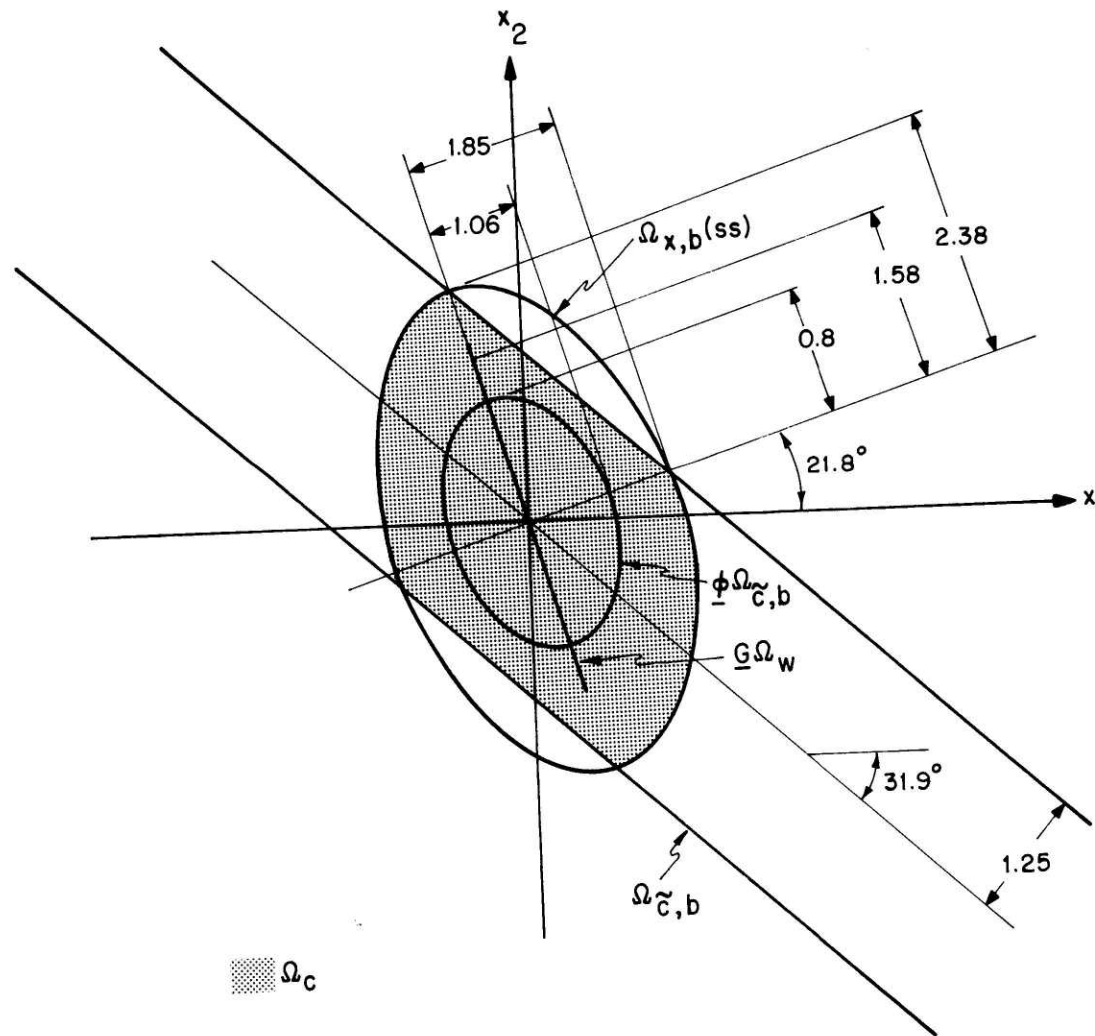
Figure 3-3   A Two Dimensional Example

C H A P T E R   4

DESIGN EXAMPLE AND RESULTS

4.1   Introduction

In this Chapter, the linear-plus-deadband control law discussed in
Chapter 3 is implemented and tested on the average system frequency model
of fig. 2-5. First a typical set of data is chosen and the continuous
time model is discretized. Then, a deadband set is designed using con-
ventional AGC first, and full state feedback second, for the linear part
of the control law. Simulations are run for both cases.

All along, computational problems are met and discussed. The computer
programs written, use subroutines from Sandell and Athans[14] as well as
modified versions thereof to accomodate the discrete nature of the problem.

4.2   Specific test system

4.2.1   Continuous time model

The hypothetical set of data to be used for the power plants is that
used by Grandez-Gomez [5] and is shown in figure 4-1. Power plants G_1 and
G_3 of the system described by figure 2-3 are given the same set of values
while power plant G_2 has a much smaller generating capacity as indicated
by its inertia coefficient. The system base is 100 MVA and, of course,

	K_1	K_2	T_1	T_1	T_V	T_S	R	M
G_1	0.2	0.25	10.5	6.0	0.45	0.4	0.01	15.6
G_2	0.2	0.25	10.5	6.0	0.45	0.4	0.06	2.4
G_3	0.2	0.25	10.5	6.0	0.45	0.4	0.01	15.6

Figure 4-1: Power Plant Data

Line	Y
ℓ_{12}	4.17
ℓ_{13}	4.17
ℓ_{23}	8.33
ℓ_{24}	8.33
ℓ_{34}	8.33

Figure 4-2: Transmission Line Admittances

60 Hz for frequency. Frequency and powers will therefore be expressed
in system p.u. values.

As mentioned above, the transmission lines are assumed to be modeled
by pure reactances. Lines ℓ_{12} and ℓ_{13} of the system given by figure 2-3
have the same length and double that of lines ℓ_{23}, ℓ_{24} and ℓ_{34}. The per
unit values of the line admittances are given in figure 4-2.

Refering to figure 2-5, matrices $\underline{A}$, $\underline{B}_c$ and $\underline{G}_c$ of the continuous time
model can be now evaluated and are given in figure 4-3. Note that due to
space limitation, the elements of $\underline{A}$ are printed out in the Fortran
(1PE8.1) Format and are therefore shown here rounded off.

A brief discussion of the model structure is useful at this point
and is motivated by the computational probems which are encountered
and described later in this section.

Recall that states x_{14} and x_{15} were only added to the model in view
of their eventual participation to the feedback control action. The
open-loop dynamics are therefore such that these two states do not couple
back into the system and, as a result, do not affect the controllability
of the remainder of the system.

Consider now the submatrix $\underline{A}_{13}$ obtained from the first thirteen rows
and columns of $\underline{A}$. Due to the similar power plant parameters, $\underline{A}_{13}$ is of
the form:

MATRIX A

```
-9.5D-02  0.0       0.0       1.6D-01   0.0       0.0       0.0       0.0       0.0       0.0       0.0       0.0       0.0       0.0       0.0
 0.0      -1.7D-01   0.0      -1.4D-01   0.0       0.0       0.0       0.0       0.0       0.0       0.0       0.0       0.0       0.0       0.0
 0.0       0.0      -2.2D+00   4.3D-01   0.0       0.0       0.0       0.0       0.0       0.0       0.0       0.0       0.0       0.0       0.0
 0.0       0.0       0.0      -2.5D+00   0.0       0.0       0.0       0.0       0.0       0.0       0.0       0.0      -2.5D+02   0.0       0.0
 0.0       0.0       0.0       0.0      -9.5D-02   0.0       0.0       1.6D-01   0.0       0.0       0.0       0.0       0.0       0.0       0.0
 0.0       0.0       0.0       0.0       0.0      -1.7D-01   0.0      -1.4D-01   0.0       0.0       0.0       0.0       0.0       0.0       0.0
 0.0       0.0       0.0       0.0       0.0       0.0      -2.2D+00   4.3D-01   0.0       0.0       0.0       0.0       0.0       0.0       0.0
 0.0       0.0       0.0       0.0       0.0       0.0       0.0      -2.5D+00   0.0       0.0       0.0       0.0      -4.2D+01   0.0       0.0
 0.0       0.0       0.0       0.0       0.0       0.0       0.0       0.0      -9.5D-02   0.0       0.0       1.6D-01   0.0       0.0       0.0
 0.0       0.0       0.0       0.0       0.0       0.0       0.0       0.0       0.0      -1.7D-01   0.0      -1.4D-01   0.0       0.0       0.0
 0.0       0.0       0.0       0.0       0.0       0.0       0.0       0.0       0.0       0.0      -2.2D+00   4.3D-01   0.0       0.0       0.0
 0.0       0.0       0.0       0.0       0.0       0.0       0.0       0.0       0.0       0.0       0.0      -2.5D+00  -2.5D+02   0.0       0.0
 3.0D-02   3.0D-02   3.0D-02   0.0       3.0D-02   3.0D-02   3.0D-02   0.0       3.0D-02   3.0D-02   3.0D-02   0.0       0.0       0.0       0.0
 0.0       0.0       0.0       0.0       0.0       0.0       0.0       0.0       0.0       0.0       0.0       0.0       1.0D+00   0.0       0.0
 5.4D-01   5.4D-01   5.4D-01   0.0      -4.6D-01  -4.6D-01  -4.6D-01   0.0      -4.6D-01  -4.6D-01  -4.6D-01   0.0       0.0       0.0       0.0
```

MATRIX BC

```
0.0           0.0           0.0
0.0           0.0           0.0
0.0           0.0           0.0
2.50000D+00   0.0           0.0
0.0           0.0           0.0
0.0           0.0           0.0
0.0           0.0           0.0
0.0           2.50000D+00   0.0
0.0           0.0           0.0
0.0           0.0           0.0
0.0           0.0           0.0
0.0           0.0           2.50000D+00
0.0           0.0           0.0
0.0           0.0           0.0
0.0           0.0           0.0
```

MATRIX GC

```
 0.0           0.0           0.0           0.0
 0.0           0.0           0.0           0.0
 0.0           0.0           0.0           0.0
 0.0           0.0           0.0           0.0
 0.0           0.0           0.0           0.0
 0.0           0.0           0.0           0.0
 0.0           0.0           0.0           0.0
 0.0           0.0           0.0           0.0
 0.0           0.0           0.0           0.0
 0.0           0.0           0.0           0.0
 0.0           0.0           0.0           0.0
 0.0           0.0           0.0           0.0
-2.97619D-02  -2.97619D-02  -2.97619D-02  -2.97619D-02
 0.0           0.0           0.0           0.0
-5.35714D-01   4.64286D-01   4.64286D-01   4.64286D-01
```

Figure 4-3

$$
\underline{A}_{13} =
\begin{bmatrix}
\underline{A}_4 & \underline{0} & \underline{0} & \underline{b} \\
\underline{0} & \underline{A}_4 & \underline{0} & \underline{c} \\
\underline{0} & \underline{0} & \underline{A}_4 & \underline{b} \\
\underline{a}' & \underline{a}' & \underline{a}' & 0
\end{bmatrix}
$$

with $\underline{a}'\ \underline{b} = \underline{a}'\ \underline{c} = 0$ and $\underline{b} = \alpha\underline{c}$ and where:

i) Blocks $\underline{A}_4$ are identical and describe the dynamics of the four individual power plant states.

ii) The 4-dimensional vectors $\underline{b}$ and $\underline{c}$ describe the effect of the average system frequency deviation on the power plant states.

iii) The last row describes the dynamics of the average system frequency deviation as affected by the power plant states.

Furthermore, the four load disturbances affect the system through x_{13}. They could be replaced by a single equivalent disturbance w with covariance (or in this case magnitude bound) computed appropriately such that $\underline{G}_{c,13}\Delta\underline{P}_L(n\Delta)$ is replaced by $\underline{G}_{c,13\ eq}w(n\Delta)$ and where

$$
\underline{G}_{c,13\ eq.} =
\begin{bmatrix}
\underline{0}_{12\times1} \\
1
\end{bmatrix}
$$

As a result,

$$\left[\; \underline{G}_{c,13\text{ eq.}} \;\vdots\; \underline{A}_{13}\,\underline{G}_{c,\,13\text{ eq.}} \;\vdots\; \underline{A}_{13}^{2}\,\underline{G}_{c,\,13\text{ eq.}} \;\vdots\; \cdots \;\vdots\; \underline{A}_{13}^{12}\,\underline{G}_{c,13\text{ eq}} \;\right]$$

$$\begin{bmatrix}
\underline{0} & \vdots & \underline{b} & \vdots & \underline{A}_4\,\underline{b} & \vdots & \underline{A}_4^{2}\,\underline{b} & \vdots & & \\
\underline{0} & \vdots & \underline{c} & \vdots & \underline{A}_4\,\underline{c} & \vdots & \underline{A}_4^{2}\,\underline{c} & \vdots & & \cdots \\
\underline{0} & \vdots & \underline{b} & \vdots & \underline{A}_4\,\underline{b} & \vdots & \underline{A}_4^{2}\,\underline{b} & \vdots & & \\
1 & \vdots & 0 & \vdots & 0 & \vdots & \underline{a}'\underline{A}_4(2\underline{b}+\underline{c}) & \vdots & &
\end{bmatrix}$$

is of rank 5 only (recall $\underline{b} = \alpha\underline{c}$) and the pair

$$\{\underline{A}_{13},\; \underline{G}_{c,\,13\text{ eq.}}\} \quad \text{is not controllable [12]}$$

Under these conditions, the continuous time model was discretized, and the design procedure described in chapter 3 was attempted. Details of such a development are treated later in this chapter. What is to be emphasized at this point, however, is that the resulting matrices $\underline{\Gamma}_{ss}$ and $\underline{\Gamma}_c$, which respectively determine ellipsoids $\Omega_{x,b}(ss)$ and $\Omega_{c,b}$ defined in chapter 3, were found to have a very large spread in their eigen-values, going down to extremely small values. Therefore, from a numerical point of view, the matrices were practically positive semi-definite and their inverses could not be properly evaluated. This also corresponds, from a geometrical point of view, to ellipsoids which are almost flat along some of their axis.

Now recall that the conditions for eq. (3.11) to have a positive definite solution $\underline{\Gamma}_{ss}$ are:

i) $\left| \lambda_i \left(\dfrac{1}{\sqrt{1-\beta}} \ \underline{\Phi}_{c\ell} \right) \right| < 1 , \qquad i = 1, \dots N_s$ (stability)

ii) the pair $\left\{ \dfrac{1}{\sqrt{1-\beta}} \ \underline{\Phi}_{c\ell}, \ \underline{G} \right\}$ or $\{ \underline{\Phi}_{c\ell}, \ \underline{G} \}$ is controllable.

As a result, it seems that in the present situation the closed loop system obtained by using a feedback control strategy retains some of the properties linked to the uncontrollability of the pair $\{\underline{A}, \underline{G}\}$ of the open loop system.

Furthermore, controllability is, in a strict sense, a Yes-No type of test without any comparative capabilities. Therefore, dissimilar power plant parameter values would make the blocks $\underline{A}_4$ mentioned above non-identical and the pair $\{\underline{A}, \underline{G}\}$ controllable. But since the parameters used here have typical values around which actual values would usually be found, the same computational problems are expected to arise if the parameters are varied.

Hence, those problems are actually related to the structure of the average system frequency model. This can be shown by a comparison with Glover's model [3] where individual machine frequencies are retained as state variables of the system. In this case load disturbances enter the model through each one of these states and the present computational problem is avoided.

Therefore, and in order to obtain numerically more robuste bounds, noise is artificially added to the models through all the previously undisturbed states. This will precisely "fatten" the ellipsoids of interest and increase the eigenvalues of $\underline{\Gamma}_{ss}$ and $\underline{\Gamma}_c$.

The new model has now matrix $\underline{G}_c$ as shown in figure 4-4. The disturbance vector is now labeled $\underline{w}$ as in chapter 3; ΔP_{L1}, of the initial model becomes w_{13} and $\Delta P_{L2}, \Delta P_{L3}, \Delta P_{L4}$ are implicitely replaced by the single equivalent disturbance w_{15}. This will be taken into account in the choice of matrix $\underline{Q}$ which determines the disturbance constraining ellipsoidal set Ω_w.

4.2.2 Discrete time model

As already mentioned in the introduction to chapter 3, because automatic generation control is a discrete time control law, and because simulations on a digital computer involve a discretization of continuous variables in any case, it was found natural in this context to convert the continuous time model to a discrete time model. The discretization time interval chosen is $\Delta = 2$ second, which is a typical value of the sampling rate for AGC, as presently used in the power industry. The control signal $\underline{u}(t)$ is therefore updated every 2 seconds and held constant over this period of time. For computational convenience, the disturbance vector $\underline{w}(t)$ is also considered to be constant over the same interval and the discrete time version is obtained as:

MATRIX GC

```
1.0D+00 0.0     0.0     0.0     0.0     0.0     0.0     0.0     0.0     0.0     0.0     0.0     0.0     0.0     0.0
0.0     1.0D+00 0.0     0.0     0.0     0.0     0.0     0.0     0.0     0.0     0.0     0.0     0.0     0.0     0.0
0.0     0.0     1.0D+00 0.0     0.0     0.0     0.0     0.0     0.0     0.0     0.0     0.0     0.0     0.0     0.0
0.0     0.0     0.0     1.0D+00 0.0     0.0     0.0     0.0     0.0     0.0     0.0     0.0     0.0     0.0     0.0
0.0     0.0     0.0     0.0     1.0D+00 0.0     0.0     0.0     0.0     0.0     0.0     0.0     0.0     0.0     0.0
0.0     0.0     0.0     0.0     0.0     1.0D+00 0.0     0.0     0.0     0.0     0.0     0.0     0.0     0.0     0.0
0.0     0.0     0.0     0.0     0.0     0.0     1.0D+00 0.0     0.0     0.0     0.0     0.0     0.0     0.0     0.0
0.0     0.0     0.0     0.0     0.0     0.0     0.0     1.0D+00 0.0     0.0     0.0     0.0     0.0     0.0     0.0
0.0     0.0     0.0     0.0     0.0     0.0     0.0     0.0     1.0D+00 0.0     0.0     0.0     0.0     0.0     0.0
0.0     0.0     0.0     0.0     0.0     0.0     0.0     0.0     0.0     1.0D+00 0.0     0.0     0.0     0.0     0.0
0.0     0.0     0.0     0.0     0.0     0.0     0.0     0.0     0.0     0.0     1.0D+00 0.0     0.0     0.0     0.0
0.0     0.0     0.0     0.0     0.0     0.0     0.0     0.0     0.0     0.0     0.0     1.0D+00 0.0     0.0     0.0
0.0     0.0     0.0     0.0     0.0     0.0     0.0     0.0     0.0     0.0     0.0     0.0     -3.0D-02 0.0    -3.0D-02
0.0     0.0     0.0     0.0     0.0     0.0     0.0     0.0     0.0     0.0     0.0     0.0     0.0     1.0D+00 0.0
0.0     0.0     0.0     0.0     0.0     0.0     0.0     0.0     0.0     0.0     0.0     0.0     -5.4D-01 0.0     4.6D-01
```

Figure 4-4

$$\underline{x}(n\Delta+\Delta) = \underline{\Phi}\ \underline{x}(n\Delta) + \underline{B}\ \underline{u}(n\Delta) + \underline{G}\ \underline{w}(n\Delta) \tag{4.1}$$

where (see [12], for example):

$$\underline{\Phi} = e^{\underline{A}\Delta}$$

$$\underline{B} = \left(\int_0^\Delta e^{\underline{A}\ (\Delta-\tau)}\ d\tau \right) \underline{B}_c$$

$$\underline{G} = \left(\int_0^\Delta e^{\underline{A}(\Delta-\tau)}\ d\tau \right) \underline{G}_c$$

are evaluated and shown in figure 4-5. The discretized version of the original matrix G_c (i.e. without the artificially added noise) is also evaluated. It will be used later in the simulations.

Furthermore the variables to be kept within limits are, as mentioned previously x_{13}, x_{14} and x_{15}. Therefore

$$\underline{y}(n\Delta) = \underline{H}\ \underline{x}(n\Delta)$$

where

$$\underline{H} = \left[\underline{0}_{3\times12}\ \vdots\ \underline{I}_{3\times3} \right]$$

and the steady state limits on $y_1 = x_{13}$, $y_2 = x_{14}$ and $y_3 = x_{15}$ are respectively given by the square root of the last three diagonal elements of $\underline{\Gamma}_{ss}$ (see section 3.2.3)

MATRIX PHI

```
 3.7D-01-4.4D-01-1.7D-01 2.9D-02-4.6D-01-4.4D-01-1.7D-01-2.5D-02-4.6D-01-4.4D-01-1.7D-01-2.5D-02-1.5D+01 0.0      0.0
 4.0D-01 1.1D+00 1.4D-01-2.2D-02 4.0D-01 3.8D-01 1.4D-01 2.2D-02 4.0D-01 3.8D-01 1.4D-01 2.2D-02 1.2D+01 0.0      0.0
-4.6D-01-4.3D-01-1.1D-01-1.7D-02-4.6D-01-4.3D-01-1.2D-01-2.5D-02-4.6D-01-4.3D-01-1.2D-01-2.5D-02-6.6D+00 0.0      0.0
-2.7D+00-2.5D+00-4.6D-01-1.3D-01-2.7D+00-2.5D+00-4.6D-01-1.3D-01-2.7D+00-2.5D+00-4.6D-01-1.3D-01-7.3D+00 0.0      0.0
-7.6D-02-7.3D-02-2.8D-02-4.2D-03 7.5D-01-7.3D-02-2.8D-02 5.0D-02-7.6D-02-7.3D-02-2.8D-02-4.2D-03-2.4D+00 0.0      0.0
 6.6D-02 6.3D-02 2.4D-02 3.7D-03 6.6D-02 7.8D-01 2.4D-02-4.0D-02 6.6D-02 6.3D-02 2.4D-02 3.7D-03 2.0D+00 0.0      0.0
-7.6D-02-7.2D-02-2.1D-02-4.1D-03-7.6D-02-7.2D-02-8.9D-03 3.6D-03-7.6D-02-7.2D-02-2.1D-02-4.1D-03-1.1D+00 0.0      0.0
-4.5D-01-4.2D-01-7.6D-02-2.2D-02-4.5D-01-4.2D-01-7.6D-02-1.5D-02-4.5D-01-4.2D-01-7.6D-02-2.2D-02-1.2D+00 0.0      0.0
-4.6D-01-4.4D-01-1.7D-01-2.5D-02-4.6D-01-4.4D-01-1.7D-01-2.5D-02 3.7D-01-4.4D-01-1.7D-01 2.9D-02-1.5D+01 0.0      0.0
 4.0D-01 3.8D-01 1.4D-01 2.2D-02 4.0D-01 3.8D-01 1.4D-01 2.2D-02 4.0D-01 1.1D+00 1.4D-01-2.2D-02 1.2D+01 0.0      0.0
-4.6D-01-4.3D-01-1.2D-01-2.5D-02-4.6D-01-4.3D-01-1.2D-01-2.5D-02-4.6D-01-4.3D-01-1.1D-01-1.7D-02-6.6D+00 0.0      0.0
-2.7D+00-2.5D+00-4.6D-01-1.3D-01-2.7D+00-2.5D+00-4.6D-01-1.3D-01-2.7D+00-2.5D+00-4.6D-01-1.3D-01-7.3D+00 0.0      0.0
 2.7D-02 2.4D-02 1.4D-03 1.1D-03 2.7D-02 2.4D-02 1.4D-03 1.1D-03 2.7D-02 2.4D-02 1.4D-03 1.1D-03-2.1D-01 0.0      0.0
 4.1D-02 3.9D-02 1.3D-02 2.2D-03 4.1D-02 3.9D-02 1.3D-02 2.2D-03 4.1D-02 3.9D-02 1.3D-02 2.2D-03 1.0D+00 1.0D+00  0.0
 9.8D-01 9.1D-01 2.4D-01 4.7D-02-8.4D-01-7.9D-01-2.1D-01-4.0D-02-8.4D-01-7.9D-01-2.1D-01-4.0D-02 1.1D-01 0.0      1.0D+00
```

MATRIX B

```
 1.93856D-01  -4.17893D-02  -4.17893D-02
-1.64646D-01   3.66683D-02   3.66683D-02
 1.29048D-01  -5.41678D-02  -5.41678D-02
 5.68730D-01  -4.24532D-01  -4.24532D-01
-6.96489D-03   2.28680D-01  -6.96489D-03
 6.11139D-03  -1.95202D-01   6.11139D-03
-9.02796D-03   1.74188D-01  -9.02796D-03
-7.07553D-02   9.22507D-01  -7.07553D-02
-4.17893D-02  -4.17893D-02   1.93856D-01
 3.66683D-02   3.66683D-02  -1.64646D-01
-5.41678D-02  -5.41678D-02   1.29048D-01
-4.24532D-01  -4.24532D-01   5.68730D-01
 5.56977D-03   5.56977D-03   5.56977D-03
 4.43758D-03   4.43758D-03   4.43758D-03
 1.36180D-01  -1.17680D-01  -1.17680D-01
```

MATRIX G

```
 1.5D+00-2.9D-01-1.4D-01 7.8D-02-3.0D-01-2.9D-01-1.4D-01-1.7D-02-3.0D-01-2.9D-01-1.4D-01-1.7D-02 4.9D-01 0.0      4.9D-01
 2.6D-01 2.0D+00 1.2D-01-6.6D-02 2.6D-01 2.6D-01 1.2D-01 1.5D-02-2.6D-01 1.5D-02-6.6D-02-4.2D-01 0.0      -4.2D-01
-3.9D-01-3.7D-01 2.8D-01 5.2D-02-3.9D-01-3.7D-01-1.7D-01-2.2D-02-3.9D-01-3.7D-01-1.7D-01-2.2D-02 4.9D-01 0.0      4.9D-01
-3.1D+00-2.9D+00-1.1D+00 2.3D-01-3.1D+00-2.9D+00-1.1D+00-1.7D-01-3.1D+00-2.9D+00-1.1D+00-1.7D-01 3.0D+00 0.0      3.0D+00
-5.0D-02-4.9D-02-2.4D-02-2.8D-03 1.8D+00-4.9D-02-2.4D-02 9.1D-02-5.0D-02-4.9D-02-2.4D-02-2.8D-03 8.1D-02 0.0      8.1D-02
 4.4D-02 4.3D-02 2.1D-02 2.4D-03 4.4D-02 1.7D+00 2.1D-02-7.8D-02 4.4D-02 4.3D-02 2.1D-02 2.4D-03-7.0D-02 0.0      -7.0D-02
-6.4D-02-6.2D-02-2.8D-02-6.4D-03-6.4D-02-6.2D-02 2.8D-02-3.6D-03 8.2D-02 0.0      8.2D-02
-5.1D-01-4.9D-01-1.9D-01-2.8D-02-5.1D-01-4.9D-01-1.9D-01 3.7D-01-5.1D-01-4.9D-01-1.9D-01-2.8D-02 5.0D-01 0.0      5.0D-01
-3.0D-01-2.9D-01-1.4D-01-1.7D-02-3.0D-01-2.9D-01-1.4D-01-1.7D-02 1.5D+00-2.9D-01-1.4D-01 7.8D-02 4.9D-01 0.0      4.9D-01
 2.6D-01 2.6D-01 1.2D-01 1.5D-02 2.6D-01 2.6D-01 1.2D-01 2.0D+00 1.2D-01-6.6D-02-4.2D-01 0.0      -4.2D-01
-3.9D-01-3.7D-01-1.7D-01-2.2D-02-3.9D-01-3.7D-01-1.7D-01-2.2D-02-3.9D-01-3.7D-01 2.8D-01 5.2D-02 4.9D-01 0.0      4.9D-01
-3.1D+00-2.9D+00-1.1D+00-1.7D-01-3.1D+00-2.9D+00-1.1D+00-1.7D-01-3.1D+00-2.9D+00-1.1D+00 2.3D-01 3.0D+00 0.0      3.0D+00
 4.1D-02 3.9D-02 1.3D-02 2.2D-03 4.1D-02 3.9D-02 1.3D-02 2.2D-03 3.9D-02 1.3D-02 2.2D-03-3.1D-02 0.0      -3.1D-02
 3.2D-02 3.1D-02 1.4D-02 1.8D-03 3.2D-02 3.1D-02 1.4D-02 1.8D-03 3.2D-02 3.1D-02 1.4D-02 1.8D-03-4.4D-02 2.0D+00-4.4D-02
 1.0D+00 9.6D-01 3.8D-01 5.4D-02-8.7D-01-8.3D-01-3.2D-01-4.7D-02-8.7D-01-8.3D-01-3.2D-01-4.7D-02-1.1D+00 0.0      9.3D-01
```

Figure 4-5

4.2.3. Disturbance bound

Refering to the discussion in chapter 3, the perturbation vector $\underline{w}(n\Delta)$ is considered to be a discrete time white unknown but bounded process.

A time invariant ellipsoidal bound:

$$\Omega_w = \{ \ \underline{w}(n\Delta) \ : \ \underline{w}'(n\Delta) \ \underline{Q}^{-1} \ \underline{w}(n\Delta) \leq 1, \ \forall n \ \}$$

is therefore chosen, where $\underline{Q}$ is a diagonal positive definite matrix, and where the diagonal elements determine the magnitude of the perturbations. [10].

In the power system model considered here, the four loads are assumed to be of the same order of magnitude (around 0.7 p.u. MW) and their perturbations to be limited in magnitude to roughly 3%, or $\left|\Delta P_{L_i}\right|^2 < 5\times10^{-4}$. For future reference, note that a load change of 0.02 pu is large compared to changes usually observed. This value was first chosen for computational convenience in an attempt to correct for the flat ellipsoids resulting from the original model. It was left unchanged when the artificial noise was added as discussed in section 4.2.1.

As for the magnitude bound of the thirteen added disturbances, the corresponding diagonal elements of $\underline{Q}$, q, had to be increased up to around 5×10^{-8} before obtaining numerically reasonable bounds. This value will be further increased to study its effect on the design results.

At this point, step (i) of the design procedure, as summarized in figure 3-2, is completed and the procedure is carried on using either one of the two proposed alternatives.

4.3 Conventional AGC

4.3.1 General description

The basic features of conventional AGC are widely presented and motivated, in the literature (e.g. [1], [3]) and can be summarized here as follows:

Each area i of an interconnected power system computes its area control error (ACE_i):

$$ACE_i(t) = \Delta P_{tie_i}(t) + B_i \Delta f_i(t)$$

where $\Delta P_{tie_i}(t)$ is the net deviation from scheduled values of tie-line power flow out of the area.

$\Delta f_i(t)$ is the deviation (from scheduled frequency) of the area frequency.

B_i is a frequency bias coefficient usually chosen to match the area frequency response characteristic.

Then, in each area, the control law u(t) is a piecewise constant function which is proportional to the integral of the ACE

$$\begin{cases} \text{IACE}_i(t) = \int_0^t \text{ACE}_i(\tau)\,d\tau & (4.2) \\ \\ \underline{u}_i(t) = -\underline{K}_i\,[\text{IACE}_i(n\Delta)] & (4.3) \\ \\ n\Delta \leq t < (n+1)\Delta \qquad ; \Delta = 2 \text{ seconds} \end{cases}$$

It is this control law which constitutes the basis for the choice of the discretization interval of section 4.2.2.

4.3.2. Design:

Refering to the model used here, only the average system frequency is assumed to prevail throughout the system. As a result, for both areas considered, $\Delta f_i(t)$ is replaced by $\Delta f_{av}(t)$. Moreover, form the configuration of the system at hand (shown in fig. 2-3)

$$\Delta P_{tie_1}(t) = -\Delta P_{tie_2}(t)$$

So that, using the terminology of fig. 2-6, (4.2) can be written as:

$$\begin{cases} \text{IACE}_1(t) = x_{15}(t) + B_1 x_{14}(t) \\ \\ \text{IACE}_2(t) = -x_{15}(t) + B_2 x_{14}(t) \end{cases} \qquad (4.4)$$

And the control law (4.3) becomes:

$$\left\{ \begin{array}{l} u_1(t) = - K_1 \ [\ x_{15}(n\Delta) + B_1 x_{14}(n\Delta) \ ] \\[2mm] u_1(t) = - K_2 \ [\ -x_{15}(n\Delta) + B_2 x_{14}(n\Delta) \ ] \\[2mm] u_3(t) = - K_3 \ [\ -x_{15}(n\Delta) + B_2 x_{14}(n\Delta) \ ] \\[4mm] \qquad n \ \Delta \ \leq t < (n+1)\Delta \end{array} \right. \qquad (4.5)$$

or, in terms of step (ii) of the design procedure

$$\underline{u}(n\Delta) = \underline{K} \ \underline{x}(n\Delta) \qquad\qquad (4.6)$$

where

$$\underline{K} = \left[\begin{array}{c|c|c} & -K_1 B_1 & -K_1 \\ \underline{0} \ _{3\times 13} & -K_2 B_2 & K_2 \\ & -K_3 B_2 & K_3 \end{array} \right]$$

Since a typical value for the area frequency response characteristic under normal conditions is about ten per cent of total power generation per Hz [3], and since the generating capacities of both areas are not too different, B_1 and B_2 are both chosen as:

$$B_1 = B_2 = 0.13 \times 60 \stackrel{\sim}{-} 8 \ \text{pu MW/pu Hz}$$

Moreover, the proportionality constants are also chosen to be the same for both areas with the AGC in area 2 to be allocated to power plants

G_2 and G_3 according to their relative capacities, i.e.

$$\begin{cases} K_2 = 0.13\ K_1 \\ K_3 = 0.87\ K_1 \end{cases}$$

Now, in view of eq. 3.11 (to be solved in step (iii)) it was shown in Chapter 3 that a necessary contition for a positive definite solution $\underline{\Gamma}_{ss}$ to exist, is that

$$\left| \lambda_i \left(\frac{1}{\sqrt{1-\beta}}\ \underline{\Phi}_{c\ell} \right) \right| < 1 \quad , \quad i=1, \ldots 15 \tag{4.7}$$

where $\lambda_i(\underline{x})$ denotes the ith eigenvalue of $\underline{x}$

(β is chosen between 0 and 1)

$\underline{\Phi}_{c\ell} = \underline{\Phi} + \underline{B}\ \underline{K}$ is the closed loop matrix with $\underline{K}$ given by (4.6)

A root locus study is therefore conducted, where the eigenvalues of $\underline{\Phi}_{c\ell}$ are computed and plotted on the complex plane for several values of K_1 starting with $K_1 = 0$ (no feedback). Only the dominant eigenvalues are shown in fig. 4-6.

$$\text{Since } \left| \lambda_i \left(\frac{1}{\sqrt{1-\beta}}\ \underline{\Phi}_{c\ell} \right) \right| = \frac{1}{\sqrt{1-\beta}}\ \left| \lambda_i(\underline{\Phi}_{c\ell}) \right| \quad ,$$

condition (4.7) is satisfied if all eigenvalues corresponding to one value
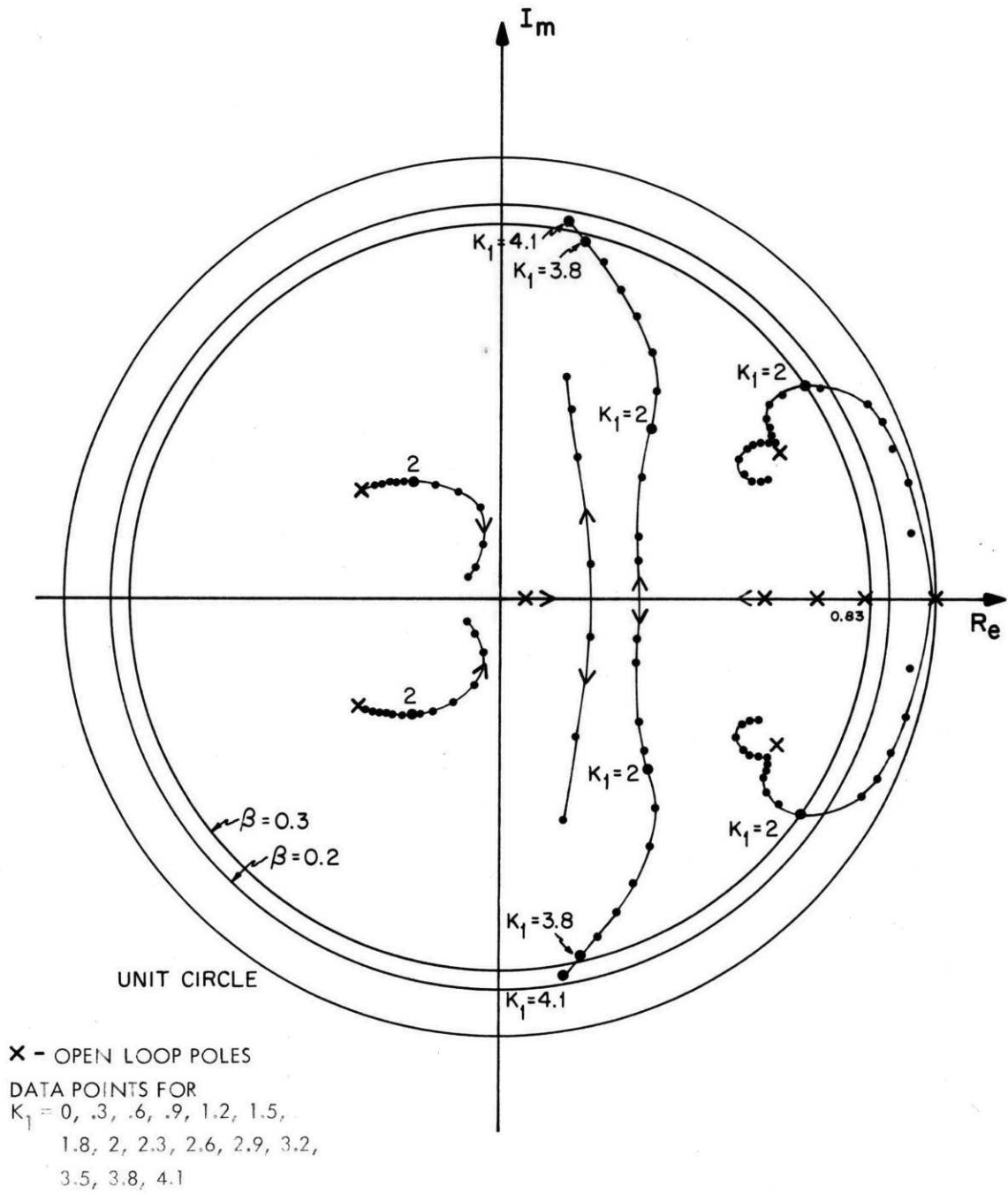
Figure 4-6

Eigenvalues of $\underline{\Phi}_{c\ell}$ for Different values of K_1

of K_1 lie within the circle of radius $\sqrt{1-\beta}$. Fig. 4-6 shows that, due to the fixed pole at 0.83, β should not exceed 0.3 and that acceptable values for K_1 are, for example:

$$2 < K_1 < 4 \qquad \text{for} \qquad \beta = 0.2 \left.\begin{array}{c} \\ \\ \end{array}\right\}$$
$$2.4 < K_1 < 3.8 \qquad \text{for} \qquad \beta = 0.3$$

(4.8)

At this point, Eq. (3.11) is solved using the matrix $\underline{G}$ which corresponds to the actual model of Chapter 2, and K_1 taking several values which span the limits given by (4.8). The values which minimize the steady state limits on:

$$\underline{y} = \underline{H}\,\underline{x}$$

or, equivalently the last three diagonal elements of $\underline{\Gamma}_{ss}$ (see section 4.2.2) are the values of K_1 and β which are retained.

In other words K_1 is chosen such that $\Omega_{x,b|y}(ss;\underline{K})$ defined in chapter 3, is roughly minimized rather than made to fit some specified Ω_y as ideally suggested. This approach is used here because the load disturbances bounds, chosen in section 4.2.3, are larger than in actual situations and the degree of freedom in the design of $\underline{K}$ is much narrower.

The square roots of the last three diagonal elements of $\underline{\Gamma}_{ss}$ are shown in figure 4-7 for different values of K_1 and β. A good compromise is for:

$$K_1 = 2.6 \qquad ; \qquad \beta = 0.3$$

	K_1	$\Delta f_{av} \times 10^3$ Max,b	$\delta \times 10^3$ Max,b	$\int \Delta P_{tie}$ Max,b
$\beta=0.2$	2.0	4.65	6.97	0.242
	2.2	4.73	7.0	0.21
	2.4	4.82	7.1	0.2
	2.6	4.9	7.15	0.19
	2.8	4.99	7.21	0.186
	3.0	5.0	7.28	0.187
	3.2	5.19	7.35	0.192
	3.4	5.3	7.43	0.2
	3.6	5.41	7.52	0.217
	3.8	5.54	7.62	0.242
	4.0	5.68	7.73	0.288
$\beta=0.3$	2.4	4.17	6.58	0.217
	2.6	4.25	6.62	0.194
	2.8	4.34	6.66	0.186
	3.0	4.43	6.7	0.188
	3.2	4.52	6.74	0.199
	3.4	4.63	6.8	0.266
	3.6	4.73	6.88	0.288
	3.8	4.87	6.96	0.198

Figure 4-7

Square root of last three diagonal elements of Γ_{ss} for different values

of K_1 and β

for which the steady state limits on Δf_{av}, $\Delta \delta_{av}$ and $\int \Delta P_{tie}$ are

$\pm 4.25 \times 10^{-3}$, $\pm 6.62 \times 10^{-3}$ and ± 0.194 respectively (in p.u).

Note that those limits are bounds on the actual limits because of the conservation inherent to the bounding process in which a bounding ellipsoid is used for the actual steady state set [Section 3.2.3]. As a matter of fact, in the simulations to be presented later, Δf_{av}, for example did not exceed $\pm 2 \times 10^{-3}$pu or ± 0.12 Hz. As expected, this value is still larger than in real situations but since the model is linear, scaled down results would be obtained with more realistic conditions; and since the main object here is the study of the deadband control effect, the same general conclusions would still be valid.

Using now $\underline{\Gamma}_{ss}$, obtained from eq. (3.11) with the modified matrix $\underline{G}$ and the selected values of K_1 and β, eq. (3.12) of step (iv) is solved with α taking several values, starting with $\alpha = 0.2$. Rather than computing directly the upper limit of α as suggested in Section 3.2.3, the iterations are simply stopped when the solution $\underline{\Gamma}_c$, which determines $\Omega_{c,b}$ defined in Chapter 3, becomes indefinite (see geometric interpretation in Section 3.2.3 and Appendix).

The eigenvalues of $\underline{\Gamma}_c$ for the different values of α are given in fig. 4-8.

The deadband sets defined by those matrices $\underline{\Gamma}_c$ intersect one another and it is no simple task to find the largest one of them. Moreover there

α	$\lambda_1 \times 10^{-3}$	$\lambda_2 \times 10^{-3}$	$\lambda_3 \times 10^2$	$\lambda_4 \times 10^2$	$\lambda_5 \times 10^2$	$\lambda_6 \times 10^3$	$\lambda_7 \times 10^3$	$\lambda_8 \times 10^4$	$\lambda_9 \times 10^4$	$\lambda_{10} \times 10^5$	$\lambda_{11} \times 10^5$	$\lambda_{12} \times 10^5$	$\lambda_{13} \times 10^6$	$\lambda_{14} \times 10^7$	$\lambda_{15} \times 10^7$
0.2	3.4	2.0	7.2	2.4	0.65	1.1	0.76	4.7	0.98	3.1	1.9	0.65	0.65	2.2	0.74
0.4	5.8	3.5	12.3	3.9	1.1	1.7	1.3	7.3	1.7	5.3	3.0	1.1	1.1	3.5	1.2
0.6	7.7	4.5	16.1	4.7	1.5	2.2	1.7	8.7	2.2	6.9	3.5	1.5	1.4	4.3	1.4
0.8	9.1	5.3	19.1	5.2	1.7	2.5	2.0	9.1	2.6	8.1	3.7	1.7	1.7	4.7	1.5
1.0	10.2	5.9	21.4	5.4	1.9	2.7	2.3	9.0	2.9	9.1	3.6	1.9	1.8	4.9	1.4
1.2	11.1	6.3	23.3	5.3	2.1	2.8	2.5	8.4	3.2	9.8	3.4	2.1	2.0	4.9	1.4
1.4	11.9	6.7	24.9	5.1	2.2	2.8	2.6	7.4	3.4	10.4	3.0	2.3	2.1	4.8	1.2
1.6	12.5	7.0	26.2	4.8	2.4	2.9	2.6	6.1	3.6	10.9	2.4	2.5	2.2	4.5	1.0
1.8	13.0	7.3	27.3	4.4	2.4	3.0	2.3	4.7	3.7	11.3	1.9	2.5	2.2	4.2	0.79
2.0	13.5	7.5	28.3	3.9	2.5	3.1	1.8	3.9	3.0	11.7	1.3	2.6	2.3	3.7	0.52
2.2	13.9	7.6	29.1	3.4	2.4	3.2	0.92	4.0	1.3	11.7	0.56	2.7	2.3	3.2	0.22

Non-positive solution for $\alpha \geq 2.4$

Figure 4-8 Eigenvalues of $\underline{\Gamma}_c$ for Different Values of α

is no obvious definition of what would be the largest. Therefore, and because the eigenvalues are an indication of the "thickness" of the ellipsoids at hand, a good compromise is found to be $\alpha = 1.6$

The four steps are now completed for a conventional controller and the whole set of results is given in fig. 4-9.

4.3.3. Simulations

A simulation is performed using the original model (i.e without the added noise)but with the matrices $\underline{\Gamma}_{ss}$ and $\underline{\Gamma}_{c}$ derived in the previous section (i.e. for the model with artificially added noise).

A random number generator is used to model the discrete time load disturbances. Since those were assumed to be only unknown but bounded, the standard deviation of the random numbers is chosen as the disturbance magnitude bound reduced by a factor of three. Moreover, the same load disturbance sequence is used in all the subsequent simulations.

Following the deadband logic described in section 3.2.3, the state $\underline{x}$ of the system is tested at every step of 2 seconds. A first test insures that $\underline{x}(n\Delta)$ is indeed within the steady state set $\Omega_{x,b}(ss)$ (Numerically: $\underline{x}' \underline{\Gamma}_{ss}^{-1} \underline{x} \le 1$), and a second test investigates wether $\underline{x}(n\Delta)$ lies in the deadband region $\Omega_{c,b}^{v}$ (Numerically $\underline{x}' \underline{\Gamma}_{c}^{-1} \underline{x} \le 1$) or not. Then, open loop $\underline{\Phi}$ or closed loop $\underline{\Phi}_{cl}$ is used for the next iteration accordingly. The outcome is shown in fig. 4-10 for 50 steps (100 seconds) and where:

K1= 2.6CCCCC   BETA= C.300000

MATRIX PHICL

```
  3.7D-01-4.4D-01-1.7C-01 2.9D-02-4.6D-01-4.4D-C1-1.7D-01-2.5D-02-4.6D-01-4.4D-01-1.7D-01-2.5C-02-1.5D+01-3.2D+00-6.1D-01
  4.0D-01 1.1D+00 1.4D-C1-2.2D-02 4.0D-01 3.8C-01 1.4C-01 2.2D-02 4.0D-01 3.8D-01 1.4D-01 2.2D-02 1.2D+01 2.7D+00 5.2D-01
 -4.6D-01-4.3D-01-1.1D-01-1.7D-02-4.6D-01-4.3D-01-1.2D-01-2.5D-02-4.6D-01-4.3D-01-1.2D-01-2.5D-02-6.6D+00-1.6D+00-4.8D-01
 -2.7D+00-2.5D+00-4.6C-01-1.3C-01-2.7D+00-2.5C+00-4.6D-01-1.3D-01-2.7D+00-2.5D+00-4.6D-01-1.3D-01-7.3D+00-3.0D+00-2.6D+00
 -7.6D-02-7.3D-02-2.8C-02-4.2D-03 7.5D-01-7.3C-02-2.8D-02 5.0D-02-7.6D-02-7.3D-02-2.8D-02-4.2D-03-2.4D+00-3.5D-01 8.0D-02
  6.6D-02 6.3D-02 2.4C-02 3.7D-03 6.6D-02 7.8C-01 2.4C-02-4.0D-02 6.6D-02 6.3D-02 2.4D-02 3.7D-03 2.0D+00 2.9D-01-6.8D-02
 -7.6D-02-7.2D-C2-2.1D-02-4.1D-03-7.6D-02-7.2C-02-8.9D-03 3.6D-03-7.6D-02-7.2D-02-2.1D-02-4.1D-03-1.1D+00-1.2D-01 6.2D-02
 -4.5D-C1-4.2D-01-7.6D-02-2.2D-02-4.5D-01-4.2C-01-7.6D-02-1.5D-02-4.5D-01-4.2D-01-7.6D-02-2.2D-02-1.2D+00 2.6D-01 3.4D-01
 -4.6D-01-4.4C-01-1.7D-01-2.5C-02-4.6D-01-4.4C-01-1.7D-01-2.5D-02 3.7D-01-4.4D-01-1.7D-01 2.9D-02-1.5D+01-2.5D+00 5.3D-01
  4.CD-01 3.8C-01 1.4C-01 2.2D-02 4.0D-01 3.8C-01 1.4C-01 2.2D-02 4.0D-01 1.1D+00 1.4C-01-2.2D-02 1.2D+01 2.1D+00-4.6D-01
 -4.6D-01-4.3C-01-1.2D-01-2.5C-02-4.6D-01-4.3D-01-1.2D-01-2.5D-02-4.6D-01-4.3D-01-1.1D-01-1.7D-02-6.6D+00-1.1D+00 4.1D-01
 -2.7D+00-2.5D+00-4.6D-01-1.3C-01-2.7D+00-2.5C+00-4.6D-01-1.3D-01 2.7D+30-2.5D+00-4.6D-01-1.3D-01-7.3D+00-3.1D+01 2.2D+00
  2.7D-C2 2.4D-C2 1.4D-03 1.1D-03 2.7D-02 2.4C-02 1.4D-03 1.1D-03 2.7D-02 2.4D-02 1.4D-03 1.1D-03-2.1D-01-2.3D-01-5.5D-17
  4.1D-02 3.9D-02 1.3D-C2 2.2D-03 4.1D-02 3.9C-02 1.3D-02 2.2D-03 4.1D-02 3.9D-02 1.3D-02 2.2D-03 1.0D+00 8.2D-01-2.8D-16
  5.8D-C1 9.1D-01 2.4D-01 4.7D-02-8.4D-01-7.9C-01-2.1D-01-4.0D-02-8.4D-01-7.9D-01-2.1D-01-4.0D-02 1.1D-01-3.8D-01 3.4D-01
```

MATRIX EIGENVALUES

```
REAL PART =  3.446459853787491D-01 IMAG PART =  5.648228978353557C-01
REAL PART =  3.446459853787491D-01 IMAG PART = -5.648228978353557D-01
REAL PART = -1.449208404453163C-01 IMAG PART =  2.489717698435161C-01
REAL PART = -1.449208404453163C-01 IMAG PART = -2.489717698435161C-01
REAL PART =  6.125174074758821C-01 IMAG PART =  4.2530283217700000D-01
REAL PART =  6.125174074758821D-01 IMAG PART = -4.2530283217700000D-01
REAL PART =  5.584395361058455C-01 IMAG PART =  3.347440986174156D-01
REAL PART =  5.584395361058455D-01 IMAG PART = -3.347440986174156D-01
REAL PART =  8.265654376242287D-01 IMAG PART =  0.0
REAL PART =  5.843350969462364C-01 IMAG PART =  0.0
REAL PART = -1.278349591097853C-02 IMAG PART =  0.0
REAL PART =  3.248145186005524C-02 IMAG PART =  0.0
REAL PART =  6.737946990085457D-03 IMAG PART =  0.0
REAL PART =  7.165313105737847D-01 IMAG PART =  0.0
REAL PART =  1.174362845702136C-02 IMAG PART =  0.0
```

MATRIX GAMMA

```
  4.9D-02-4.2D-02 7.5D-03 2.8D-02-5.0D-03 4.1D-03-9.7D-05-1.1D-03-3.4D-02 2.8D-02-9.8D-04-8.1D-03-1.6D-05-4.3D-04 2.4D-02
 -4.2D-02 3.8D-02-1.00D-02-4.4D-02 4.5D-03-3.9C-03 4.9D-04 3.0D-03 3.1D-02-2.7D-02 3.6D-03 2.1D-03 4.5D-05 3.6D-04-1.7D-02
  7.5D-03-1.0C-02 1.6C-02 8.5C-02-1.5D-03 1.6C-03-1.2D-03 1.8D-03-9.8D-03 1.1D-02-8.4D-03-4.2D-02-2.5D-04-1.8D-05-9.1D-03
  2.8D-02-4.4C-02 8.5D-02 4.8D-C1-8.1D-03 9.1C-03-6.5C-03-2.9D-02-5.3D-02 6.0D-02-4.6D-02-2.1D-01-1.7D-03 3.2D-04-5.5D-02
 -5.0D-03 4.5C-03-1.5D-03-8.1C-03 1.3D-01 3.4C-03 1.6D-04 5.9D-04 8.1D-03-7.0D-03 1.1D-03 4.5D-03 5.1D-05-1.00-04-2.2D-03
  4.1D-03-3.9D-03 1.6D-03 9.1C-03-1.1D-03 9.6C-04-2.3D-04-9.7D-04-6.9D-03 6.2D-03-1.6D-03-6.9D-03-3.9D-05 1.1D-04 1.0D-03
 -9.7D-05 4.9D-04-1.2D-03-6.5D-03 1.6D-04-2.3D-04 3.0D-04 1.5D-03 9.5D-04-1.4D-03 1.9D-03 9.9D-03-1.7D-05-5.8D-05 2.1D-03
 -1.1D-03 3.0D-03-5.8C-03-2.9C-02 5.9D-04-9.7C-04-1.5D-03 8.2D-03 3.5D-03-6.1D-03 9.8D-03 5.3D-02-1.5D-02-2.4D-04 1.1D-02
 -3.4D-02 3.1D-C2-9.8D-03-5.3D-02 8.1D-03-6.9C-03 9.5D-04 3.5D-03 5.3D-02-4.5D-02 6.9D-03 2.7D-02 3.3D-04-6.2D-04-1.5D-02
  2.8D-02-2.7D-02 1.1D-C2 6.00-02-7.0D-03 6.2C-03-1.4D-03-6.1D-03-4.5D-02 4.1D-02-9.9D-03-4.3D-02-2.6D-04 6.5D-04 7.6D-03
 -9.8D-04 3.6D-03-8.4D-03-4.6D-02 1.1D-03-1.6C-03 1.9D-03 9.8D-03 6.9D-03-9.9D-03 1.3D-02 6.5D-02-8.8D-05-3.8D-04 1.3D-02
 -8.1D-03 2.1D-02-4.2D-02-2.1D-01 4.5D-03-6.9C-03 9.9D-03 5.3D-02 2.7D-02-4.3D-02 6.5D-02 3.5D-01-1.8-04-1.6D-03 7.0D-02
 -1.6D-05 4.5D-05-2.5D-04-1.7C-03 5.1D-05-3.9C-05-1.7D-05-1.5D-04 3.3D-04-2.6D-04-8.8D-05 8.2D-04 1.8D-05-2.2D-06-7.0D-05
 -4.3D-04 3.6D-04-1.8C-05 3.2D-04-1.0D-04 1.1C-04-5.8C-05-2.4D-04-6.2D-04 6.5D-04-3.8D-04-1.6D-03-2.2D-06 4.5D-05-4.0D-04
  2.4D-02-1.7C-02-9.1C-03-5.5D-02-2.2D-03 1.0D-03 2.1D-03 1.1D-02-1.5D-02 7.6D-03 1.3D-02 7.0D-02-7.0D-05-4.0D-04 3.7D-02
```

ALPHA= 1.630000

DEADBAND SET GAMDB

```
  2.2D+01-2.0D+01 1.7D+02-3.7D+02-1.3D+00 1.2C+00-1.3D+01 1.4D+01-9.3D+00 8.6D+00-8.8D+01 1.0D+02-5.8D-01 1.6D-01-4.4D+01
 -2.0D+01 1.9D+01-1.6D+02 3.4D+02 1.2D+30-1.1C+00 1.2D+01-1.3D+01 8.6D+00-8.0D+00 8.1D+01-9.4D+01 5.3D-01-1.5D-01 4.0D+01
  1.7D+02-1.6D+02 1.4D+03-2.9D+03-1.5D+01 1.4D+01-1.4D+02 2.0D+02-1.0D+02 9.6D+01-9.2D+02 1.4D+03-2.8D+00 7.8D-01-3.9D+02
 -3.7D+02 3.4D+02-2.9D+03 6.8D+03 6.4D+3C-5.8C+00 9.8C+01 9.5D+01 5.3D+01-4.9D+01 7.1D+02 3.5D+02 1.6D+01-4.5D+00 6.0D+02
 -1.3D+00 1.2D+00-1.5C+01 6.4C+00-7.2D-01-6.7C-01 5.5D+00-1.4D+01 4.7D+00-4.3D+00 3.6D+01-8.7D-01-2.1D-01 5.8D-02 8.6D+00
  1.2D+00-1.1D+C0 1.4D+01-5.8D+00-6.7D-01 6.2C-01-5.1D+00 1.3D+01-4.3C+00 4.0D+00-3.3D+01 8.1D+01 1.9D-01-5.4D-02-8.0D+00
 -1.3D+C1 1.2D+01-1.4D+02 9.8D+01 5.5D+30-5.1D+00 4.2D+01-1.0D+02 3.6D+01-3.3D+01 2.8D+02-6.6D+02-1.5D+00 4.1D-01 7.0D+01
  1.4D+01-1.3D+01 2.0D+02 9.5D+01-1.4D+01 1.3C+01-1.0D+02 2.6D+02-8.8D+01 8.1D+01-6.7D+02 1.7D+03 4.5D+00-1.3D+00-1.5D+02
 -9.3D+00 8.6D+00-1.0C+02 5.3D+01 4.7D+00-4.3D+00 3.6D+01-8.8D+01 3.1D+01-2.8D+01 2.4D+02-5.7D+02-1.3D+00 3.7D-01 5.7D+01
  8.6D+3C-8.0D+00 9.6D+01-4.9D+01-4.3D+30 4.0D+00-3.3D+01 8.1D+01-2.8D+01 2.6D+01-2.2D+02 5.2D+02 1.2D+00-3.4D-01-5.3D+01
 -8.8D+01 8.1D+01-9.2D+02 7.1C+02 3.6D+01-3.3C+01 2.8D+02-6.7D+02 2.4D+02-2.2D+02 1.8D+03-4.3D+03-9.5D+00 2.6D+00 4.6D+02
  1.0D+02-9.4D+01 1.4D+03 3.5D+02-8.7D+01 8.1C+01-6.6C+02 1.7D+03-5.7D+02 5.2D+02-4.3D+03 1.1D+04 2.8D+01-7.9D+00-9.6D+02
 -5.8D-01 5.3D-01-2.8C+00 1.6D+01-2.1D-01 1.9C-01-1.5C+00 4.5D+00-1.3D+00 1.2D+00-9.5D+00 2.8D+01 1.1D-01-3.0D-02-1.1D+00
  1.6D-C1-1.5D-01 7.8D-01-4.5D+00 5.8D-02-5.4C-02 4.1D-01-1.3D+00 3.7D-01-3.4D-01 2.6D+00-7.9D+00-3.0D-02 8.4D-03 3.1D-01
 -4.4D+01 4.0D+01-3.9D+02 6.0D+02 8.6D+3C-8.0C+00 7.0D+01-1.5D+02 5.7D+01-5.3D+01 4.6D+02-9.6C+02-1.1D+00 3.1D-01 1.4D+02
```

Figure 4-9

STEP	TEST	T1	T2
1	0	C.0	C.0
2	1	0.2392D+00	C.3C13D+C1
3	1	0.1494D+00	0.7256D+01
4	1	0.1C34D+00	0.1892D+01
5	1	0.8661D-01	0.1530D+01
6	1	0.1271D+00	0.1352D+C2
7	1	C.1945D+00	C.1349D+01
8	1	0.3507D+00	0.8459D+C2
9	1	0.2874D+00	0.7727D+C2
10	1	C.4C6CD+00	0.2C98D+C2
11	0	C.2257D+00	C.3799D+CC
12	1	0.3375D+00	0.1623D+01
13	1	C.4C77D+CC	0.1669D+C2
14	1	C.2272D+00	C.4291D+C1
15	1	C.1776D+00	0.3217D+C2
16	1	C.1312D+00	0.1C66D+C2
17	1	C.859CD-C1	C.1C86D+C2
18	1	C.1254D+00	0.211CD+C1
19	1	C.1941D+00	0.2965D+C2
2C	1	C.1355D+00	C.1566D+C2
21	1	C.1823D+00	C.2258D+01
22	1	0.2118D+00	0.1783D+01
23	0	C.1272D+00	0.5962D+CC
24	1	C.4257D+00	0.5112D+C2
25	1	0.2452D+00	0.5321D+C2
26	1	0.2287D+00	C.2017D+C1
27	1	C.1972D+00	C.1740D+C1
28	1	0.2192D+00	C.5651D+C1
29	0	0.2134D+00	0.8844D+CC
3C	1	C.2264D+00	0.1258D+C1
31	1	0.1188D+00	C.1832D+C2
32	0	0.7689D-01	0.5910D+CC
33	1	C.1143D+00	C.7CC9D+C1
34	1	0.9124D-01	0.2252D+C1
35	1	C.1748D+00	0.1551D+C2
36	0	C.1423D+00	C.4405D+C0
37	0	C.1418D+00	C.4886D+CC
38	1	0.9582D-01	0.1488D+C1
39	1	C.9403D-01	0.1348D+C2
40	1	C.9313D-01	C.1638D+C2
41	1	0.1265D+00	C.2275D+C1
42	1	C.1294D+00	0.2261D+C2
43	0	C.8827D-01	C.1534D+CC
44	1	0.1542D+00	C.3232D+C1
45	0	0.1917D+00	0.8442D+00
46	1	C.3683D+00	0.3835D+C2
47	1	C.1593D+00	0.5493D+C1
48	0	0.2377D+00	0.6975D+CC
49	1	C.4805D+CC	C.3257D+C2
5C	1	0.2716D+00	C.8928D+C1

MONITCR= 4C

Figure 4-10   Simulation #1 ($q=5\times10^{-8}$)

i) Column labeled TEST indicates 0 if no control action is taken and 1 otherwise.

ii) Columns T_1 and T_2 indicate the numerical outcome of both tests mentioned above.

iii) MONITOR gives the total number of steps for which a control action is taken.

As mentioned in Section 4.2.1, it is to make these tests T_1 and T_2 numerically possible that artificial noise was added to the model used to derive $\underline{\Gamma}_{ss}$ and $\underline{\Gamma}_c$.

Plots of Δf_{av}, $\Delta \delta_{av}$ and $\int \Delta P_{tie}$ are shown in figures 4-11, 4-12 and 4-13 respectively. Plots of ΔP_{M_1}, Δw_1, ΔP_{M_2}, Δw_2, ΔP_{M_3}, Δw_3 (refer to fig. 2.6 for symbols) were also obtained; but since they follow similar patterns only ΔP_{M_1} and Δw_1 are shown here, in fig. 4-14 and 4-15. The figures also give, for comparison, the behavior of the corresponding variables when the system is left completely uncontrolled.

Then, using the same values for K_1, β and α, larger deadband regions are derived by increasing the added diagonal elements of $\underline{Q}$ from 5×10^{-8} to 5×10^{-7}, 5×10^{-6} and 5×10^{-5} successively. Simulations are also run using each of those deadband regions and the results are given in figures 4-16, 4-17 and 4-18 respectively. The corresponding maximum deviations of the variables mentioned above are given in fig. 4-19.

These results show reductions of successively 20%, 40%, 74% and 80%
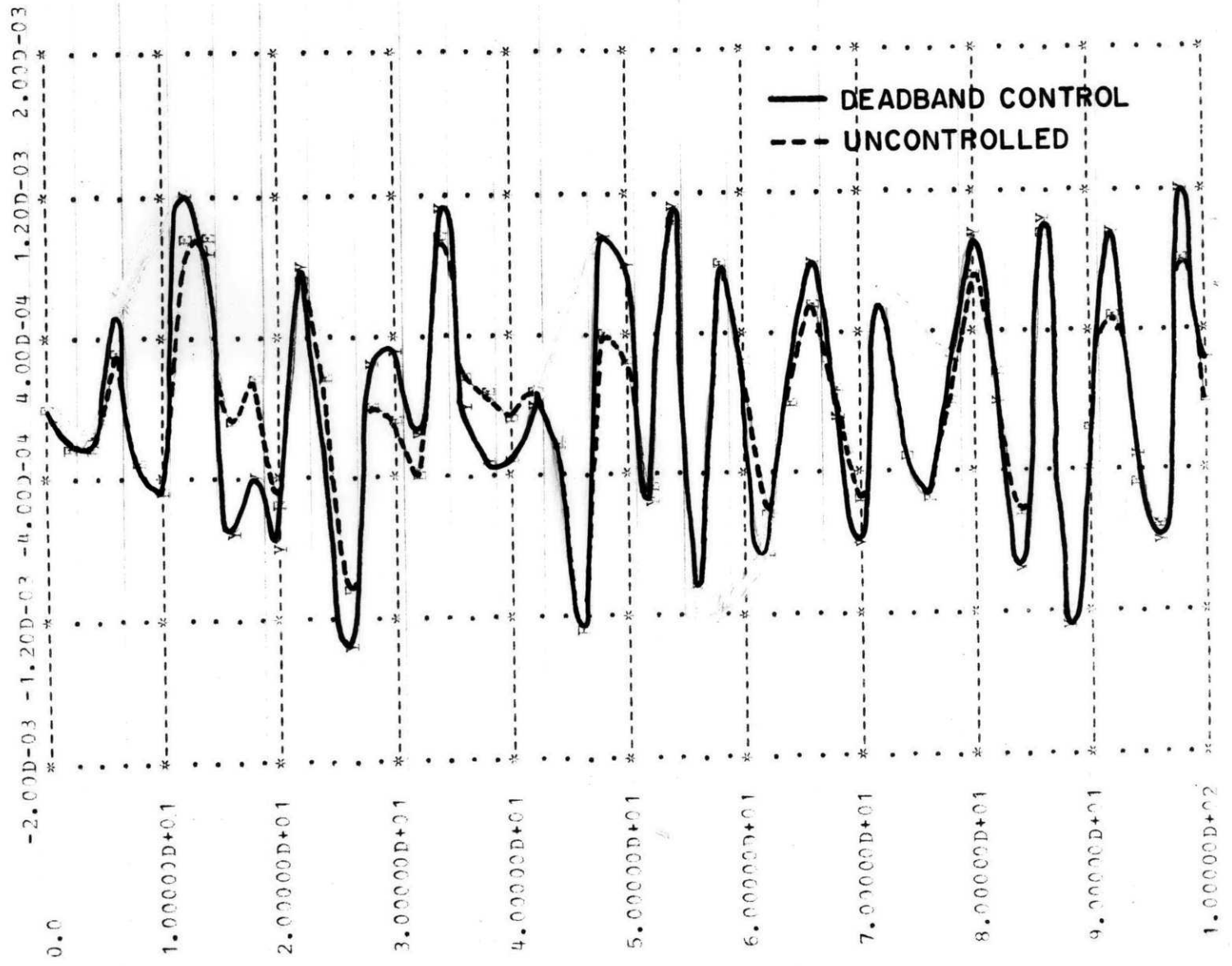
Figure 4-11 Δf_{av} versus time (Simulation #1)
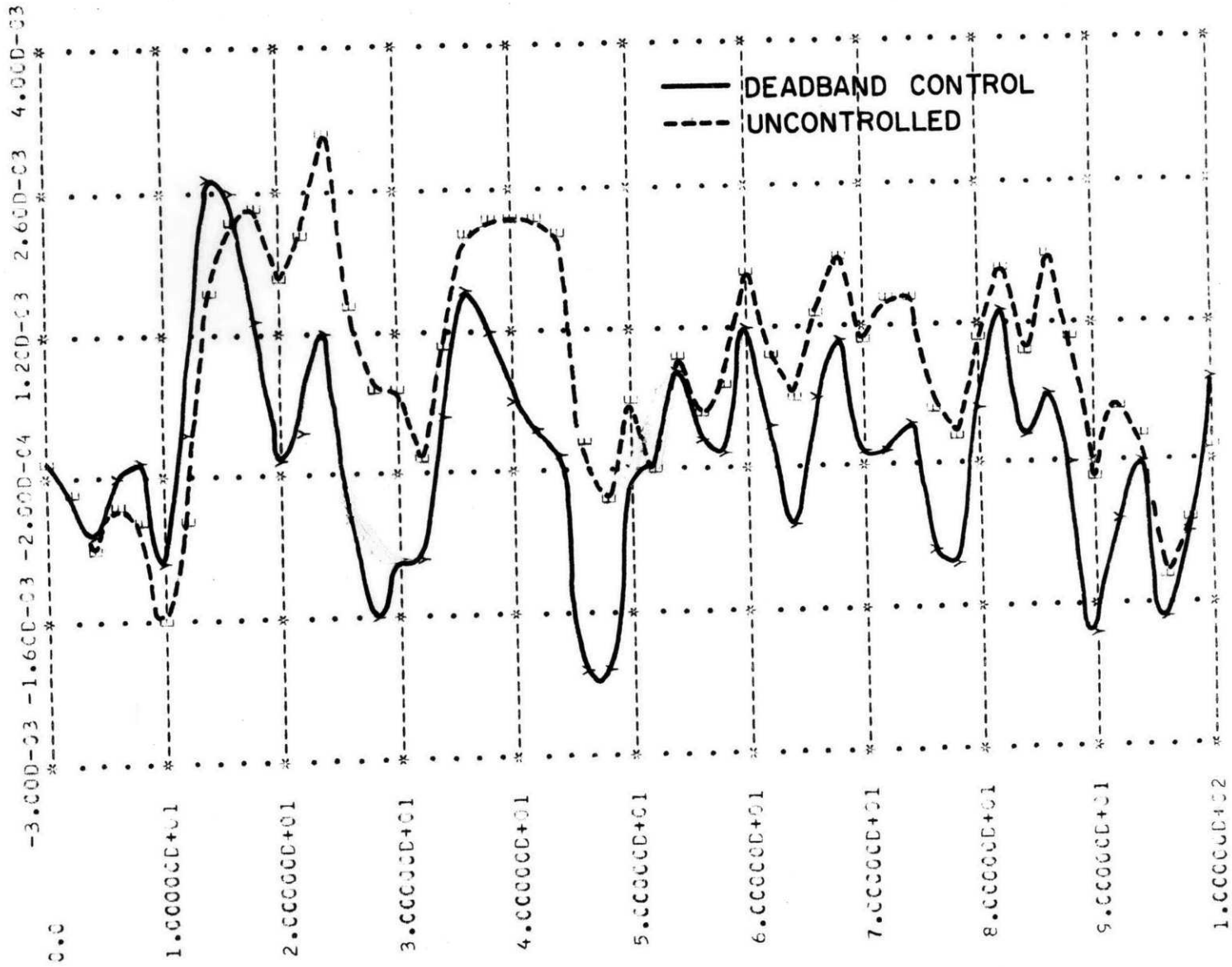
Figure 4-12 $\Delta\delta_{av}$ versus time (Simulation #1)
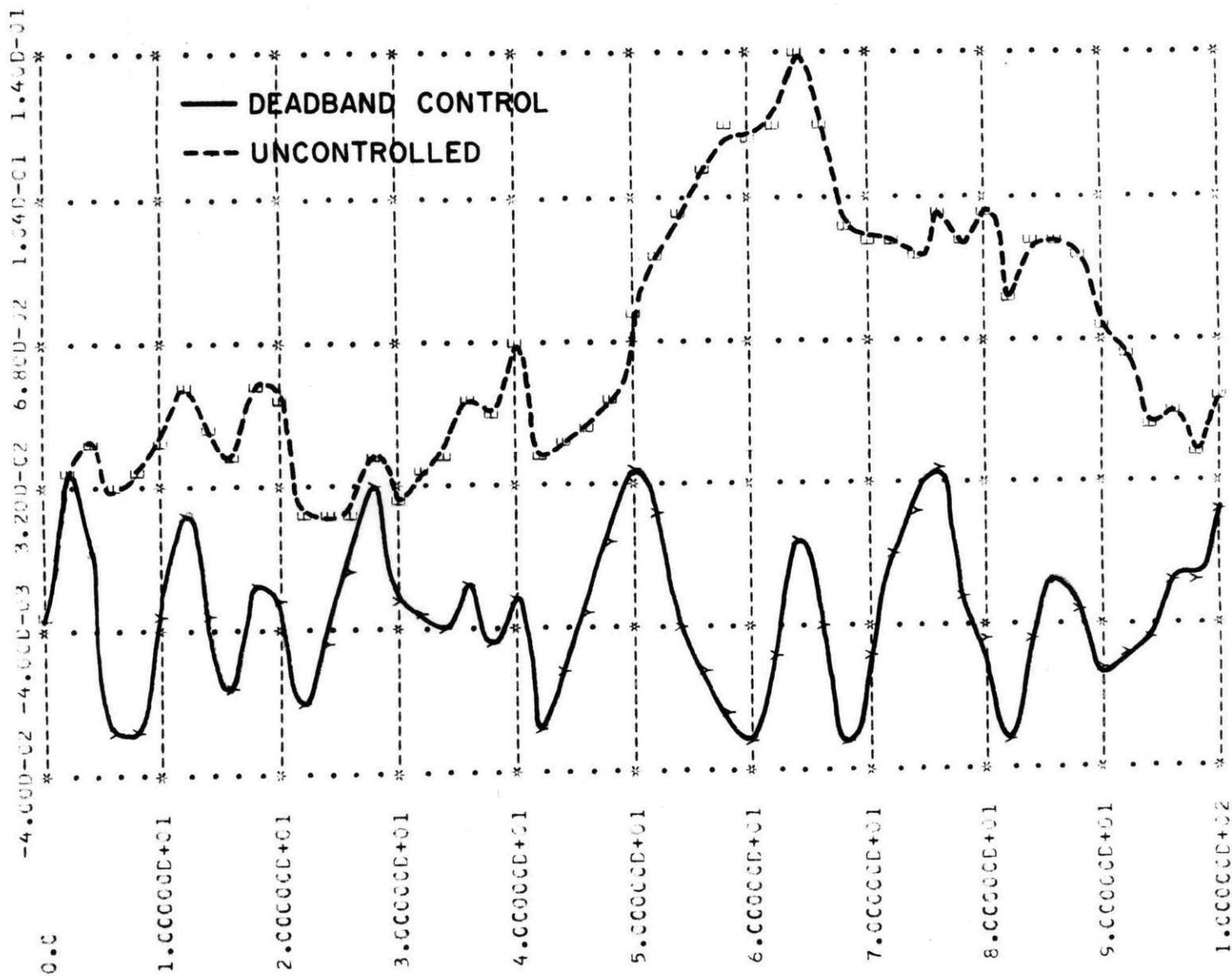
Figure 4-13 $\int \Delta P_{tie}$ versus time (Simulation #1)
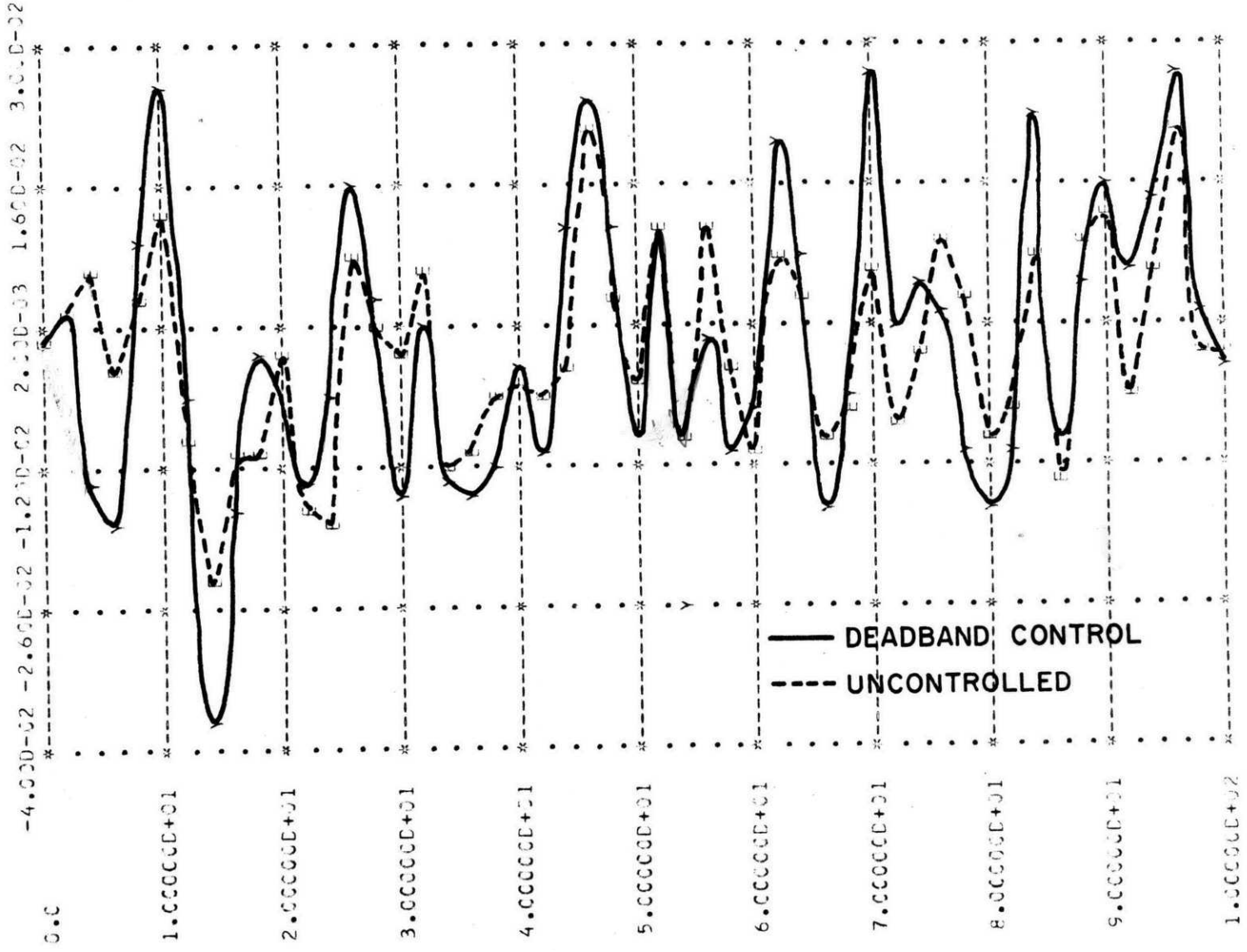
Figure 4-14 ΔP_{Ml} versus time (Simulation #1)
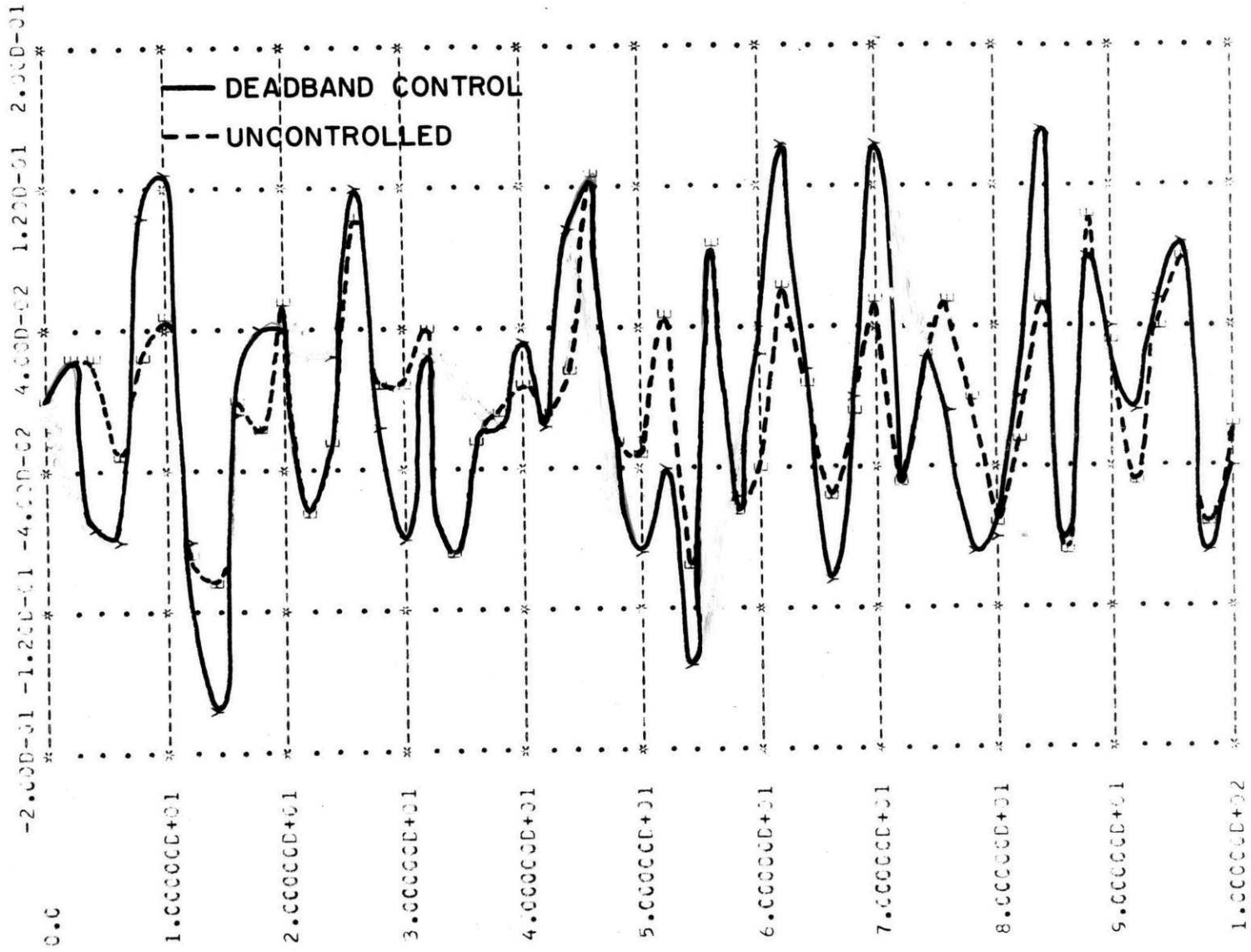
Figure 4-15 Δw_1 versus time (Simulation #1)

STEP	TEST	T1	T2
1	0	0.0	0.0
2	1	0.2366D+00	0.2106D+01
3	1	0.1471D+00	0.1334D+01
4	1	0.1013D+00	0.1439D+01
5	1	0.8376D-01	0.1412D+01
6	1	0.1241D+00	0.1642D+01
7	0	0.1915D+00	0.9521D+00
8	1	0.4455D+00	0.1029D+02
9	1	0.3159D+00	0.9574D+01
10	1	0.4172D+00	0.2869D+01
11	0	0.2289D+00	0.2875D+00
12	1	0.3752D+00	0.2783D+01
13	1	0.4347D+00	0.2898D+01
14	0	0.2193D+00	0.7957D+00
15	1	0.3386D+00	0.6806D+01
16	1	0.1603D+00	0.2708D+01
17	1	0.8461D-01	0.1581D+01
18	0	0.1155D+00	0.4396D+00
19	1	0.1824D+00	0.3703D+01
20	1	0.1126D+00	0.3018D+01
21	0	0.1700D+00	0.4623D+00
22	1	0.2354D+00	0.1027D+01
23	0	0.1147D+00	0.2490D+00
24	1	0.3380D+00	0.5463D+01
25	1	0.2127D+00	0.6105D+01
26	1	0.2113D+00	0.1650D+01
27	0	0.1823D+00	0.8127D+00
28	0	0.4256D+00	0.8193D+00
29	0	0.3247D+00	0.2536D+00
30	0	0.1958D+00	0.1968D+00
31	1	0.1121D+00	0.3125D+01
32	0	0.9831D-01	0.7488D+00
33	0	0.1005D+00	0.6824D+00
34	1	0.2173D+00	0.1251D+01
35	1	0.1857D+00	0.3223D+01
36	0	0.1447D+00	0.2402D+00
37	1	0.1310D+00	0.1341D+01
38	1	0.7468D-01	0.1212D+01
39	1	0.7250D-01	0.2333D+01
40	1	0.8058D-01	0.1913D+01
41	0	0.1201D+00	0.4580D+00
42	1	0.2475D+00	0.4288D+01
43	0	0.9608D-01	0.2772D+00
44	0	0.1570D+00	0.6090D+00
45	0	0.2375D+00	0.1343D+00
46	1	0.2100D+00	0.2960D+01
47	0	0.1280D+00	0.4398D+00
48	0	0.3284D+00	0.4220D+00
49	1	0.4565D+00	0.4866D+01
50	1	0.2907D+00	0.1474D+01

MONITOR= 30

Figure 4-16 Simulation #2 (q=5×10^{-7})

STEP	TEST	T1	T2
1	0	0.0	0.0
2	1	0.2187D+00	0.1770D+01
3	0	0.1297D+00	0.5709D+00
4	0	0.7475D-01	0.5418D+00
5	1	0.1179D+00	0.1001D+01
6	0	0.1232D+00	0.6064D+00
7	0	0.1551D+00	0.8823D-01
8	0	0.2011D+00	0.9282D+00
9	1	0.2782D+00	0.1428D+01
10	0	0.3487D+00	0.9512D+00
11	0	0.2532D+00	0.5901D+00
12	0	0.2927D+00	0.5596D+00
13	0	0.2860D+00	0.8877D+00
14	0	0.2369D+00	0.3939D+00
15	1	0.2187D+00	0.1439D+01
16	0	0.1227D+00	0.1208D+00
17	0	0.8567D-01	0.1139D+00
18	0	0.1377D+00	0.1302D+00
19	0	0.1083D+00	0.3479D+00
20	0	0.1042D+00	0.4552D+00
21	0	0.1308D+00	0.3702D+00
22	1	0.1957D+00	0.1845D+01
23	0	0.1012D+00	0.6554D+00
24	0	0.4275D+00	0.6291D+00
25	0	0.2270D+00	0.8407D+00
26	1	0.4018D+00	0.2763D+01
27	1	0.2339D+00	0.2426D+01
28	0	0.2201D+00	0.2060D+00
29	0	0.2215D+00	0.7922D+00
30	1	0.1716D+00	0.1785D+01
31	1	0.9021D-01	0.2629D+01
32	0	0.7426D-01	0.3316D+00
33	0	0.5918D-01	0.6082D+00
34	0	0.1078D+00	0.1462D+00
35	0	0.8262D-01	0.2365D+00
36	0	0.1038D+00	0.6706D-01
37	0	0.7440D-01	0.1511D+00
38	0	0.3936D-01	0.2919D+00
39	1	0.1227D+00	0.1676D+01
40	0	0.8828D-01	0.3910D+00
41	0	0.2214D+00	0.1283D+00
42	0	0.6026D-01	0.6420D+00
43	0	0.1014D+00	0.2416D+00
44	0	0.1304D+00	0.8985D+00
45	1	0.3981D+00	0.1342D+01
46	1	0.3299D+00	0.1598D+01
47	0	0.1532D+00	0.1913D+00
48	0	0.2456D+00	0.2582D+00
49	1	0.3228D+00	0.1869D+01
50	0	0.2019D+00	0.9347D+00

MONITOR= 13

Figure 4-17   Simulation #3 (q=5×10^{-6})

STEP	TEST	T1	T2
1	0	0.0	0.0
2	0	0.1589D+00	0.9788D+00
3	1	0.2005D+00	0.1261D+01
4	0	0.7797D-01	0.5124D-01
5	0	0.3580D-01	0.2943D+00
6	0	0.1116D+00	0.5397D+00
7	0	0.8391D-01	0.6724D+00
8	1	0.2550D+00	0.2405D+01
9	1	0.1321D+00	0.1264D+01
10	0	0.2017D+00	0.5287D+00
11	1	0.1231D+00	0.2001D+01
12	0	0.2122D+00	0.2890D+00
13	0	0.1645D+00	0.1538D+00
14	0	0.6954D-01	0.1681D+00
15	0	0.1327D+00	0.7123D+00
16	0	0.6298D-01	0.3794D+00
17	0	0.1365D+00	0.9292D+00
18	1	0.3325D+00	0.1062D+01
19	0	0.1192D+00	0.4782D+00
20	0	0.8974D-01	0.7381D-01
21	0	0.7186D-01	0.7213D-01
22	1	0.1154D+00	0.1339D+01
23	0	0.4234D-01	0.5476D+00
24	0	0.3052D+00	0.2305D+00
25	0	0.4603D-01	0.8757D-01
26	0	0.7307D-01	0.4425D+00
27	1	0.1992D+00	0.1512D+01
28	0	0.1712D+00	0.6443D+00
29	0	0.2282D+00	0.3711D+00
30	0	0.1990D+00	0.2955D+00
31	0	0.7199D-01	0.6651D-01
32	0	0.4877D-01	0.5391D-01
33	0	0.3216D-01	0.2743D-01
34	0	0.5146D-01	0.4904D+00
35	1	0.3424D+00	0.2697D+01
36	0	0.1428D+00	0.6957D+00
37	0	0.1158D+00	0.5619D-01
38	0	0.3372D-01	0.1147D+00
39	1	0.8270D-01	0.1155D+01
40	0	0.3533D-01	0.4333D+00
41	0	0.1975D+00	0.4413D+00
42	0	0.1937D-01	0.5792D-01
43	0	0.6455D-01	0.3355D+00
44	0	0.2132D+00	0.3041D+00
45	0	0.1149D+00	0.2112D+00
46	0	0.2694D-01	0.4731D-01
47	0	0.3093D-01	0.1540D+00
48	0	0.2020D+00	0.7482D+00
49	0	0.3552D+00	0.9217D+00
50	1	0.2672D+00	0.1535D+01

MCNITOR= 10

Figure 4-18   Simulation #4 (q=5×10^{-5})

	$\Delta P_{M_1} \times 10^2$ Max	Δw_1 Max	$\Delta P_{M_2} \times 10^2$ Max	Δw_2 Max	$\Delta P_{M_3} \times 10^2$ Max	Δw_3 Max	$\Delta f_{av} \times 10^3$ Max	$\Delta \delta_{av} \times 10^3$ Max	$\int \Delta P_{tie}$ Max
No deadband used	3.7	0.18	0.5	0.02	3.1	0.13	1.36	2.7	0.039
case #1 20% saving	3.7	0.18	0.5	0.02	3.1	0.12	1.36	2.7	0.036
case #2 40% saving	3.2	0.15	0.54	0.02	3.5	0.12	1.36	2.7	0.040
case #3 74% saving	3.5	0.16	0.52	0.02	3.3	0.15	1.36	2.6	0.039
case #4 80% saving	3.5	0.2	0.52	0.02	3.4	0.14	1.52	2.3	0.061
No control used	2.2	0.13	0.4	0.02	2.3	0.13	1.20	3.16	0.14

Figure 4-19

Maximum deviations corresponding to the different deadbands used with conventional AGC

in the number of control signals sent to power plants. The larger savings
are obtained by using deadband regions derived for models to which a
relatively sizeable artificial noise was added. But figure 4-19 shows no
significant change in the maximum deviationsof the original model variables
as compared to those when no deadband is used. This, again, is essentially
due to the conservative nature of the ellipsoidal bounds.

One can note, in passing, (from figures 4-11 to 4-13) that the main
effect of the control here, is to reduce the maximum deviation in area inter-
change of energy from 0.14 pu for the uncontrolled system to 0.04 pu for
the controlled system. This is done at the expense of sometimes larger
deviations of the other variables of the system.

Finally, recall that one of the assumptions which lead to the linear
model at hand was that the values of the power plant turbines do not hit
their limits. (±0.065 pu for G, and G_3, ±0.01 pu for G_2, as given by the
source of the data of figure 4-1. [5]). Now the plots of Δw_1, Δw_2 and Δw_3
show that this is not the case here. However, as was already argued above
for Δf_{av}, the load disturbance bounds, chosen in section 4.2.3, are much
larger than in actual situations and scaled down results would be obtained
with more realistic conditions. Moreover the main purpose of this study
was to investigate the potential of the control strategy proposed in Chapter
3 and any further research will definitely have to take into account the

problem of valve limits.

To conclude this section, note that conventional AGC is, in effect, a feedback of only two variables: the integral of frequency deviation and that of tie-line power flow deviation. As a result, one would expect further savings when the control signals carry more information about the system. This is the motivation of the next section where a full state feedback is used for control.

4.4 Full State Feedback Controller

4.4.1: General description

Optimal linear regulator theory is found in many standard references in modern control systems (e.g. [13]) and has been frequently applied to power systems (e.g. [2], [3]). One can summarize the results to be used here as follows:

Given a linear time invariant system represented by

$$\underline{x}(n\Delta+\Delta) = \underline{\Phi}\underline{x}(n\Delta) + \underline{B}\underline{u}(n\Delta)$$

and a quadratic cost function of the form:

$$J = \sum_{n=0}^{\infty} [\underline{x}'(n\Delta)\ \underline{Q}_w\ \underline{x}(n\Delta) + \underline{u}'(n\Delta)\ \underline{R}_w\ \underline{u}(n\Delta)]$$

where $\underline{Q}_w$ and $\underline{R}_w$ are respectively positive semi - definite and positive

definite weighting matrices of proper dimensions, the control law which minimizes the cost function J is

$$\underline{u}(n\Delta) = \underline{K} \; \underline{x}(n\Delta)$$

where the feedback gain matrix $\underline{K}$ is given by:

$$\begin{cases} \underline{K} = - \; (\underline{B}' \; \underline{S} \; \underline{B} + \underline{R}_w)^{-1} \; \underline{B}' \; \underline{S} \; \underline{\Phi} \\ \\ \underline{S} = \underline{Q}_w + \underline{\Phi}' \; \underline{S} \; \underline{\Phi} - \underline{\Phi}' \; \underline{S} \; \underline{B} \; (\underline{B}' \; \underline{S} \; \underline{B} + \underline{R}_w)^{-1} \; \underline{B}' \; \underline{S} \; \underline{\Phi} \end{cases} \tag{4.9}$$

4.4.2 Design

The choice of the weighting matrices $\underline{Q}_w$ and $\underline{R}_w$ is the most subjective factor of such a design and is guided by the extent to which deviations of the different state variables and controls are to be minimized. Following Glover's example [3], $\underline{Q}_w$ is chosen at this point such that x_{13} and x_{15} (i.e Δf_{av} and $\int \Delta P_{tie}$) are equally penalized , x_{14} ($\Delta \delta_{av}$) is penalized to a lesser extent and x_1 through x_{12} are not at all. This choice, given in fig. 4-20, will be later modified.

As for $\underline{R}_w$, it is chosen such that the control signals are weighted more heavily than the state variables. Taking also into account their relative orders of magnitude (from the simulations of the previous section, say) a first choice for $\underline{R}_w$ is $0.01 \times \underline{I}_{3\times 3}$ But then, solving Eqs. (4.9) for $\underline{K}$ and evaluating the eigenvalues of the resulting closed loop

MATRIX QW

0.0	0.0	0.0	0.0	0.0	0.0	0.0	0.0	0.0	0.0	0.0	0.0	0.0	0.0	0.0
0.0	0.0	0.0	0.0	0.0	0.0	0.0	0.0	0.0	0.0	0.0	0.0	0.0	0.0	0.0
0.0	0.0	0.0	0.0	0.0	0.0	0.0	0.0	0.0	0.0	0.0	0.0	0.0	0.0	0.0
0.0	0.0	0.0	0.0	0.0	0.0	0.0	0.0	0.0	0.0	0.0	0.0	0.0	0.0	0.0
0.0	0.0	0.0	0.0	0.0	0.0	0.0	0.0	0.0	0.0	0.0	0.0	0.0	0.0	0.0
0.0	0.0	0.0	0.0	0.0	0.0	0.0	0.0	0.0	0.0	0.0	0.0	0.0	0.0	0.0
0.0	0.0	0.0	0.0	0.0	0.0	0.0	0.0	0.0	0.0	0.0	0.0	0.0	0.0	0.0
0.0	0.0	0.0	0.0	0.0	0.0	0.0	0.0	0.0	0.0	0.0	0.0	0.0	0.0	0.0
0.0	0.0	0.0	0.0	0.0	0.0	0.0	0.0	0.0	0.0	0.0	0.0	0.0	0.0	0.0
0.0	0.0	0.0	0.0	0.0	0.0	0.0	0.0	0.0	0.0	0.0	0.0	0.0	0.0	0.0
0.0	0.0	0.0	0.0	0.0	0.0	0.0	0.0	0.0	0.0	0.0	0.0	0.0	0.0	0.0
0.0	0.0	0.0	0.0	0.0	0.0	0.0	0.0	0.0	0.0	0.0	0.0	0.0	0.0	0.0
0.0	0.0	0.0	0.0	0.0	0.0	0.0	0.0	0.0	0.0	0.0	0.0	1.0D+00	0.0	0.0
0.0	0.0	0.0	0.0	0.0	0.0	0.0	0.0	0.0	0.0	0.0	0.0	0.0	1.0D-01	0.0
0.0	0.0	0.0	0.0	0.0	0.0	0.0	0.0	0.0	0.0	0.0	0.0	0.0	0.0	1.0D+00

MATRIX RW

0.5000D-03	0.0	0.0
0.0	0.5000D-03	0.0
0.0	0.0	0.5000D-03

Figure 4-20

matrix $\underline{\Phi}_{c\ell} = \underline{\Phi} + \underline{B}\,\underline{K}$ yields a pole at 0.95. Arguments similar to those used for the root locus study of section 4.3.2 show that the choice of β for eq. (3.11) would therefore be limited to extremely small values. As a result, the diagonal elements of $\underline{R}_w$ are decreased until the largest closed loop pole is at 0.83. As before, this then allows a β of 0.3. The new matrix $\underline{R}_w$ is also given in fig. 4.20.

Following exactly the same steps of section 4.3.2, Eq. (3.11) is then solved for $\underline{\Gamma}_{ss}$. Using this last result Eq. (3.12) is solved with several values of α. Comparing the eigenvalues of the different matrices $\underline{\Gamma}_c$ a value of α is then chosen to be:

$$\alpha = 1.2$$

A whole set of results is given in fig. 4.21 for $q = 5 \times 10^{-8}$.

4.4.3. Simulations

A set of simulations, equivalent to those of section 4.3.3., can now be performed. The results for $q = 5 \times 10^{-8}$, 5×10^{-7}, 5×10^{-6} and 5×10^{-5} are given in figures 4-22, 4-28, 4-29 and 4-30 respectively. Plots of Δf_{av}, $\Delta \delta_{av}$, $\int \Delta P_{tie}$, ΔP_{M_1} and ΔW_1, corresponding to the first run, are also given in figures 4-23 to 4-27. The maximum deviations of the variables of interest are given, for all four runs in fig. 4.31.

The simulation results show reductions of succesively 42%, 60%, 78% and

58% in the number of control signals. A comparison with the results of the conventional controller (section 4.3.3) shows that for a same value of q, i.e. for the same amount of artificial noise added to the model, one gets a larger deadband region and therefore a greater saving in control action. As a result, and as confirmed by figures 4-19 and 4-31, greater savings in control action are obtained for equal or even smaller maximum deviations in the output variables.

An exception however, is for the last run where even with a larger deadband region more control action had to be taken as compared to the preceeding case. This indicates that at some point, it no longer pays to enlarge the deadband region; because then, trying to decrease control action further results in driving the states more often out of this new deadband region and the purpose is defeated.

Here also, the plots show that the main effect of the control is to reduce the maximum deviation (from schedule) in area interchange of energy. Because no weight was assigned to the first twelve variables in the choice of Q_w, this is still done at the expense of larger savings of those variables. But now, the maximum deviation of Δw_2 in particular is much larger than in the case where a conventional controller is used. It is therefore felt that the arguments pertaining to this problem in section 4.3.3 do not hold here, and another design is carried out with a new weighting matrix Q_w. The first twelve diagonal elements of Q_w are now set to 0.1

and the fourteenth to 0.5; the frequency and tie-line interchange weights are kept at the same value 1.0.

Then, simulations are run with $q=5\times10^{-7}$, 5×10^{-6} and 5×10^{-5} and results are given in figures 4-32, 4-33 and 4-34. A sample plot of $\int \Delta P_{tie}$ is given in figure 4-35. The three curves, plotted on the same graph for comparison, correspond to the behavior of x_{15} when no deadband is used (continuous control action), when the deadband designed with $q=5\times10^{-6}$ is used (54% **saving** in control action) and when no control action is taken at all.

Finally, figure 4-36 shows the maximum deviations of the different variables for the new set of runs. Now the deviations of Δw_1, Δw_2 and Δw_3 are brought down to levels comparable to those of the conventional design but it is only for the last case that we have a greater saving (88%) for equivalent maximum deviations.

MATRIX PHICL

```
-5.4D-01-1.3D+00-3.6D-01-1.2D-02 1.1D-01 9.9D-02-1.8D-02 2.1D-03 1.1D-01 9.9D-02-1.8D-02 2.1D-03-1.5D+01-1.3D+00-7.7D-01
 1.2D+00 1.8D+00 3.1D-01 1.3D-02-8.8D-02-8.2D-02 1.5D-02-1.6D-03-8.8D-02-8.2D-02 1.5D-02-1.6D-03 1.2D+01 1.1D+00 6.6D-01
-1.2D+00-1.1D+00-2.7D-01-4.9D-02 4.8D-02 4.4D-02 3.5D-03-5.9D-04 4.4D-02 3.5D-03-6.0D-04-6.7D+00-6.0D-01-6.4D-01
-6.5D+00-6.0D+00-1.3D+00-3.0D-01 4.1D-01 4.0D-01 3.0D-01 1.5D-02 4.1D-01 4.0D-01 3.0D-01 1.5D-02-7.8D+00-7.0D-01-3.7D+00
 3.5D-01 3.4D-01 9.4D-02 1.7D-02 2.0D-01-5.8D-01-1.5D-01 2.5D-02-6.3D-01-5.8D-01-1.5D-01-2.9D-02-2.5D+00-1.1D+00 5.4D-01
-3.2D-01-2.9D-01-8.1D-02-1.5D-02 5.4D-01 1.2D+00 1.3D-01-1.9D-02 5.4D-01 5.0D-01 1.3D-01 2.5D-02 2.1D+00 9.4D-01-4.6D-01
 2.6D-01 2.5D-01 7.4D-02 1.3D-02-5.0D-01-4.6D-01-9.9D-02-1.6D-02 5.0D-01-4.6D-01-1.5D-01-2.3D-02-1.1D+00-7.8D-01 4.1D-01
 1.4D+00 1.3D+00 4.3D-01 6.9D-02-2.7D+00-2.4D+00-5.6D-01-1.2D-01-2.7D+00-2.4D+00-5.6D-01-1.2D-01-1.3D+00-3.8D+00 2.2D+00
-1.9D-02-2.3D-02-5.6D-02-4.2D-03-9.1D-01-8.5D-01-2.7D-01-4.6D-02-7.9D-02-8.5D-01-2.7D-01 8.0D-03-1.4D+01-4.2D-01 4.8D-01
 2.1D-02 2.5D-02 4.9D-02 7.8D-01 7.3D-01 2.3D-01 4.0D-02 7.8D-01 1.4D+00 2.3D-01-4.2D-03 1.2D+01 3.4D-01-4.1D-01
-1.1D-01-1.1D-01-4.3D-02-8.5D-03-7.4D-01-6.9D-01-1.9D-01-3.8D-02-7.4D-01-6.9D-01-1.8D-01-3.0D-02-6.5D+00 9.8D-02 3.4D-01
-7.9D-01-7.7D-01-5.3D-02-4.6D-02-3.9D+00-3.6D+00-7.7D-01-1.9D-01-3.9D+00-3.6D+00-7.7D-01-1.8D-01-6.9D+00 3.1D+00 1.6D+00
 2.5D-02 2.4D-02 3.0D-03 1.1D-03 1.0D-02 9.6D-03-1.3D-03 3.5D-04 1.0D-02 9.6D-03-1.3D-03 3.5D-04-2.2D-01-1.1D-01 9.6D-03
 4.0D-02 3.9D-02 1.5D-02 2.3D-03 2.8D-02 2.8D-02 1.1D-02 1.7D-03 2.8D-02 2.8D-02 1.1D-02 1.7D-03 1.0D+00 9.1D-01 7.6D-03
 2.0D-02 2.0D-02 9.8D-03 1.6D-03-1.7D-02-1.7D-02-8.3D-03-1.3D-03-1.7D-02-1.7D-02-8.3D-03-1.3D-03 6.7D-03 1.0D-03 4.1D-02
```

PHICL EIGENVALUES

```
0.6294D+00   +J    0.3256D+00
0.6294D+00   +J   -0.3256D+00
0.6337D+00   +J    0.2949D+00
0.6337D+00   +J   -0.2949D+00
0.8264D+00   +J    0.0
0.8161D+00   +J    0.0
-0.6248D+00  +J    0.0
-0.3181D+00  +J    0.2000D+00
-0.3181D+00  +J   -0.2000D+00
0.7164D+00   +J    0.0
-0.1491D-01  +J    0.0
0.1176D-01   +J    0.0
0.6660D-02   +J    0.0
0.1005D-03   +J    0.0
0.6650D-03   +J    0.0
```

BETA= 0.200000

MATRIX GAMMA

```
 1.0D-02-8.5D-03 2.9D-03 1.4D-02-3.0D-03 2.1D-03-6.2D-04-3.4D-03 2.1D-03-2.0D-03 9.5D-04 3.9D-03-7.8D-05-3.0D-04 1.3D-03
-8.5D-03 7.7D-03-3.4D-03-1.7D-02 2.6D-03-2.1D-03 8.4D-04 4.5D-03-9.7D-04 1.3D-03-8.7D-04-3.9D-03 9.5D-05 2.1D-04-1.1D-03
 2.9D-03-3.4D-03 9.0D-03 6.0D-02-3.7D-03 3.6D-03-4.9D-03-2.6D-02-5.3D-03 4.4D-03-2.9D-03-6.9D-03-3.0D-04 6.2D-05 9.6D-04
 1.4D-02-1.7D-02 6.0D-02 4.1D-01-2.5D-02 2.4D-02-3.6D-02-1.9D-01-4.1D-02 3.4D-02-2.7D-02-3.9D-02-2.0D-03 6.6D-04 5.3D-03
-3.0D-03 2.6D-03-3.7D-03-2.5D-02 2.1D-03-2.1D-03 4.4D-03 2.3D-02-2.0D-01 1.1D-02 1.2D-03 2.8D-03 2.8D-03-4.1D-03 5.0D-04
 2.1D-03-2.1D-03 3.6D-03 2.4D-02-2.0D-03 6.1D-03-3.1D-03-1.6D-02 1.1D-02 2.2D-03-2.5D-03-9.6D-03-1.2D-04 4.3D-04-4.5D-04
-6.2D-04 8.4D-04-4.9D-03-3.6D-02 4.4D-03-3.1D-03 5.2D-03 2.8D-03-3.4D-03-4.2D-03 6.2D-03 2.7D-02 1.0D-04-1.7D-04 6.4D-04
-3.4D-03 4.5D-03-2.6D-02-1.9D-01 2.3D-02-1.6D-02 2.8D-02 1.5D-01 1.6D-02-2.2D-02 3.4D-02 1.5D-01 5.1D-04-8.8D-04 3.6D-03
 2.1D-03-9.7D-04-5.3D-03-4.1D-02-2.0D-01 1.1D-02 3.0D-03 1.6D-02 2.2D-01-2.7D-02 6.8D-03 2.6D-02-3.4D-05 1.3D-03 1.8D-03
-2.3D-03 1.3D-03 4.4D-03 3.4D-02 1.1D-02 2.2D-03-2.4D-02-3.2D-02 1.3D-02-5.9D-03-2.6D-02-6.9D-05 1.6D-05-1.6D-04 1.8D-03
 9.5D-04-8.7D-04-2.9D-03-2.7D-02 1.2D-03-2.5D-03 6.2D-03 3.4D-02 6.8D-03-5.9D-03 9.6D-03 4.5D-02-2.4D-05-1.6D-04 1.8D-03
 3.9D-03-3.9D-03-6.9D-03-7.3D-02 1.2D-03-9.6D-03 2.7D-02 1.5D-01 2.6D-02-2.3D-02 4.5D-02 2.2D-01-5.0D-04-6.2D-04 1.0D-02
-7.8D-05 3.5D-05-3.0D-04-2.0D-03 2.8D-04-1.2D-04 1.0D-04 5.1D-04-3.4D-05-6.9D-05-2.4D-05-5.0D-04 1.5D-05-5.7D-06-7.7D-05
-3.0D-04 2.1D-04 6.2D-05 6.6D-04-1.9D-03 4.3D-04-1.7D-04-8.8D-04 1.3D-03 1.6D-05-1.6D-04-6.2D-04-5.7D-06 7.8D-05-1.4D-04
 1.3D-03-1.1D-03 9.6D-04 5.3D-03 5.0D-04-4.5D-04 6.4D-04 3.6D-03 1.8D-03-1.6D-03 1.8D-03 1.0D-02-7.7D-05-1.4D-04 6.2D-03
```

ALPHA= 1.200000

DEADBAND SET GAMDB

```
 7.0D+00-6.6D+00 6.8D+01-8.3D+01-6.4D+00 5.8D+00-5.2D+01 9.8D+01-7.1D+00 6.8D+00-5.7D+01 1.3D+02 3.2D-01-7.4D-02-2.7D+01
-6.6D+00 6.1D+00-6.3D+01 8.2D+01 6.0D+00-5.4D+00 4.8D+01-9.2D+01 6.7D+00-6.4D+00 5.4D+01-1.3D+02-3.0D-01 7.1D-02 2.6D+01
 6.8D+01-6.3D+01 6.8D+02-7.5D+02-7.2D+01 6.6D+01-5.9D+02 1.1D+03-8.8D+01 8.3D+01-6.7D+02 1.7D+03 4.5D+00-1.1D+00-3.0D+02
-8.8D+01 8.2D+01-7.5D+02 1.4D+03 5.0D+01-4.2D+01 3.8D+02-6.7D+02 3.4D+01-3.6D+01 3.5D+02-6.0D+02 2.7D+00-2.3D+00 2.3D+02
-6.4D+00 6.0D+00-7.2D+01 5.0D+01 9.3D+00-8.6D+00 7.7D+01-1.5D+02 1.3D+01-1.2D+01 9.2D+01-2.4D+02-7.6D+01 2.3D-01 3.7D+01
 5.8D+00-5.4D+00 6.6D+01-4.2D+01-8.6D+00 8.0D+00-7.2D+01 1.4D+02-1.2D+01 1.1D+01-8.6D+01 2.3D+02 7.3D-01-1.9D-01-3.4D+01
-5.2D+01 4.8D+01-5.9D+02 3.8D+02 7.7D+01-7.2D+01 6.4D+02-1.3D+03 1.1D+02-9.8D+01 7.7D+02-2.0D+03-6.5D+00 1.7D+00 3.1D+02
 9.8D+01-9.2D+01 1.1D+03-6.7D+02-1.5D+02 1.4D+02-1.3D+03 2.5D+03-2.1D+02 1.9D+02-1.5D+03 4.1D+03 1.3D-01-3.4D+00-6.0D+02
-7.1D+00 6.7D+00-8.8D+01 3.4D+01 1.3D+01-1.2D+01 1.1D+02-2.1D+02 1.9D+01-1.7D+01 1.3D+02-3.6D+02-1.2D+00 3.1D-01 3.7D+01
 6.8D+00-6.4D+00 8.3D+01-3.6D+01-1.2D+01 1.1D+01-9.8D+01 1.9D+02-1.7D+01 1.6D+01-1.2D+02 3.3D+02 1.1D+00-2.8D-01-4.6D+01
-5.7D+01 5.4D+01-6.7D+02 3.5D+02 9.2D+01-8.6D+01 7.7D+02-1.5D+03 1.3D+02-1.2D+02 9.5D+02-2.5D+03-8.2D+00 2.1D+00 3.7D+02
 1.3D+02-1.3D+02 1.7D+03-6.0D+02-2.4D+02 2.3D+02-2.0D+03 4.1D+03-3.6D+02 3.3D+02-2.5D+03 6.9D+03 2.3D+01-6.0D+00-9.6D+02
 3.2D-01-3.0D-01 4.5D+00 2.7D-01-7.6D-01 7.3D-01-6.5D+00 1.3D+01-1.2D+00 1.1D+00-8.2D+00 2.3D+01 8.0D-02-2.1D-02-2.9D+00
-7.4D-02 7.1D-02-1.1D+00-2.3D-01 2.0D-01-1.9D-01 1.7D+00-3.4D+00 3.1D-01-2.8D-01 2.1D+00-6.0D+00-2.1D-02 5.7D-03 7.5D-01
-2.7D+01 2.6D+01-3.0D+02 2.3D+02 3.7D+01-3.4D+01 3.1D+02-6.0D+02 5.0D+01-4.6D+01 3.7D+02-9.6D+02-2.9D+00 7.5D-01 1.5D+02
```

Figure 4-21

STEP	TFSI	T1	T2
1	0	0.0	0.0
2	1	0.2396D+00	0.1519D+01
3	1	0.1904D+00	0.1899D+01
4	0	0.1429D+00	0.5878D+00
5	0	0.1791D+00	0.1978D+00
6	0	0.1539D+00	0.1414D+00
7	1	0.1950D+00	0.1863D+01
8	1	0.3540D+00	0.2218D+01
9	0	0.2823D+00	0.4831D+00
10	1	0.5099D+00	0.1290D+01
11	1	0.3334D+00	0.1889D+01
12	0	0.4214D+00	0.8065D+00
13	1	0.4404D+00	0.1184D+01
14	1	0.2167D+00	0.4707D+01
15	1	0.1915D+00	0.2831D+01
16	1	0.1557D+00	0.4180D+01
17	1	0.1318D+00	0.4745D+01
18	1	0.1704D+00	0.2058D+01
19	1	0.2209D+00	0.2090D+01
20	1	0.1597D+00	0.4305D+01
21	1	0.1931D+00	0.1999D+01
22	1	0.2543D+00	0.6087D+01
23	1	0.1818D+00	0.2480D+01
24	1	0.3476D+00	0.9263D+01
25	0	0.2461D+00	0.8631D+00
26	1	0.5530D+00	0.3323D+01
27	1	0.3798D+00	0.4571D+01
28	0	0.3324D+00	0.9340D+00
29	1	0.3748D+00	0.2254D+01
30	1	0.2141D+00	0.1165D+01
31	0	0.1457D+00	0.6358D+00
32	0	0.2133D+00	0.4323D+00
33	0	0.1033D+00	0.3433D+00
34	1	0.1479D+00	0.1751D+01
35	0	0.1912D+00	0.6212D+00
36	0	0.2238D+00	0.2088D+00
37	1	0.1188D+00	0.1210D+01
38	0	0.8007D-01	0.1193D+00
39	0	0.9858D-01	0.6958D+00
40	0	0.1322D+00	0.4934D+00
41	1	0.3127D+00	0.1702D+01
42	1	0.2601D+00	0.2852D+01
43	1	0.2095D+00	0.2473D+01
44	1	0.2453D+00	0.1638D+01
45	0	0.2358D+00	0.8247D+00
46	0	0.3500D+00	0.5849D+00
47	0	0.2531D+00	0.6733D+00
48	0	0.3500D+00	0.6459D+00
49	0	0.5327D+00	0.8449D+00
50	1	0.3785D+00	0.2078D+01

MONITOR= 29

Figure 4-22   Simulation #5 (q=5×10^{-8})

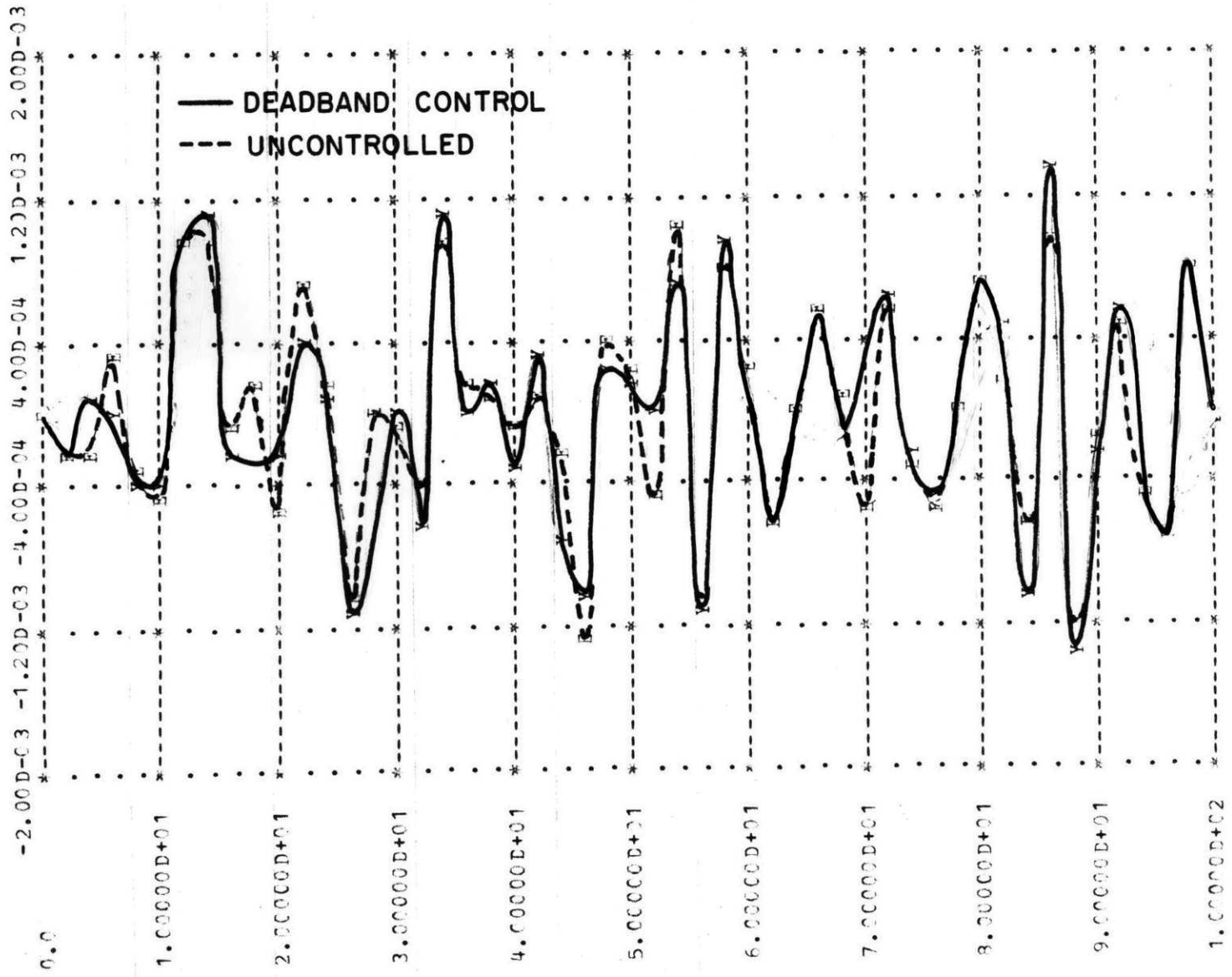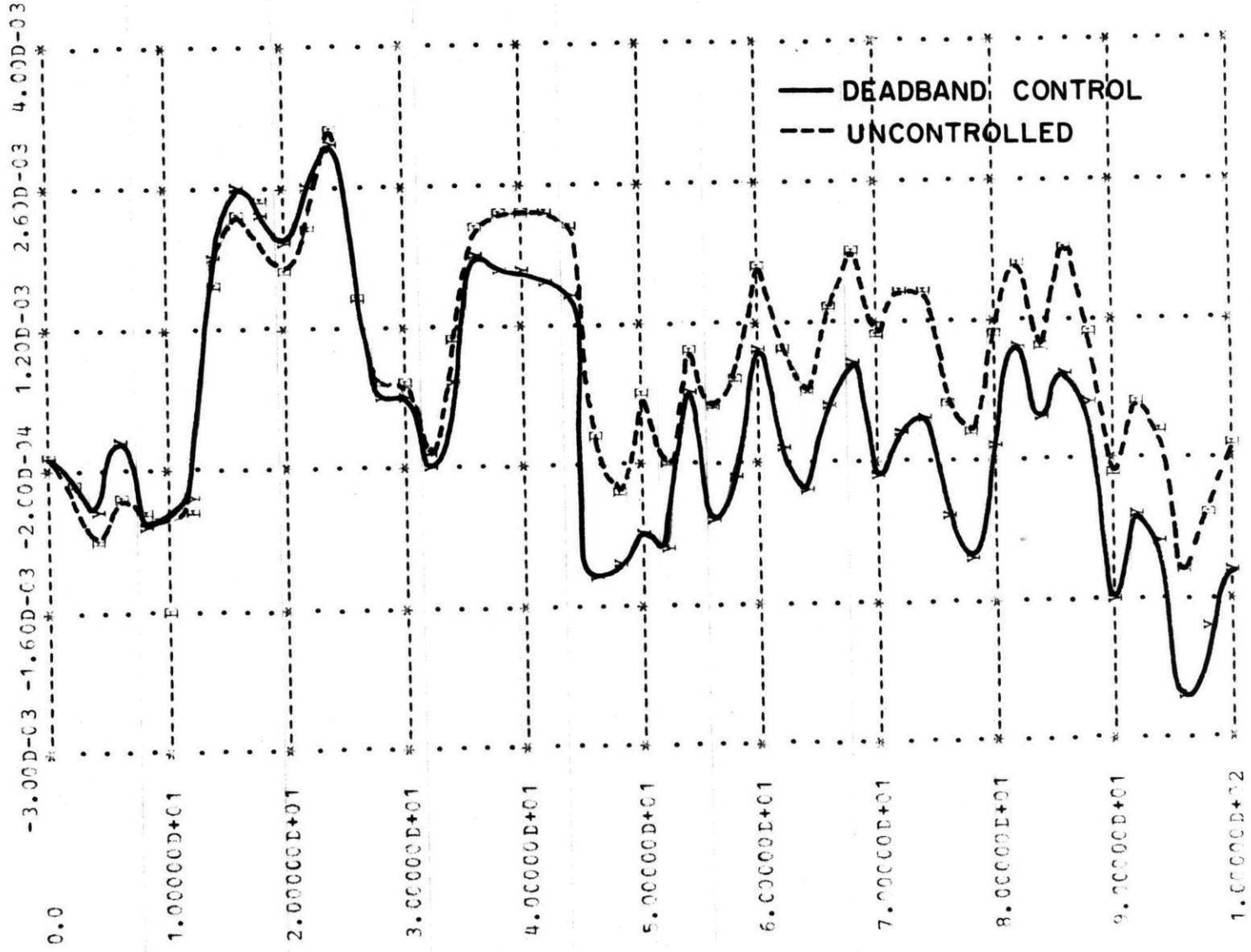Figure 4-23 Δf_{av} versus time (Simulation #5)

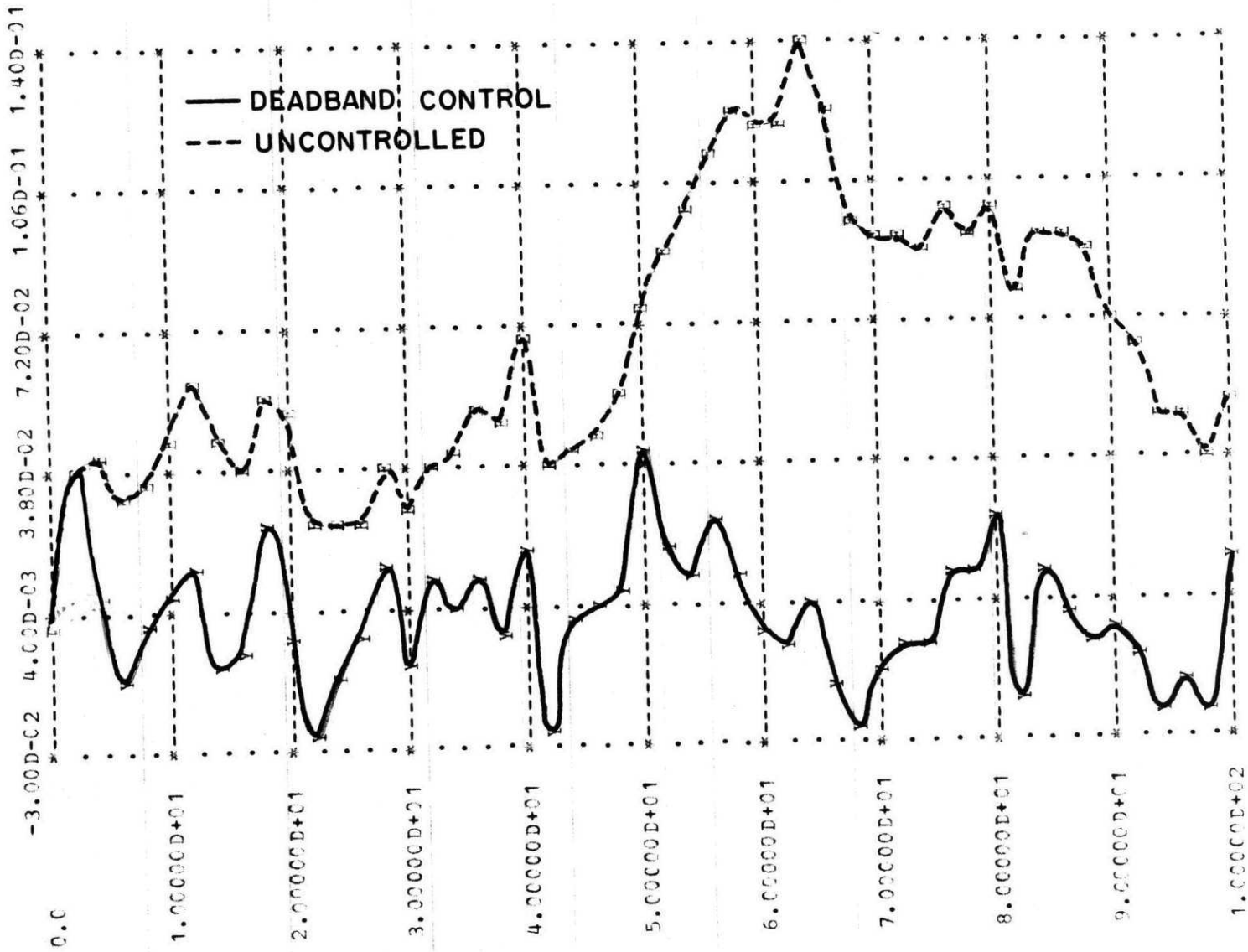Figure 4-24 $\Delta\delta_{av}$ versus time (Simulation #5)

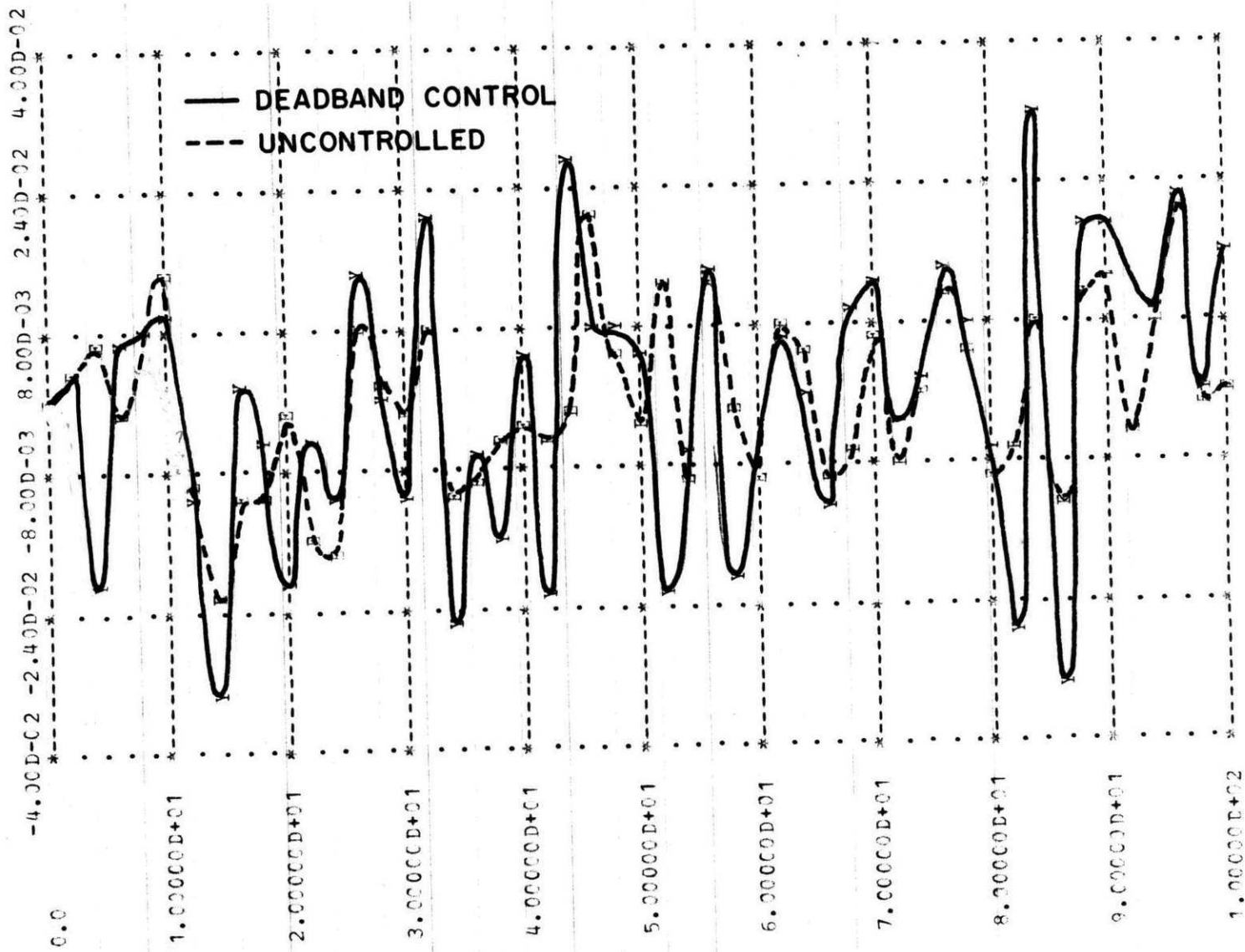Figure 4-25 $\int \Delta P_{tie}$ versus time (Simulation #5)

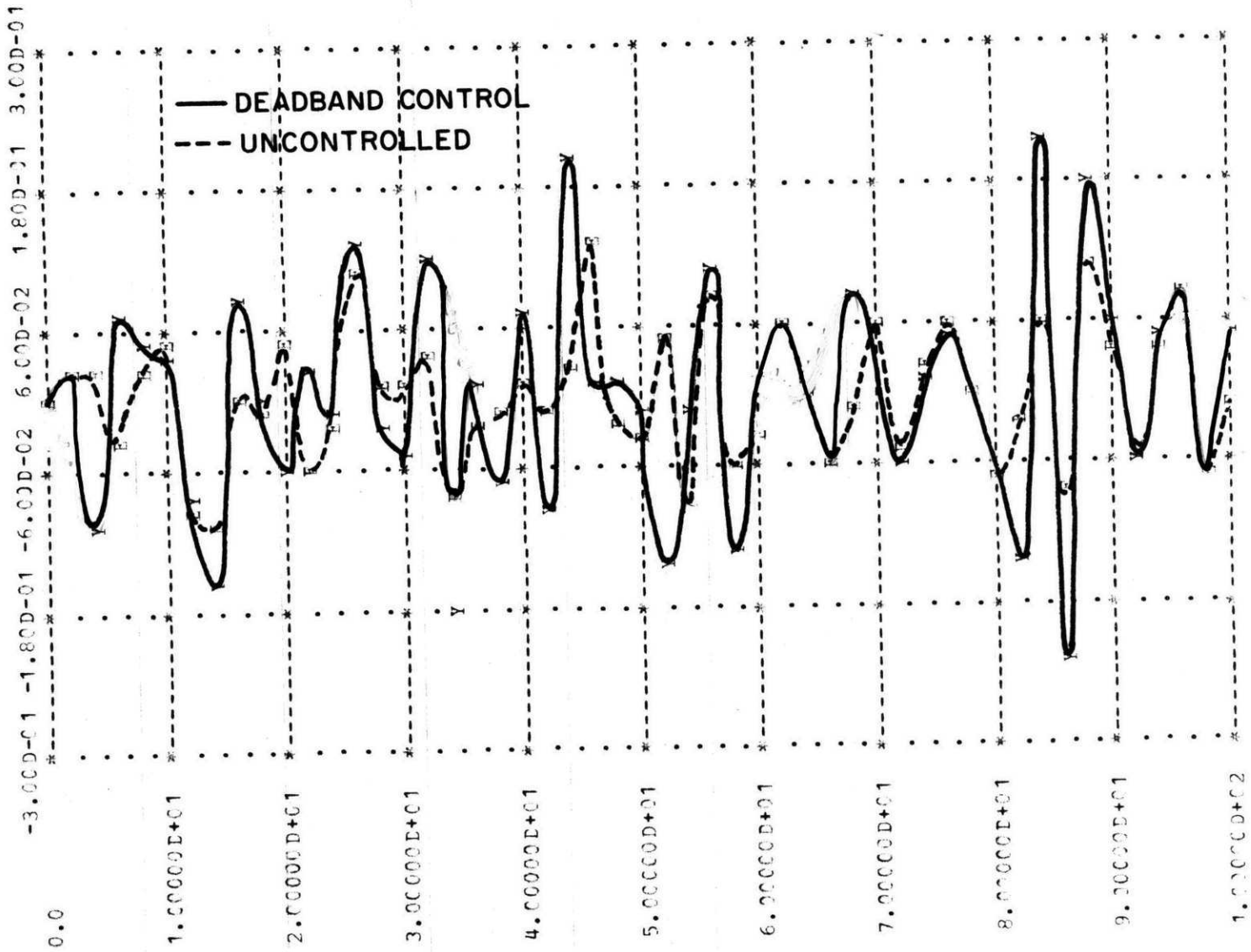Figure 4-26 ΔP_{M1} versus time (Simulation #5)

Figure 4-27 Δw_1 versus time (Simulation #5)

STEP	TEST	T1	T2
1	0	0.0	0.0
2	1	0.2392D+00	0.1487D+01
3	1	0.1881D+00	0.1442D+01
4	0	0.1350D+00	0.1936D+00
5	0	0.1009D+00	0.9087D-01
6	0	0.1313D+00	0.1262D+00
7	0	0.1878D+00	0.4746D+00
8	0	0.3921D+00	0.5511D+00
9	0	0.3065D+00	0.4253D+00
10	0	0.3115D+00	0.4097D+00
11	0	0.1949D+00	0.2488D+00
12	1	0.3273D+00	0.1219D+01
13	1	0.4136D+00	0.1052D+01
14	1	0.2247D+00	0.1057D+01
15	1	0.1979D+00	0.1079D+01
16	1	0.1489D+00	0.1612D+01
17	1	0.1164D+00	0.1550D+01
18	0	0.1661D+00	0.8648D+00
19	0	0.2525D+00	0.7549D+00
20	1	0.2501D+00	0.1511D+01
21	1	0.2321D+00	0.1608D+01
22	1	0.2561D+00	0.3986D+01
23	1	0.1828D+00	0.2474D+01
24	1	0.3414D+00	0.1802D+01
25	0	0.2445D+00	0.8866D+00
26	1	0.5595D+00	0.2917D+01
27	1	0.3745D+00	0.1863D+01
28	0	0.3281D+00	0.5247D+00
29	0	0.2927D+00	0.7863D+00
30	0	0.3836D+00	0.6755D+00
31	0	0.2367D+00	0.2740D+00
32	0	0.1229D+00	0.1256D+00
33	0	0.1359D+00	0.3706D+00
34	0	0.7201D-01	0.1856D+00
35	1	0.2138D+00	0.1355D+01
36	1	0.1626D+00	0.1142D+01
37	0	0.1451D+00	0.3149D+00
38	0	0.1526D+00	0.2405D+00
39	0	0.1135D+00	0.1574D+00
40	0	0.9300D-01	0.7143D-01
41	0	0.1010D+00	0.1771D+00
42	0	0.7877D-01	0.1868D+00
43	0	0.5568D-01	0.9579D-01
44	0	0.1627D+00	0.3113D+00
45	0	0.2133D+00	0.3564D+00
46	0	0.3077D+00	0.3873D+00
47	0	0.1826D+00	0.6047D+00
48	1	0.4656D+00	0.1679D+01
49	1	0.5736D+00	0.2708D+01
50	1	0.3865D+00	0.1107D+01

MONITOR = 20

Figure 4-28   Simulation #6 (q=5×10^{-7})

STEP	TEST	T1	T2
1	0	0.0	0.0
2	1	0.2360D+00	0.1458D+01
3	1	0.1728D+00	0.1297D+01
4	0	0.1095D+00	0.1245D+00
5	0	0.7288D-01	0.6866D-01
6	0	0.1203D+00	0.1060D+00
7	0	0.1763D+00	0.3120D+00
8	0	0.3489D+00	0.3234D+00
9	0	0.2356D+00	0.3467D+00
10	0	0.2732D+00	0.3238D+00
11	0	0.1526D+00	0.1895D+00
12	1	0.2893D+00	0.1112D+01
13	0	0.3614D+00	0.9715D+00
14	1	0.2601D+00	0.1738D+01
15	0	0.2071D+00	0.3129D+00
16	0	0.1836D+00	0.5974D+00
17	0	0.1316D+00	0.4695D+00
18	0	0.1341D+00	0.6766D+00
19	0	0.1445D+00	0.4508D+00
20	0	0.1386D+00	0.9664D+00
21	0	0.9707D-01	0.4620D+00
22	1	0.3784D+00	0.2789D+01
23	1	0.2364D+00	0.2532D+01
24	0	0.3507D+00	0.7868D+00
25	0	0.2618D+00	0.2350D+00
26	0	0.1528D+00	0.4326D+00
27	1	0.2059D+00	0.1223D+01
28	0	0.2326D+00	0.9173D+00
29	1	0.4382D+00	0.1171D+01
30	0	0.2877D+00	0.4647D+00
31	0	0.1662D+00	0.1599D+00
32	0	0.6639D-01	0.1349D+00
33	0	0.1428D+00	0.6361D+00
34	0	0.9016D-01	0.1304D+00
35	0	0.9066D-01	0.4384D+00
36	0	0.1752D+00	0.5911D+00
37	0	0.1084D+00	0.5922D+00
38	0	0.1819D+00	0.7857D+00
39	0	0.1535D+00	0.3254D+00
40	0	0.1918D+00	0.5772D+00
41	0	0.7314D-01	0.2733D+00
42	1	0.2267D+00	0.1270D+01
43	1	0.1730D+00	0.2572D+01
44	1	0.2167D+00	0.1052D+01
45	0	0.2358D+00	0.5744D+00
46	0	0.2634D+00	0.2888D+00
47	0	0.1255D+00	0.1215D+00
48	0	0.1615D+00	0.2039D+00
49	0	0.3759D+00	0.3747D+00
50	0	0.2158D+00	0.2549D+00

MONITOR= 11

Figure 4-29 Simulation #7 (q=5×10^{-6})

STEP	TEST	T1	T2
1	0	0.0	0.0
2	1	0.2198D+00	0.1289D+01
3	0	0.1099D+00	0.9106D+00
4	1	0.3237D+00	0.3380D+01
5	1	0.1666D+00	0.1750D+01
6	0	0.1546D+00	0.4216D+00
7	0	0.1115D+00	0.2514D+00
8	0	0.2631D+00	0.9693D+00
9	1	0.2769D+00	0.1857D+01
10	1	0.3027D+00	0.2444D+01
11	1	0.1228D+00	0.1202D+01
12	0	0.2536D+00	0.2494D+00
13	0	0.2422D+00	0.1623D+00
14	0	0.6826D-01	0.3031D+00
15	1	0.1952D+00	0.1477D+01
16	1	0.1052D+00	0.1488D+01
17	1	0.7752D-01	0.1194D+01
18	0	0.1368D+00	0.6488D+00
19	0	0.1360D+00	0.5147D+00
20	1	0.1409D+00	0.1350D+01
21	1	0.1423D+00	0.1576D+01
22	1	0.1617D+00	0.3109D+01
23	1	0.1038D+00	0.1944D+01
24	0	0.2775D+00	0.5639D+00
25	0	0.1546D+00	0.2012D+00
26	0	0.4828D-01	0.5633D-01
27	0	0.1004D+00	0.3153D+00
28	0	0.2737D+00	0.5582D+00
29	0	0.2464D+00	0.9097D+00
30	1	0.4022D+00	0.1224D+01
31	1	0.1735D+00	0.1574D+01
32	0	0.9600D-01	0.4046D+00
33	1	0.2511D+00	0.1143D+01
34	1	0.1352D+00	0.2149D+01
35	0	0.1890D+00	0.1571D+00
36	0	0.9827D-01	0.1094D+00
37	0	0.9167D-01	0.2473D+00
38	0	0.4911D-01	0.3758D+00
39	1	0.1488D+00	0.1568D+01
40	1	0.1065D+00	0.1241D+01
41	0	0.1090D+00	0.7993D+00
42	0	0.7664D-01	0.1571D+00
43	0	0.9851D-01	0.8373D+00
44	1	0.3807D+00	0.1196D+01
45	1	0.2296D+00	0.1016D+01
46	0	0.2041D+00	0.1113D+00
47	0	0.5513D-01	0.5767D-01
48	0	0.1902D+00	0.4704D+00
49	0	0.4393D+00	0.5333D+00
50	0	0.2381D+00	0.6643D+00

MONITOR= 21

Figure 4-30 Simulation #8 (q=5×10^{-5})

	$\Delta P_{M_1} \times 10^2$ Max	Δw_1 Max	$\Delta P_{M_2} \times 10^2$ Max	Δw_2 Max	$\Delta P_{M_3} \times 10^2$ Max	Δw_3 Max	$\Delta f_{av} \times 10^3$ Max	$\Delta \delta_{av} \times 10^3$ Max	$\int \Delta P_{tie}$ Max
No deadband used	3.4	0.2	0.25	0.12	4.3	0.22	1.36	3	0.038
case #5 42% saving	3.4	0.2	0.23	0.11	4.2	0.15	1.36	2.3	0.041
Case #6 60% saving	3.1	0.22	0.26	0.12	4.4	0.22	1.2	3	0.04
Case #7 78% saving	3.4	0.24	0.24	0.11	4.2	0.22	1.36	3	0.042
Case #8 58% saving	4.3	0.26	0.28	0.13	4.5	0.23	1.2	2.7	0.042
No control used	2.2	0.13	0.4	0.02	2.3	0.13	1.20	3.16	0.14

Figure 4-31

Maximum deviations corresponding to the different deadbands used with full

state feedback control

STEP	TEST	T1	T2
1	0	0.0	0.0
2	1	0.2376D+00	0.3011D+01
3	1	0.1876D+00	0.5035D+01
4	0	0.1325D+00	0.4643D+00
5	1	0.1315D+00	0.4384D+01
6	1	0.1744D+00	0.2114D+02
7	1	0.2198D+00	0.1210D+01
8	1	0.3565D+00	0.4402D+02
9	1	0.3017D+00	0.4989D+02
10	1	0.3902D+00	0.7452D+02
11	1	0.2190D+00	0.2847D+02
12	1	0.3270D+00	0.7532D+02
13	1	0.3898D+00	0.5995D+02
14	0	0.2761D+00	0.8874D+00
15	1	0.3161D+00	0.1300D+01
16	1	0.1900D+00	0.9272D+01
17	1	0.1364D+00	0.3695D+02
18	1	0.1531D+00	0.2405D+01
19	0	0.2156D+00	0.9489D+00
20	1	0.2837D+00	0.1760D+01
21	1	0.2373D+00	0.1704D+01
22	1	0.2638D+00	0.4972D+01
23	0	0.1750D+00	0.3917D+00
24	1	0.4288D+00	0.5087D+02
25	1	0.2453D+00	0.2955D+02
26	1	0.2495D+00	0.2320D+02
27	1	0.1835D+00	0.5115D+02
28	0	0.2138D+00	0.5611D+00
29	1	0.3717D+00	0.2649D+02
30	1	0.2798D+00	0.1023D+01
31	1	0.1928D+00	0.4625D+01
32	0	0.1339D+00	0.4791D+00
33	0	0.2004D+00	0.2421D+00
34	1	0.1338D+00	0.8315D+01
35	1	0.1737D+00	0.1014D+02
36	0	0.1402D+00	0.3649D+00
37	1	0.2142D+00	0.7210D+01
38	0	0.1074D+00	0.1724D+00
39	1	0.1147D+00	0.7919D+01
40	1	0.1009D+00	0.8037D+01
41	0	0.1411D+00	0.7806D+00
42	1	0.2719D+00	0.3320D+01
43	1	0.8207D-01	0.1795D+01
44	1	0.1566D+00	0.2183D+02
45	1	0.1957D+00	0.5881D+01
46	1	0.2740D+00	0.8968D+01
47	1	0.1668D+00	0.1713D+01
48	1	0.2155D+00	0.1628D+02
49	1	0.3711D+00	0.6774D+02
50	1	0.2742D+00	0.1350D+02

MCNITOR= 39

Figure 4-32 Simulation #9 ($q=5\times10^{-7}$)

STEP	TEST	T1	T2
1	0	0.0	0.0
2	1	0.2234D+00	0.1584D+01
3	0	0.1666D+00	0.7103D+00
4	0	0.1788D+00	0.2191D+00
5	0	0.7824D-01	0.6500D+00
6	1	0.2293D+00	0.2228D+01
7	0	0.2283D+00	0.2809D+00
8	1	0.2945D+00	0.4772D+01
9	1	0.2489D+00	0.5473D+01
10	1	0.3648D+00	0.7736D+01
11	1	0.1867D+00	0.2874D+01
12	1	0.2802D+00	0.8490D+01
13	1	0.3666D+00	0.6098D+01
14	0	0.2449D+00	0.2340D+00
15	0	0.1654D+00	0.6073D+00
16	1	0.1034D+00	0.1235D+01
17	1	0.9020D-01	0.4115D+01
18	0	0.1364D+00	0.4759D+00
19	0	0.1913D+00	0.3747D+00
20	0	0.1424D+00	0.3777D+00
21	0	0.2796D+00	0.7538D+00
22	0	0.9711D-01	0.4513D+00
23	0	0.1272D+00	0.2368D+00
24	1	0.3891D+00	0.5723D+01
25	1	0.2568D+00	0.3693D+01
26	1	0.2409D+00	0.3345D+01
27	1	0.1669D+00	0.6381D+01
28	0	0.1938D+00	0.2291D+00
29	1	0.2416D+00	0.3330D+01
30	0	0.2053D+00	0.2360D+00
31	0	0.1225D+00	0.5529D+00
32	0	0.2036D+00	0.3344D+00
33	0	0.1020D+00	0.8481D-01
34	1	0.9738D-01	0.1567D+01
35	1	0.1681D+00	0.2180D+01
36	0	0.1384D+00	0.1786D+00
37	0	0.1113D+00	0.7328D+00
38	0	0.2130D+00	0.1354D+00
39	1	0.1160D+00	0.1521D+01
40	0	0.1003D+00	0.9156D+00
41	0	0.3197D+00	0.3706D+00
42	0	0.1257D+00	0.4431D+00
43	0	0.1455D+00	0.3449D+00
44	1	0.2639D+00	0.2204D+01
45	0	0.1942D+00	0.7552D+00
46	1	0.3408D+00	0.1476D+01
47	0	0.1701D+00	0.4524D+00
48	1	0.3430D+00	0.1958D+01
49	1	0.4567D+00	0.7232D+01
50	1	0.2714D+00	0.1872D+01

MONITOR= 23

Figure **4-33** Simulation #10 (q=5×10^{-6})

STEP	TEST	T1	T2
1	0	0.0	0.0
2	0	0.1707D+00	0.9519D+00
3	1	0.2159D+00	0.1318D+01
4	0	0.9835D-01	0.8772D-01
5	0	0.4587D-01	0.1210D+00
6	0	0.1008D+00	0.2970D+00
7	0	0.1589D+00	0.1797D+00
8	1	0.3020D+00	0.1153D+01
9	0	0.2146D+00	0.8866D+00
10	0	0.3389D+00	0.9452D+00
11	0	0.2596D+00	0.4178D+00
12	1	0.2967D+00	0.1812D+01
13	0	0.3057D+00	0.7892D+00
14	0	0.2492D+00	0.2933D+00
15	0	0.1480D+00	0.2953D+00
16	0	0.3025D-01	0.2004D+00
17	0	0.9841D-01	0.9683D+00
18	1	0.4001D+00	0.1147D+01
19	0	0.3014D+00	0.3953D+00
20	0	0.1330D+00	0.2270D+00
21	0	0.2102D+00	0.4842D+00
22	0	0.5209D-01	0.2107D+00
23	0	0.4037D-01	0.1865D+00
24	0	0.3285D+00	0.6820D+00
25	0	0.2150D+00	0.3607D+00
26	0	0.1610D+00	0.2299D+00
27	0	0.1451D+00	0.8519D+00
28	0	0.4098D+00	0.7471D+00
29	1	0.3120D+00	0.1435D+01
30	0	0.2102D+00	0.1934D+00
31	0	0.7522D-01	0.8756D-01
32	0	0.5943D-01	0.8180D-01
33	0	0.6270D-01	0.7789D-01
34	0	0.5937D-01	0.3258D+00
35	1	0.2506D+00	0.1898D+01
36	0	0.1651D+00	0.2061D+00
37	0	0.7994D-01	0.1439D+00
38	0	0.6161D-01	0.1005D+00
39	0	0.7956D-01	0.2711D+00
40	0	0.6927D-01	0.2551D+00
41	0	0.1649D+00	0.3798D+00
42	0	0.4683D-01	0.7331D-01
43	0	0.7570D-01	0.5289D+00
44	0	0.3014D+00	0.7375D+00
45	0	0.2029D+00	0.8718D+00
46	0	0.1787D+00	0.5364D+00
47	0	0.1131D+00	0.1784D+00
48	0	0.7798D-01	0.2285D+00
49	0	0.2683D+00	0.9082D+00
50	0	0.2331D+00	0.3341D+00

MONITOR= 6

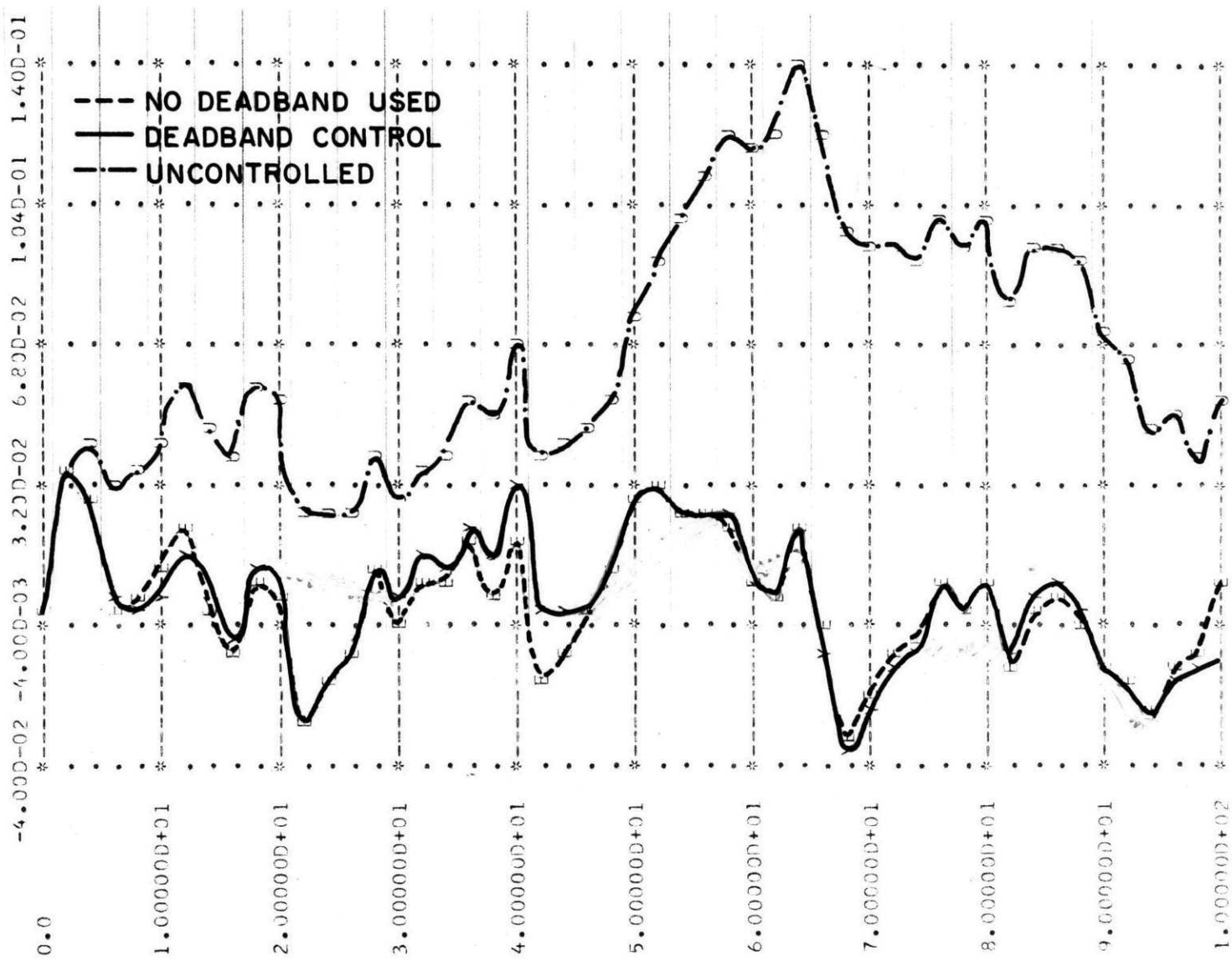Figure 4-34 Simulation #11 ($q=5\times10^{-5}$)

Figure 4-35 P_{tie} versus time (Simulation #10)

	$\Delta P_{M_1} \times 10^2$ Max	Δw_1 Max	$\Delta P_{M_2} \times 10^2$ Max	Δw_2 Max	$\Delta P_{M_3} \times 10^2$ Max	Δw_3 Max	$\Delta f_{av} \times 10^3$ Max	$\Delta \delta_{av} \times 10^3$ Max	$\int \Delta P_{tie}$ Max
No deadband used	2.8	0.14	0.7	0.03	2.7	0.12	1.44	8.4	0.036
Case #9 22% saving	2.6	0.12	0.7	0.03	2.6	0.1	1.44	8.4	0.033
Case #10 54% saving	2.2	0.11	0.74	0.03	2.3	0.1	1.36	9.0	0.036
Case #11 88% saving	2.8	0.13	0.65	0.03	2.5	0.09	1.12	4.0	0.043
No control used	2.2	0.13	0.4	0.02	2.3	0.13	1.20	3.16	0.14

Figure 4-36

Maximum deviations corresponding to different deadbands used with full state feedback control

and modified $\underline{Q}_w$

CHAPTER   5

CONCLUSION AND SUGGESTIONS FOR FUTURE RESEARCH

In this thesis, a linear-plus-deadband controller is implemented on
an average system frequency model of a power system. This model essential-
ly ignores the relatively fast dynamics of the intermachine oscillations
Furthermore, normal mode (non emergency) operation is assumed and only un-
known-but-bounded disturbances of the loads are considered. As for the
linear part of the control, two avenues are taken: conventional AGC and full
state feedback. The deadband is imposed on the controller for both cases.
Its design is based on set-theoretic relations which are then translated
to relations between bounding ellipsoids.

When applied to a simple working example, computational problems, link-
ed to the form of the average frequency model, are encountered. These are
solved by adding fake noise to the model during the design process. Owing
partly to the conservative nature of the ellipsoidal bounds, this additional
degree of freedom results in sizeable savings in control signals. The
deviations of frequency and tie-line flow between areas are not significantly
increased as compared to the case where no deadband is used (i.e.the control
action is continuous). Moreover, slightly better results are obtained for the

full state feedback deadband controller.

The main criterion used all along, is the maximum deviations of the variables of interest. However, in actual situations this is only but one of many other considerations and as high savings as 88% (simulation #11) may not at all be feasable or even desirable. But it is only meant here to illustrate the promissing potentials of such an approach.

It is therefore suggested that future research along those lines should take into account important non linearities such as the turbine valve limits, and be extended to include a full blown nonlinear simulation. It has also been assumed all along that the state variables are perfectly known. In particular the average frequency is not a directly measurable physical variable. A state estimator should therefore be included in a further study. Finally, an extension of the deadband controller design to situations where the loads have different models (superimposed steps, ramps...) seems also necessary.

APPENDIX

This appendix presents the relevant mathematical material for Chapter 3. It is composed mainly of extracts from Chapter H and Appendix H of [10] and from Appendix A of [11].

1. Ellipsoids

An ellipsoid Ω with center $\underline{m}$ can be defined by

$$\Omega = \{\underline{x}: [\underline{x}-\underline{m}]' \ \underline{\Gamma}^{-1} [\underline{x}-\underline{m}] \leq 1\} \tag{A.1}$$

where $\underline{\Gamma}$ is a positive definite matrix. The direction of the axis of Ω are determined by the eigenvectors of $\underline{\Gamma}$ and the lengths of the semimajor axes of Ω are equal to the roots of the corresponding eigenvalues. (Appendix H, [10]). The eigenvalues of $\underline{\Gamma}$ thus give an idea of the thickness of the ellipsoid in the corresponding directions.

$$\text{Let} \quad \Omega_x = \left\{ \underline{x}: (\underline{x}-\underline{m})' \ \underline{\Gamma}^{-1} (\underline{x}-\underline{m}) \leq 1 \right\}$$

$$\underline{x}_1 : K_1\text{-dimensional}$$

$$\Omega_y = \left\{ \underline{y} : \underline{y} = \underline{H} \ \underline{x} \pm \underline{h}, \ \underline{x} \ \varepsilon \ \Omega_x \right\}$$

$$\underline{y} \quad : K_2\text{-dimensional}$$

Then, (Appendix H, [10])

$$\Omega_y = \left\{ \underline{y} : (\underline{y} - \underline{h} - \underline{H}\,\underline{m})' \, [\underline{H}\,\underline{\Gamma}\,\underline{H}']^{-1} \, (\underline{y} - \underline{h} - \underline{H}\,\underline{m}) \leq 1 \right\}$$

In chapter 3, the ellipsoids of interest are centered at the origin and the transformations encountered are of the form $\underline{y} = \underline{H}\,\underline{x}$. Under those conditions

$$\Omega_y = \left\{ \underline{y} : \underline{y}' \, (\underline{H}\,\underline{\Gamma}\,\underline{H}')^{-1} \, \underline{y} \leq 1 \right\}$$

If $[\underline{H}\,\underline{\Gamma}\,\underline{H}']^{-1}$ does not exist, Ω_y is defined with the aid of support functions.

2. Support functions:

The support function $s(\underline{\eta})$ of a closed convex set Ω is defined by

$$\left\{ \begin{array}{l} s(\underline{\eta}) = \text{maximum } (\underline{x}'\,\underline{\eta}) \\[1em] \qquad \forall\,\underline{x} \; \epsilon \; \Omega \\[1em] \underline{\eta}'\,\underline{\eta} = 1 \end{array} \right.$$

and the set Ω can be expressed as

$$\Omega : \left\{ \underline{x} : \underline{x}' \, \underline{\eta} \leq s(\underline{\eta}) \qquad \forall\,\underline{\eta},\; \underline{\eta}'\,\underline{\eta} = 1 \right\}$$

(see Fig. A.I)

Let Ω_1 and Ω_2 have support functions $s_1(\underline{n})$ and $s_2(\underline{n})$ respectively, and let

$$\Omega \triangleq \Omega_1 \oplus \Omega_2 \triangleq \left\{ \underline{x} : \underline{x} = \underline{x}_1 + \underline{x}_2, \quad \forall \underline{x}_1 \in \Omega_1, \quad \forall \underline{x}_2 \in \Omega_2 \right\}$$

Then, the support function of Ω is (Appendix G, [10])

$$s(\underline{n}) = s_1(\underline{n}) + s_2(\underline{n}) \tag{A.2}$$

Moreover, $\Omega_2 \subset \Omega_1$ if and only if

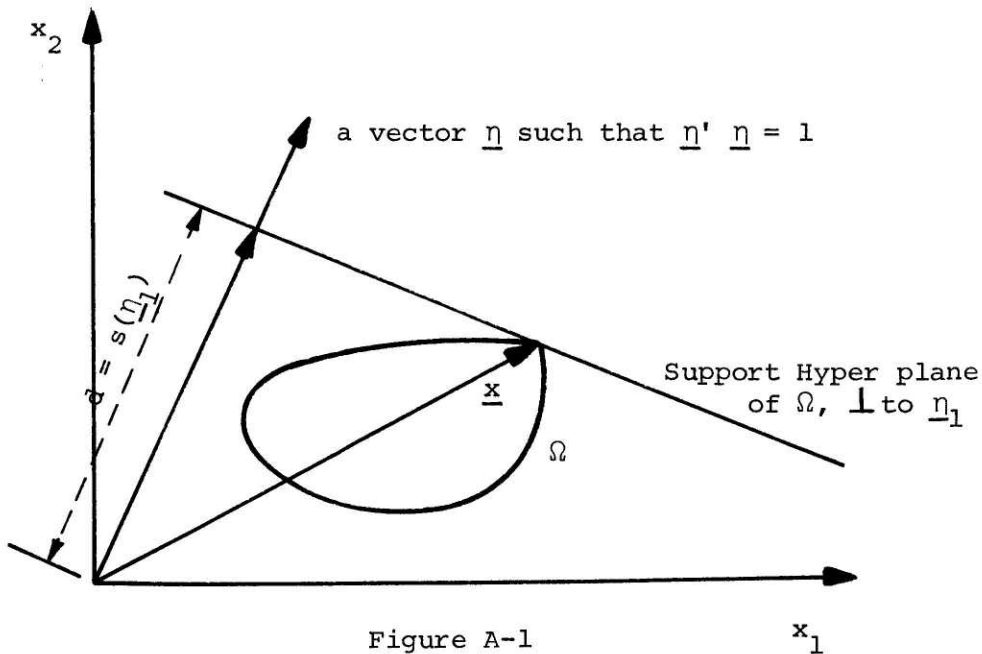$$s_2(\underline{n}) \le s_1(\underline{n}) \quad \forall \underline{n} \tag{A.3}$$

Figure A-1

Example of geometry of support funtion (Fig.G.2,[10])

Finally, the support function of the ellipsoid given by (A.1) is:

$$s(\underline{\eta}) = \underline{x}' \; \underline{m} + (\underline{\eta}' \; \underline{\Gamma} \; \underline{\eta})^{\frac{1}{2}} \tag{A.4}$$

3. Bounding ellipsoids ([10], [11])

Let Ω_1 and Ω_2 be two ellipsoids as defined by (A.1) with $m_1 = m_2 = 0$. In view of (A.4)

$$s_1(\underline{\eta}) = (\underline{\eta}' \; \underline{\Gamma}_1 \; \underline{\eta})^{\frac{1}{2}} \tag{A.5}$$

$$s_2(\underline{\eta}) = (\underline{\eta}' \underline{\Gamma}_2 \; \underline{\eta})^{\frac{1}{2}}$$

Let $\Omega = \Omega_1 \oplus \Omega_2$. Then (A.2)

$$s(\underline{\eta}) = (\underline{\eta}' \; \underline{\Gamma}_1 \; \underline{\eta})^{\frac{1}{2}} + (\underline{\eta}' \; \underline{\Gamma}_2 \; \underline{\eta})^{\frac{1}{2}} \tag{A.6}$$

is not in general the support function of an ellipsoid.

Using H older's inequality

$$(b_1 + b_2)^2 \leq \frac{1}{1-\beta} \; b_1^2 + \frac{1}{\beta} b_2^2 \qquad 0 \leq \beta \leq 1$$

(A.6) gives:

$$s(\underline{\eta}) \leq \left[\underline{\eta}' \left(\frac{1}{1-\beta} \; \underline{\Gamma}_1 + \frac{1}{\beta} \; \underline{\Gamma}_2 \right) \; \underline{\eta} \right]^{\frac{1}{2}} = s_{b_1}(\underline{\eta})$$

In view of (A.4), $s_{b_1}(\underline{\eta})$ is the support function of the ellipsoid

$$
\begin{cases}
\Omega_{b_1} = \{\underline{x} : \underline{x}' \; \underline{\Gamma}_{b_1}^{-1} \; \underline{\eta} \le 1 \} \\[3mm]
\underline{\Gamma}_{b_1} = \dfrac{1}{1-\beta} \; \underline{\Gamma}_1 + \dfrac{1}{\beta} \; \Gamma_2 \\[3mm]
0 \le \beta \le 1
\end{cases}
\qquad (A.6)
$$

and in view of (A.4)

$$
\Omega = \Omega_1 \oplus \Omega_2 \subset \Omega_{b_1}
$$

so that Ω_b is an ellipsoidal outer bound of Ω.

Refering to the dynamic system of chapter 3, let

$$
\underline{x}(n\Delta+\Delta) = \underline{\Phi}_{c\ell}\underline{x}(n\Delta) + \underline{G} \; \underline{w}(n\Delta)
$$

where

$$
\underline{w}(n\Delta) \; \varepsilon \; \Omega_w = \{ \underline{w}: \underline{w}' \; \underline{Q}^{-1} \; \underline{w} \le 1 \}
$$

and let

$\Omega_x(n\Delta)$ be the smallest set that contains $\underline{x}(n\Delta)$, $\forall \underline{w}(k\Delta) \; \varepsilon \; \Omega_w$,

$$
k = 0, \; \dots \; n-1.
$$

then

$$
\Omega_x(n\Delta+\Delta) = \underline{\Phi}_{c\ell} \; \Omega_x(n\Delta) \oplus \underline{G} \; \underline{\Omega}_w
$$

If $\underline{\Phi}_{c\ell}$ is stable, $\Omega_x(n\Delta)$ will reach a steady state value $\Omega_x(ss)$ given by

$$\Omega_x(ss) = \underline{\Phi}_{c\ell} \; \Omega_x(ss) \; \oplus \; \underline{G} \; \Omega_w$$

In view of (A.6), Eq.(3.11) of chapter 3 then follows.

Suppose now $\Omega_2 \subset \Omega_1$ or, equivalently, $\underline{\Gamma}_1 - \underline{\Gamma}_2 > 0$ (from A.3 and A.5). Let

$$\Omega_{b_2} = \{ \; \underline{x} \; : \; \underline{x}' \; \Gamma_{b_2}^{-1} \; \underline{x} \leq 1 \; \}$$

be an ellipsoid such that

$$\Omega_{b_2} \; \oplus \; \Omega_2 \subset \Omega_1 \tag{A.7}$$

From (A.6) we must have

$$\underline{\Gamma}_1 = \frac{\underline{\Gamma}_2}{\beta} + \frac{\Gamma_{b_2}}{1-\beta}$$

or

$$\underline{\Gamma}_{b_2} = \frac{\alpha}{1+\alpha} \underline{\Gamma}_1 - \alpha \; \underline{\Gamma}_2 \quad \text{where} \quad \alpha = \frac{1}{\beta} - 1 \tag{A.8}$$

and since $\underline{\Gamma}_{b_2}$ must be positive definite β cannot take any value between 0 and 1 or equivalently α any value between 0 and ∞.

We then must have

$$\frac{\alpha}{1+\alpha} \ \underline{\Gamma}_1 \ - \ \alpha\underline{\Gamma}_2 \ > \ 0$$

or

$$\underline{\Gamma}_1 \ - \ (1+\alpha) \ \underline{\Gamma}_2 \ > \ 0 \qquad\qquad\qquad (A.9)$$

Let $\underline{\Theta}$ be the matrix such that $\underline{\Theta}' \ \underline{\Gamma}_2 \ \underline{\Theta} = \underline{I}$ (i.e change coordinates such that Ω_2 is transformed into a shpere of unit radius). Then (A.9) becomes

$$\underline{\Theta}' \ \underline{\Gamma}_1 \ \underline{\Theta} \ - \ (1+\alpha) \ \underline{I} \ > \ 0 \qquad\qquad\qquad (A.10)$$

Let $\underline{V}$ be the matrix of eigenvectors of $\underline{\Theta}' \ \underline{\Gamma}_1 \ \underline{\Theta}$. Then $\underline{V}^{-1} \ \underline{\Theta}' \ \underline{\Gamma}_1 \ \underline{\Theta} \ \underline{V}$ is diagonal and the diagonal elements are the eigenvalues of $\underline{\Theta}' \ \underline{\Gamma}_1 \ \underline{\Theta}$. Then (A.10) becomes

$$(\ \underline{V}^{-1} \ \underline{\Theta}' \ \underline{\Gamma}_1 \ \underline{\Theta} \ \underline{V} \ ) \ - \ (1 + \alpha) \ \underline{I} \ > \ 0$$

or

$$\lambda_i \ (\ \underline{\Theta}' \ \underline{\Gamma}_1 \ \underline{\Theta} \ ) \ - \ (1 + \alpha) \ > \ 0 \qquad i = 1, \ \dots \ n$$

Therefore, α should satisfy

$$\alpha \ < \ \left[\lambda_{\min} \ (\ \underline{\Theta}' \ \underline{\Gamma}_1 \ \underline{\Theta} \ ) \ - \ 1 \right] \qquad\qquad\qquad (A.11)$$

Geometrically, this means that if α is increased beyond a certain limit one cannot find an ellipsoid which satisfies (A.7). This is because $\underline{\Gamma}_2$ (weighted by α) is more amplified than $\underline{\Gamma}_1$ (weighted by $\frac{\alpha}{1+\alpha}$ as α increases, and the "fit" is too close.

Referring again to the system of chapter 3, Eq. (3.12) follows now from (A.8) and (A.11).

REFERENCES

[1]. N. Cohn, <u>Control of Generation and Power Flow on Interconnected Systems</u>, John Wiley and Sons, Inc., New York 1966.

[2]. C.E. Fosha, Jr. and O.I. Elgerd, "The Megawatt-Frequency Control Problem: A New Approach via Optimal Control Theory", <u>IEEE Trans. on PAS</u>, Vol. PAS 89, pp. 563-578, April 1970.

[3]. J.D. Glover, F.C. Schweppe, "Advanced Load Frequency Control", <u>IEEE Trans. on PAS</u>, Vol. PAS 91, No. 4, pp.1637-1642, July 1972. Also <u>EPSEL Report No. 26</u>, M.I.T., February 1971.

[4]. C.W. Ross, "Error Adaptive Control Computer for Interconnected Power Systems". <u>IEEE Trans. on PAS</u>, Vol. PAS 85, No.7, pp. 742-749, July 1966.

[5]. David Grandez-Gomez, "Average System Frequency Approach to Slow Speed Power System Dynamics", <u>EPSEL Report No. 37</u>, M.I.T., June 1972.

[6]. James B. Woodard Jr., "Power System Model Reduction - A Canonical Representation", <u>EPSEL Report No. 35</u>, M.I.T., February 1972.

[7]. M.L. Chan, R. Dunlop, F.C. Schweppe, "Dynamic Equivalents for Average System Frequency Behavior Following Major Disturbances, <u>EPSEL Report No. 32</u>, M.I.T. March 1971.

[8]. M.L. Baugham, F.C. Schweppe, "Contingency Evaluation: Real Power Flows from a Linear Model", <u>IEEE Summer Power Meeting & EHV Conference</u>, Los Angeles, California, July 12-17, 1970.

[9]. D.N. Ewart, "Automatic Generation Control", <u>Engineering Foundation Conference</u>, New England College, Henniker, New Hampshire, August 1975.

[10]. F.C. Schweppe, <u>Uncertain Dynamic Systems</u>, Prentice Hall, New Jersey 1973.

[11]. J.D. Glover, F.C. Schweppe, "Control of Linear Dynamic Systems with Unknown but Bounded Disturbances", <u>IEEE Trans. on Automatic Control</u>, Vol. AC-16, pp. 411-423, October 1972.

[12]. R.W. Brockett, _Finite Dimensional Linear Systems_, Wiley, New York, 1970.

[13]. M. Athans, P. Falb, _Optimal Control_, McGraw-Hill, New York, 1966.

[14]. N.R. Sandell Jr., M. Athans, _Computer Subroutines for Modern Control Theory_, M.I.T. Center for Advanced Engineering Study, Cambridge, Mass. 1974.

[15]. M. Aoki, "Control of Large-Scale Dynamic Systems by Aggregation", _IEEE Trans. on Automatic Control_, Vol. AC-13, No.3, June 1968.